

Quantum Transport

Lecture Notes

Yuri M. Galperin

*Lund University
November 1998*

E-mail: yurig@teorfys.lu.se

Permanent address:

*Department of Physics, P.O. Box 1048 Blindern, 0316 Oslo
Phone: +47 22 85 64 95, E-mail: iouri.galperine@fys.uio.no*

Preface

This course is an attempt to provide an overview of basic concepts of quantum transport through modern small-size structures. It is a very hot topic at present time because it is relevant to fundamental principles of quantum mechanics and statistical physics, as well as to various applications in modern electronics.

Several excellent books [1, 2, 3, 4, 5, 6] and review articles (e. g. [7, 8, 9, 10, 11, 12, 13, 14, 15, 16, 17, 18, 19]) are written on this subject. This list is far from being complete.

In the present course I try to select only few topics from the broad area to provide a general introduction to the subject. The reference list includes only few selected papers rather than a more or less complete overview of the literature. I tried to concentrate on the basic concepts rather than on historical aspects.

Any comments and criticism will be gratefully appreciated.

October 1998

Yuri Galperin

Contents

1	Preliminary Concepts	1
1.1	Two-Dimensional Electron Gas	1
1.2	Basic Properties	2
1.3	Degenerate and non-degenerate electron gas	12
1.4	Relevant length scales	13
2	Diffusive transport	17
2.1	Classical transport in diffusive regime	17
2.2	Linear response in quantum mechanics	20
2.3	Shubnikov-de Haas effect	23
2.4	Weak localization	24
2.5	Weak localization .. magnetic field	27
2.6	Aharonov-Bohm effect	28
2.7	$e - e$ interaction	30
2.8	Anderson localization	32
3	Ballistic Transport	37
3.1	Landauer formula	37
3.2	Application of Landauer formula	42
3.3	Additional aspects of ballistic transport	47
3.4	$e - e$ interaction in ballistic systems	48
4	Tunneling and Coulomb blockage	55
4.1	Tunneling	55
4.2	Coulomb blockade	59
5	Conductance Fluctuations	67
5.1	General considerations	67
5.2	Universal conductance fluctuations	67
5.3	Temperature effects	69
5.4	Magnetoconductance fluctuations	70
5.5	$I - V$ -curve of a metallic wire	72
5.6	Random matrix theory	73

6	Quantum Hall Effect	77
6.1	Ordinary Hall effect	77
6.2	Integer Quantum Hall effect - General Picture	77
6.3	Edge Channels and Adiabatic Transport	81
6.4	Fractional Quantum Hall Effect	85
7	Noise in mesoscopic systems	93
7.1	Current fluctuations	93
7.2	Two Simple Applications	97
7.3	Phase Breaking, Thermalization, and Inelastic Scattering	98
7.4	Double-Barrier Junction	101
A	Second quantization	109
B	Quantum corrections to conductivity	113
B.1	Diagrammatic perturbation theory	113
B.2	Kubo-Greenwood formula	116
B.3	Weak localization corrections	117
C	Derivation of Landauer formula.	123
D	Coulomb blockade in a non-stationary case	127

Chapter 1

Preliminary Concepts

1.1 Two-Dimensional Electron Gas

An important system where quantum effects were observed is two-dimensional electron gas (2DEG). There are two basic systems where 2DEG has been studied. One of them is Si MOSFETs (metal-oxide-semiconductor field-effect transistors). A very good review of such systems is given in Ref. [7]. A typical device is shown in Fig. 1.1. A (100)Si surface serves

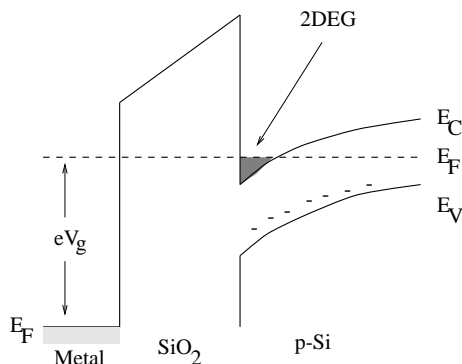


Figure 1.1: Band diagram showing conduction band E_C , valence band E_V and quasi-Fermi level E_F . A 2DEG is formed at the interface between the oxide (SiO_2) and p -type silicon substrate as a consequence of the gate voltage V_g .

as a substrate while SiO_2 layer behaves as an insulator. 2DEG is induced electrostatically by application a positive voltage V_g . The sheet density of 2DEG can be described as

$$n_s = \frac{\epsilon_{\text{ox}}}{ed_{\text{ox}}}(V_g - V_t)$$

where V_t is the threshold voltage for the barrier's creation

Another important systems with 2DEG involve modulation-doped GaAs-AlGaAs heterostructures. The bandgap in AlGaAs is wider than in GaAs. By variation of doping it is possible to move the Fermi level inside the forbidden gap. When the materials are

put together, a unified level of chemical potential is established, and an inversion layer is formed at the interface.

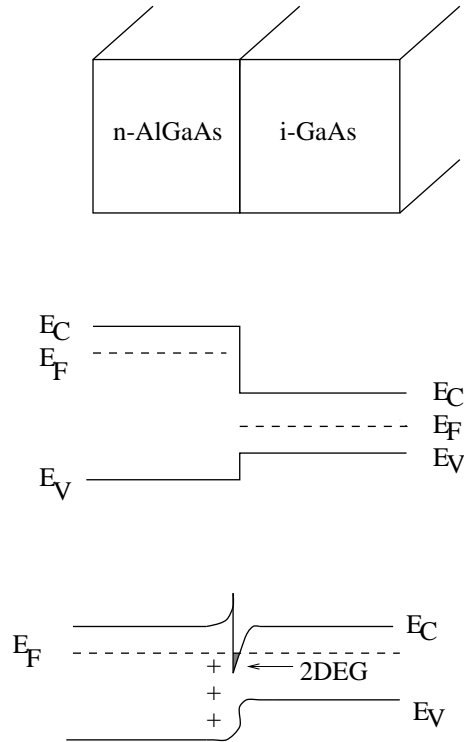


Figure 1.2: Band structure of the interface between *n*-AlGaAs and intrinsic GaAs, (a) before and (b) after the charge transfer.

The 2DEG created by a modulation doping can be squeezed into narrow channels by selective depletion in spatially separated regions. The simplest lateral confinement technique is to create split metallic gates in a way shown in Fig. 1.3 A typical nanostructure is shown in Fig. 1.4.

1.2 Basic Properties of Low-Dimensional Systems

Wave Functions

Let us direct z -axis perpendicular to the plane of 2DEG. The wave function can be decoupled as

$$\Psi(\mathbf{r}, z) = \chi(z) \psi(\mathbf{r})$$

where \mathbf{r} is the vector in plane of 2DEG. Throughout our considerations we will assume that all the distances are much larger than interatomic distance and thus we will use the effective

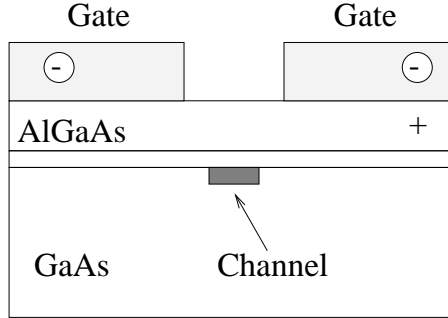


Figure 1.3: On the formation of a narrow channel by a split gate.

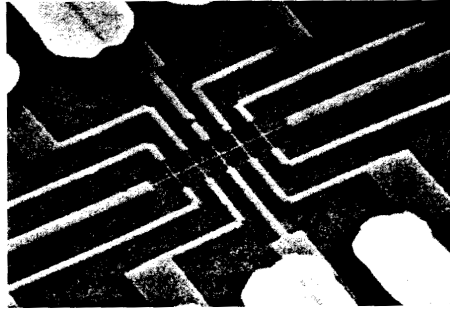


Figure 1.4: Scanning electron microphotographs of nanostructures in GaAs-AlGaAs heterostructures. Taken from M. L. Roukes *et al.*, Phys. Rev. Lett. **59**, 3011 (1987).

mass approximation. A good approximation for the confining potential is a triangular one,

$$U(z) = \begin{cases} \infty & \text{at } z < 0; \\ Fz & \text{at } z > 0. \end{cases}$$

Then one can write the Schrödinger equation for the wave function $\chi(z)$ as

$$\frac{\partial^2 \chi}{\partial z^2} + \frac{2m}{\hbar^2} (E - Fz) \chi = 0. \quad (1.1)$$

Instead z we introduce a dimensionless variable

$$\zeta = \left(z - \frac{E}{F} \right) \left(\frac{2mF}{\hbar^2} \right)^{1/3}.$$

The quantity

$$\ell_F = \left(\frac{2mF}{\hbar^2} \right)^{-1/3}$$

plays the role of characteristic localization length in z direction. Then Eq. (1.1) acquires the form

$$\chi'' - \zeta \chi = 0$$

which should be solved with the boundary conditions of finiteness at infinity and zero at $z = 0$. Such a solution has the form

$$\chi(\zeta) = A \text{Ai}(\zeta).$$

Here $\text{Ai}(\zeta)$ is the *Airy function* defined as

$$\text{Ai}(\zeta) = \frac{1}{\sqrt{\pi}} \int_0^\infty \cos(u^3/3 + u\zeta) du.$$

For large positive ζ it decays exponentially,

$$\text{Ai}(\zeta) \approx \frac{1}{2\zeta^{1/4}} e^{-(2/3)\zeta^{3/2}},$$

while for large negative ζ it is oscillatory,

$$\text{Ai}(\zeta) \approx \frac{1}{|\zeta|^{1/4}} \sin\left(\frac{2}{3}|\zeta|^{3/2} + \frac{\pi}{4}\right).$$

The energy spectrum E is defined by the roots ζ_n of the equation

$$\text{Ai}(\zeta) = 0, \quad \rightarrow \quad E_n = -E_0\zeta_n.$$

Here

$$E_0 = \left(\frac{\hbar^2 F^2}{2m}\right)^{1/3}.$$

We have $\zeta_1 \approx -2.337$, $\zeta_2 \approx -4.088$. The normalization constants A_n for each level are defined as

$$A_n^{-1} = \int_0^\infty dz |\chi_n(z)|^2.$$

Normalized electron densities $A_n |\chi_n(z)|^2$ are shown in Fig. 1.5. Each level creates a subband for the in-plane motion, the energy being

$$E_{n,\mathbf{k}} = E_n + E(\mathbf{k}) = E_n + \frac{\hbar^2 k^2}{2m}.$$

Note that the effective mass m is considerably smaller than the mass of a free electron.

Density of States

The density of states $g(\epsilon)$ is defined as number of states per the energy interval ϵ , $\epsilon + d\epsilon$. It is clear that

$$g(\epsilon) = \sum_{\alpha} \delta(\epsilon - \epsilon_{\alpha})$$

where α is the set of quantum numbers characterizing the states. In the present case it includes the subband quantum number n , spin quantum number σ , valley quantum number

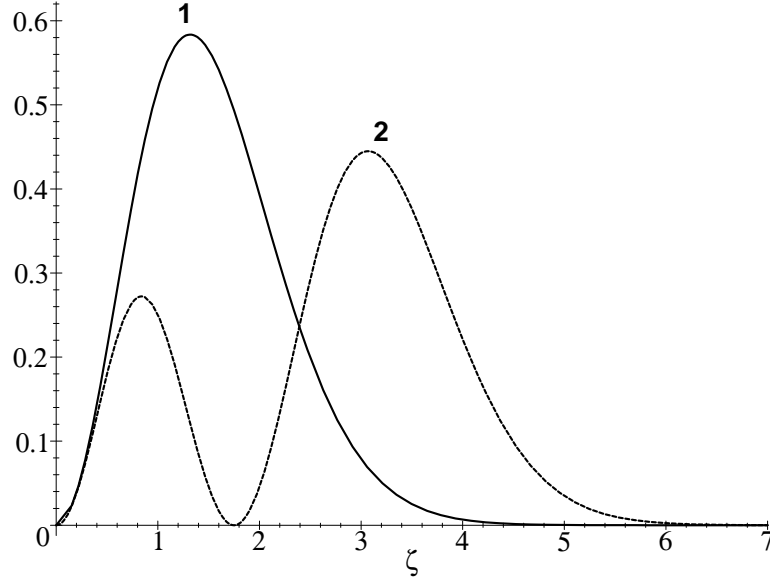


Figure 1.5: Normalized electron densities $A_n |\chi_n(z/\ell_F)|^2$ for the first (1) and second (2) subbands in a triangle potential with the slope F , $\ell_F = (\hbar^2/2mF)^{1/3}$.

v (for n -type materials), and in-plane quasimomentum \mathbf{k} . If the spectrum is degenerate with respect to spin and valleys one can define the spin degeneracy ν_s and valley degeneracy ν_v to get

$$g(\epsilon) = \frac{\nu_s \nu_v}{(2\pi)^d} \sum_n \int d^d k \delta(\epsilon - E_{n,\mathbf{k}}) .$$

Here we calculate the number on states per unit volume, d being the dimension of the space. For 2D case we obtain easily

$$g(\epsilon) = \frac{\nu_s \nu_v m}{2\pi \hbar^2} \sum_n \Theta(\epsilon - E_n) .$$

Within a given subband it appears energy-independent. Since there can exist several subbands in the confining potential (see Fig. 1.6, inset), the total density of states can be represented as a set of steps, as shown in Fig. 1.6. At low temperature ($kT \ll E_F$) all the states are filled up to the Fermi level. Because of energy-independent density of states the sheet electron density is linear in the Fermi energy,

$$n_s = \mathcal{N} \frac{\nu_s \nu_v m E_F}{2\pi \hbar^2} + \text{const}$$

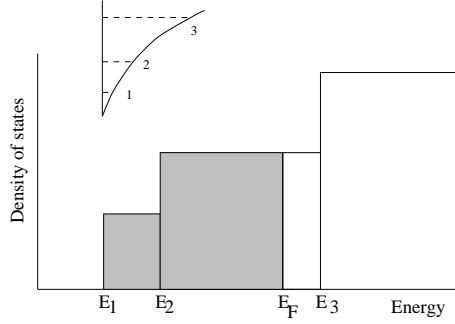


Figure 1.6: Density of states for a quasi-2D system.

while the Fermi momentum in each subband can be determined as

$$k_{Fn} = \frac{1}{\hbar} \sqrt{2m(E_F - E_n)}.$$

Here \mathcal{N} is the number of transverse modes having the edges E_n below the Fermi energy. The situation is more complicated if the gas is confined into a narrow channel, say, along y -axis. In a similar way, the in-plane wave function can be decoupled as a product

$$\psi(\mathbf{r}) = \eta(y) \frac{1}{N} e^{ik_x x},$$

where N is a proper normalization factor, the energy being

$$E_{n,s,k} = E_n + E_s(k_x) = E_n + E_s + \frac{\hbar^2 k_x^2}{2m}.$$

Here $E_{ns} \equiv E_n + E_s$ characterizes the energy level in the potential confined in both (z and y) directions. For square-box confinement the terms are

$$E_s = \frac{(s\pi\hbar)^2}{2mW^2},$$

where W is the channel width, while for the parabolic confinement $U(y) = (1/2)m\omega_0^2 y^2$ (typical for split-gate structures)

$$E_s = (s - 1/2)\hbar\omega_0.$$

It is conventional to introduce partial densities of states for the states with $k_x > 0$ and $k_x < 0$, g^\pm , respectively. We have,

$$g_s^+(\epsilon) = \frac{\nu_s \nu_v}{2\pi} \left(\frac{dE_s(k_x)}{dk_x} \right)^{-1} = \frac{\nu_s \nu_v \sqrt{m}}{2^{3/2} \pi \hbar} \frac{1}{\sqrt{\epsilon - E_{ns}}}. \quad (1.2)$$

The total density of states is

$$g^+(\epsilon) = \frac{\nu_s \nu_v \sqrt{m}}{2^{3/2} \pi \hbar} \sum_{ns} \frac{\Theta(\epsilon - E_{ns})}{\sqrt{\epsilon - E_{ns}}}. \quad (1.3)$$

The energy dependence of the density of states for the case of parabolic confinement is shown in Fig. 1.7.

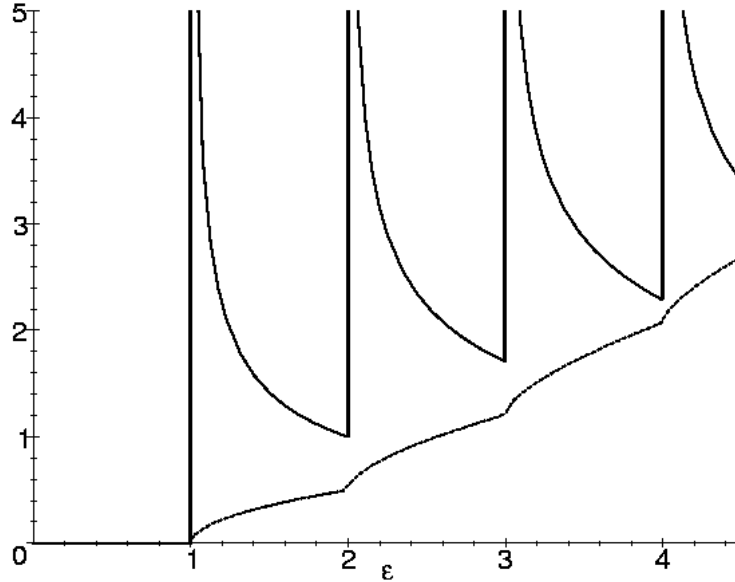


Figure 1.7: Density of states for a quasi-1D system (solid line) and the number of states (dashed lines).

Motion in a perpendicular magnetic field

2DEG in a perpendicular magnetic field gives an example of 0-dimensional electronic system. Indeed, according to the classical theory the Hamilton's function of a charged particle in an external electromagnetic field is

$$\mathcal{H} = \frac{1}{2m} \left(\mathbf{p} - \frac{e}{c} \mathbf{A} \right)^2 + e\phi,$$

where ϕ is the scalar and \mathbf{A} is the vector potential of the field, and \mathbf{p} is the generalized momentum of the particle. According to the rules of quantum mechanics, one should replace the canonical momentum \mathbf{p} by the operator

$$\mathbf{p} \rightarrow \hat{\mathbf{p}} = -i\hbar\nabla$$

and add also an extra spin term $-\boldsymbol{\mu}\mathbf{H}$ where $\boldsymbol{\mu} = \mu_B \hat{\mathbf{s}}/s$. Here $\mu_B = e/2mc$ is the *Bohr magneton* while $\hat{\mathbf{s}}$ is the spin operator. Generally, interaction with periodic potential of the crystalline lattice leads to renormalization of the spin splitting $\mu_B \rightarrow \mu^= g_f \mu_B$ where g_f is called the spectroscopic spin splitting factor.

Finally we get,

$$\begin{aligned} \mathcal{H} &= \frac{1}{2m} \left(\hat{\mathbf{p}} - \frac{e}{c} \mathbf{A} \right)^2 - \boldsymbol{\mu}\mathbf{H} + e\phi \\ &= \frac{\mathbf{p}^2}{2m} - \frac{e}{2mc} (\mathbf{A} \cdot \mathbf{p} + \mathbf{p} \cdot \mathbf{A}) + \frac{e^2 \mathbf{A}^2}{mc^2} - \frac{\mu}{s} \hat{\mathbf{s}} \cdot \mathbf{H} + e\phi. \end{aligned}$$

Since

$$\hat{\mathbf{p}} \cdot \mathbf{A} - \mathbf{A} \cdot \hat{\mathbf{p}} = -i\hbar \operatorname{div} \mathbf{A},$$

those operator commute if $\operatorname{div} \mathbf{A} = 0$. It holds in a uniform field with

$$\mathbf{A} = \frac{1}{2} \mathbf{H} \times \mathbf{r}.$$

The wave function in a magnetic field is not uniquely defined: it is defined only within the *gauge transform*

$$\mathbf{A} \rightarrow \mathbf{A} + \nabla f, \quad \phi \rightarrow \phi - \frac{1}{c} \frac{\partial f}{\partial t},$$

where f is an arbitrary function of coordinates and time. Under such a transform only the phase of wave function is changed by the quantity $ef/\hbar c$ that does not affect the observable quantities.

In classical mechanics, the generalized momentum of the particle is related to its velocity by the Hamilton equations,

$$m\mathbf{v} = \mathbf{p} - e\mathbf{A}/c.$$

According to the quantum mechanics we arrive at a similar expression. However different components of velocity do not commute, the commutation rules being

$$\begin{aligned} \{\hat{v}_x, \hat{v}_y\} &= i(e\hbar/m^2c)H_z, \\ \{\hat{v}_y, \hat{v}_z\} &= i(e\hbar/m^2c)H_x, \\ \{\hat{v}_z, \hat{v}_x\} &= i(e\hbar/m^2c)H_y. \end{aligned}$$

That means that the particle cannot simultaneously have definite velocities in all three directions.

Let us determine the energy levels in a 3-dimensional system embedded into a uniform magnetic field with a vector potential

$$A_x = -Hy, \quad A_y = A_z = 0.$$

The Hamiltonian then becomes

$$\mathcal{H} = \frac{1}{2m} \left(\hat{p}_x + \frac{eHy}{c} \right)^2 + \frac{\hat{p}_y^2}{2m} + \frac{\hat{p}_z^2}{2m} - \frac{\mu}{s} \hat{s}_z H.$$

First, the operator \hat{s}_z commutes with the Hamiltonian. Thus z -component of spin is conserved and can be replaced by its eigenvalue σ . Thus one can analyze the Schrödinger equation for an ordinary coordinate function,

$$\frac{1}{2m} \left[\left(\hat{p}_x + \frac{eH}{c} y \right)^2 + \hat{p}_y^2 + \hat{p}_z^2 \right] \psi - \frac{\mu}{s} \sigma H \psi = E \psi.$$

It is naturally to search for solution in the form

$$\psi = e^{i(p_x x + p_z z)/\hbar} \phi(y).$$

The eigenvalues p_x and p_z take all values from $-\infty$ to ∞ . Since $A_z = 0$ we get

$$p_z = mv_z.$$

Thus the motion along magnetic field in 3D system is not quantized. For a motion in the xy -plane we have the following Schrödinger equation,

$$\phi'' + \frac{2m}{\hbar^2} \left[\left(E + \frac{\mu\sigma}{s}H - \frac{p_z^2}{2m} \right) - \frac{1}{2}m\omega_c^2(y - y_0)^2 \right] \phi = 0. \quad (1.4)$$

Here

$$y_0 = -cp_x/eH = -a_H^2 k_x, \quad a_H = (c\hbar/eH)^{1/2}, \quad \omega_c = |e|H/mc. \quad (1.5)$$

Since this equation is the same as the Schrödinger equation for a harmonic oscillator, we obtain

$$E = (n + 1/2)\hbar\omega_c - (\mu\sigma/s)H + p_z^2/2m, \quad n = 0, 1, \dots \quad (1.6)$$

The first term gives discrete levels which corresponds to the finite motion in the xy -plane, they are called *Landau levels*. For an electron, $\mu/s = -|e|\hbar/mc$, and the energy spectrum reads as

$$E = \left(n + \frac{1}{2} + \sigma \right) \hbar\omega_c + \frac{p_z^2}{2m}. \quad (1.7)$$

The eigenfunctions $\phi_n(y)$ are

$$\phi_n(y) = \frac{1}{\pi^{1/4} a_H^{1/2} \sqrt{2^n n!}} \exp \left[-\frac{(y - y_0)^2}{2a_H^2} \right] H_n \left[\frac{y - y_0}{a_H} \right]. \quad (1.8)$$

Here H_n is the Hermite polynomial.

In classical mechanics the motion in a magnetic field in xy -plane takes place in a circle about a fixed center. Here the conserved quantity y_0 corresponds to y coordinate of the center of the circle. It is easy to see that the combination

$$x_0 = cp_y/eH + x$$

is also conserved, it commutes with the Hamiltonian. The quantity x_0 corresponds to a classical x coordinate of the circle center. However, the operators \hat{y}_0 and \hat{x}_0 do not commute. That means that the coordinates x_0 and y_0 cannot take definite values simultaneously.¹

One can ask: why the coordinates x and y are not equivalent? The reason is that the wave functions (1.8) correspond to the energy independent of k_y . Consequently, any function of the type

$$\sum_{k_x} C(k_x) \psi_{N, k_x, k_z}$$

¹ In a classical mechanics, the radius of the circle is $r_c = cmv_t/eH = v_t/\omega_c$. Here v_t is the tangential component of the velocity. Thus we have,

$$y = y_0 + r_c(v_x/v_t), \quad x = x_0 - r_c(v_y/v_t).$$

corresponds to the same energy and one can chose convenient linear combinations to get correct asymptotic behavior.

To calculate the density of states in a magnetic field first we should count the number of the values k_y corresponding to the energy ε_α (the so-called *degeneracy factor*). As usual, we apply cyclic boundary conditions along y and z -axes and get

$$k_x = \frac{2\pi}{L_x}n_y, \quad k_z = \frac{2\pi}{L_z}n_z.$$

At the same time, we assume that the solution exists only in the region

$$0 < y_0 < L_y.$$

So, the degeneracy factor is

$$\frac{L_x}{2\pi}|k_x|^{\max} = \frac{L_x}{2\pi a_H^2}y_0^{\max} = \frac{L_y L_x}{2\pi a_H^2}. \quad (1.9)$$

This is very important relation which shows that one can imagine Landau states as cells with the area a_H^2 . We will come back to this property later.

Now it is easy to calculate number of states in a 3D system treating the k_z variable as for the usual 1D motion

$$\frac{2|k_z|L_z}{2\pi} = \frac{2\sqrt{2m}L_z}{2\pi\hbar} \sqrt{\varepsilon - \hbar\omega_c(N + 1/2)}$$

for each state with a given N . Finally, the total number of states per volume for a given spin is

$$Z_s(\varepsilon) = \sum_N Z_{sN}(\varepsilon) = \frac{2\sqrt{2m}}{(2\pi)^2 \hbar a_H^2} \sum_N \sqrt{\varepsilon - \hbar\omega_c(N + 1/2)}$$

where one has to sum over all the values of N with non-negative $\varepsilon - \hbar\omega_c(N + 1/2)$. The total number of sates is $Z(\varepsilon) = 2Z_s(\varepsilon)$. To get DOS one should to differentiate this equation with respect to ε . The result is

$$g_s(\varepsilon) = \frac{dZ(\varepsilon)}{d\varepsilon} = \frac{\sqrt{2m}}{(2\pi)^2 \hbar a_H^2} \sum_N \frac{\Theta[\varepsilon - \hbar\omega_c(N + 1/2)]}{\sqrt{\varepsilon - \hbar\omega_c(N + 1/2)}}.$$

Here

$$\Theta(x) = \begin{cases} 1 & \text{for } x > 0; \\ 1/2 & \text{for } x = 0; \\ 0 & \text{for } x < 0 \end{cases}$$

is the Heaviside step function. To take the spin into account one should add the spin splitting $\pm\mu_B g_f H$ to the energy levels. If we ignore the spin splitting we can assume spin degeneracy and multiply all the formulas by the factor 2. We take it into account automatically using $g(\varepsilon) = 2g_s(\varepsilon)$.

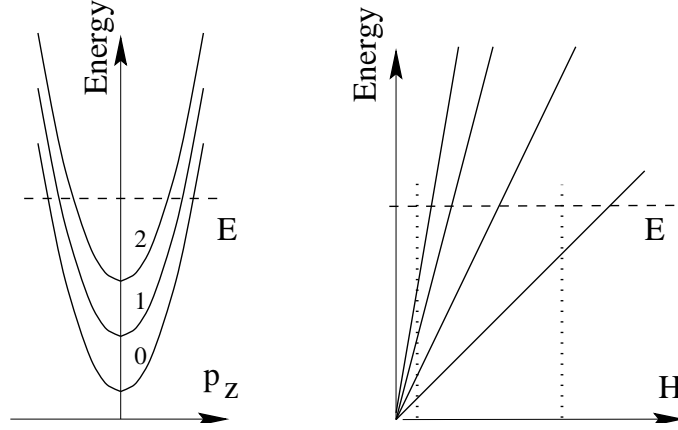


Figure 1.8: Landau levels as functions of p_z (left panel) and of H (right panel). The Fermi level is assumed to be fixed by external conditions.

The behavior of the density of states could be interpreted qualitatively in the following way. The Landau levels as functions of magnetic field for a given value of p_z are shown in Fig. 1.8. As a function of magnetic field, they form the so-called *Landau fan*. The Fermi level is also shown. At low magnetic fields its dependence on magnetic field is very weak. We see that if magnetic field is small many levels are filled. Let us start with some value of magnetic field and follow the upper filled level N . As the field increases, the slopes of the “fan” also increase and at a given threshold value H_N for which

$$\varepsilon_N(H_N) = \epsilon_F.$$

As the field increases the electrons are transferred from the N -th Landau level to the other ones. Then, for the field H_{N-1} determined from the equation $\varepsilon_{N-1}(H_{N-1}) = \epsilon_F$ the $(N-1)$ becomes empty. We get

$$H_N \approx \frac{m_c c \epsilon_F}{e \hbar} \frac{1}{N}, \quad \text{so} \quad \Delta \left(\frac{1}{H} \right) \approx \frac{e \hbar}{m_c c \epsilon_F}.$$

Here m_c is the so-called cyclotron effective mass which in the case of isotropic spectrum is the same as the density-of-states effective mass. We observe that DOS in a given magnetic field oscillated with the increase in energy just similar to the case of quasi 1D systems. Here Landau sub-bands play the same role as the modes of transverse quantization for quantum channels.

For a 2DEG the motion along z -direction is quantized, and instead of $e^{ip_z z/\hbar}$ we have $\chi_s(z)$. This means that for each subband of spatial quantization we have a sharp Landau level, the density of states (per area) being

$$g(\epsilon) = \frac{\nu_v e H}{4\pi^2 \hbar^2 c} \sum_{n,s,\sigma} \delta(\epsilon - E_{n,s,\sigma}).$$

Thus the density of states has sharp maxima at the energy levels that is a feature of so-called 0-dimensional system. In real samples the peaks are smeared by disorder.

1.3 Degenerate and non-degenerate electron gas

At equilibrium the states are filled according to the Fermi function

$$f_0(\epsilon) = \frac{1}{\exp[(\epsilon - \mu)/kT] + 1},$$

where μ is the chemical potential while k is the Boltzmann constant. The chemical potential is determined by the normalization to the total number of electrons as

$$n = \int_0^\infty g(\epsilon) f_0(\epsilon) d\epsilon$$

where n is the *electron density*. At zero temperature the chemical potential is called *the Fermi energy*, ϵ_F . The graph of the Fermi function and its energy derivative is given in Fig. 1.9

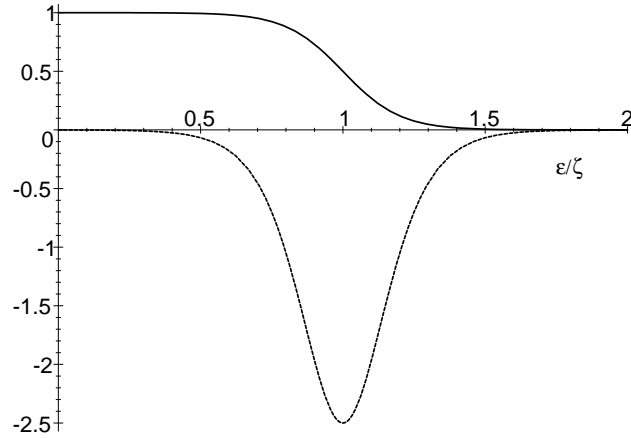


Figure 1.9: The Fermi distribution (solid line) and its energy derivative multiplied by kT (dashed line) for $\zeta/kT = 10$.

Since at $T = 0$

$$f_0(\epsilon) \approx \Theta(\epsilon - \zeta),$$

the Fermi energy is given by the equation

$$n = \int_0^{\epsilon_F} g(\epsilon) d\epsilon. \quad (1.10)$$

The limiting case $T = 0$ is actually means the the inequality $kT \ll \epsilon_F$ is met. In the opposite limiting case, $kT \gg \epsilon_F$, we get

$$f_0(\epsilon) \approx e^{(\zeta - \epsilon)/kT}, \quad n = e^{\zeta/kT} \int_0^\infty g(\epsilon) e^{-\epsilon/kT} d\epsilon.$$

Thus,

$$f_0(\epsilon) = A(T) e^{-\epsilon/kT}, \quad \frac{1}{A(T)} = \frac{1}{n} \int_0^\infty g(\epsilon) e^{-\epsilon/kT} d\epsilon. \quad (1.11)$$

This distribution is called the *Boltzmann* one.

1.4 Relevant length scales

One can discriminate between several important length scales in low-dimensional systems. They are shown in the Table 1.1.

1 mm	Mean free path in the quantum Hall regime
100 μm	Mean free path/Phase relaxation length in high-mobility semiconductor at $T < 4$ K
10 μm	
1 μm	Commercial semiconductor devices (1990)
100 nm	
10 nm	de Broglie wave length in semiconductors. Mean free path in polycrystalline metallic films
1 nm	
	de Broglie wave length in metals Distance between atoms
1 \AA	

Table 1.1: A few relevant length scales. Note that $1 \mu\text{m} = 10^{-6} \text{ m} = 10^{-4} \text{ cm}$; $1 \text{ nm} = 10^{-9} \text{ m} = 10 \text{ \AA}$.

The above mentioned scales have the following physical meaning:

De Broglie wave length, λ . This length is defined as

$$\lambda = \frac{2\pi\hbar}{p} = \frac{2\pi}{k}$$

where p (k) is the typical electron momentum (wave vector). For Fermi gas the characteristic momentum is just the Fermi momentum. For the case of a single filled band in 2DEG,

$$\lambda = 2\pi/k_F = \sqrt{2\pi/n_s}$$

where n_s is the sheet density. For the Boltzmann gas, $p \approx \sqrt{2mkT}$, and

$$\lambda = \frac{2\pi\hbar}{\sqrt{2mkT}}.$$

Mean free path, ℓ . This is a characteristic length between the collisions with impurities or phonons. It is defined as

$$\ell = v\tau_{\text{tr}}$$

where v is the typical velocity while τ_{tr} is the so-called *transport relaxation time*. It is defined as

$$\frac{1}{\tau_{\text{tr}}} \propto \int d\theta \sin\theta W(\theta) (1 - \cos\theta)$$

where θ is the scattering angle while $W(\theta)$ is the scattering probability. Usually the transport is characterized by the *mobility*

$$u = \frac{e\tau_{\text{tr}}}{m}.$$

The physical meaning of mobility is that a typical electron drift velocity acquired in an external electric field E is given by the relation

$$v_d = uE.$$

Phase-relaxation length, L_φ . This is a specially quantum mechanical relaxation length which has no analogs in classical physics. Namely, classical motion can be described as evolution of the *probability* to find a particle at a given point at a given time. However, in quantum mechanics the state is characterized by the *wave function* which has a *phase*. The phase is important in the so-called interference phenomena, where the electron wave functions having different pre-history are collected at the same point. If the phases of the waves are not destroyed, a specific quantum interference phenomena can be observed and important. The phase-relaxation time, τ_φ , describes relaxation of the phase memory.

It is clear that scattering against any static spin-independent potential cannot lead to the phase relaxation. Indeed, in any stationary potential the equations of motion are *time-reversible*. The only processes which can be responsible for phase relaxation are the ones which broke the symmetry with respect to time-reversal. Among them are inelastic scattering by phonons, electron-electron collisions, spin-flip processes, etc. An important feature of such processes is that an electron suffers many elastic collisions during a typical time τ_φ . Since it moves *diffusively* a proper way to estimate the relevant length L_φ is as follows:

$$L_\varphi = \sqrt{D\tau_\varphi},$$

where $D = (1/d)v\ell$ is the diffusion constant (d is the dimensionality of the electron gas).

Thermal dephasing length, L_T . The above mentioned relaxation process is relevant to the interference of the wave functions belonging to a single-electron state. However, interference can be also important for the interaction of *two electrons* having close

energies. Indeed, if the energy difference between the electrons is $\approx kT$ they travel almost coherently during the time \hbar/kT . Thus the characteristic length of coherent propagation is estimated as

$$L_T = \sqrt{\hbar D/kT}.$$

Comparing mean free path ℓ with characteristic dimensions of the system, L , one can discriminate between *diffusive*, $\ell \ll L$ and *ballistic*, $\ell \geq L$, transport. Such a classification appears incomplete in the situation where different dimensions of the sample are substantially different. The situation is illustrated in Fig. 1.10 for the case where the length L of the sample is much larger than its width, W . If phase coherence is taken into account, the

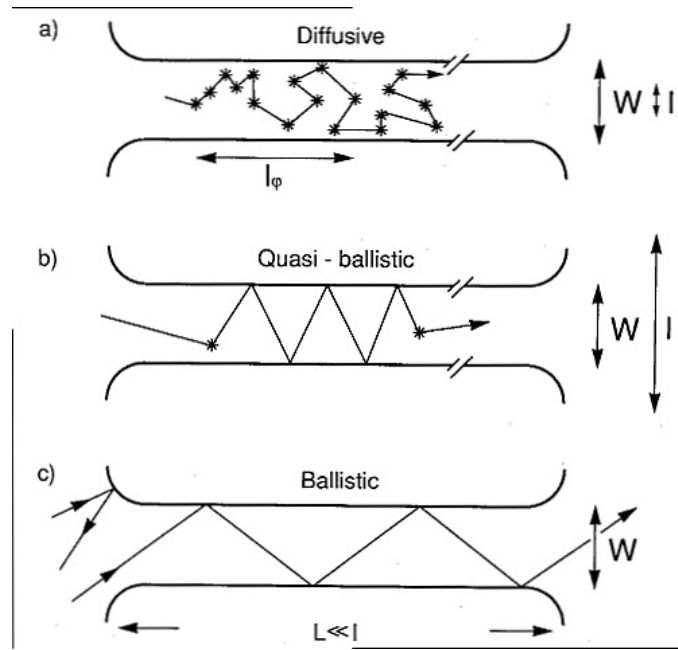


Figure 1.10: Electron trajectories for the diffusive ($\ell < W, L$), quasi-ballistic ($W < \ell < L$) and ballistic ($\ell > W, L$) transport regimes. From [11].

scales L_φ and L_T become important, and the situation appears more rich and interesting. Mesoscopic conductors are usually fabricated by patterning a planar conductor that has one very small dimension to start with. Although some of the pioneering experiments in this field were performed using metallic conductors, most of the recent work has been based on the gallium arsenide (GaAs)–aluminum gallium arsenide (AlGaAs) material system. Some important parameters for such systems are shown in Fig. 1.11.

		GaAs(100)	Si (100)	UNITS
Effective Mass	m	0.067	0.19	$m_e = 9.1 \times 10^{-28} \text{ g}$
Spin Degeneracy	g_s	2	2	
Valley Degeneracy	g_v	1	2	
Dielectric Constant	ϵ	13.1	11.9	$\epsilon_0 = 8.9 \times 10^{-12} \text{ F m}^{-1}$
Density of States Electronic Sheet	$\rho(E) = g_s g_v (m/2\pi\hbar^2)$	0.28	1.59	$10^{11} \text{ cm}^{-2} \text{ meV}^{-1}$
Density ^a	n_s	4	1-10	10^{11} cm^{-2}
Fermi Wave Vector	$k_F = (4\pi n_s / g_s g_v)^{1/2}$	1.58	0.56-1.77	10^6 cm^{-1}
Fermi Velocity	$v_F = \hbar k_F / m$	2.7	0.34-1.1	10^7 cm/s
Fermi Energy	$E_F = (\hbar k_F)^2 / 2m$	14	0.63-6.3	meV
Electron Mobility ^a	μ_e	$10^4 - 10^6$	10^4	$\text{cm}^2/\text{V} \cdot \text{s}$
Scattering Time	$\tau = m\mu_e/e$	0.38-38	1.1	ps
Diffusion Constant	$D = v_F^2 \tau / 2$	140-14000	6.4-64	cm^2/s
Resistivity	$\rho = (n_s e \mu_e)^{-1}$	1.6-0.016	6.3-0.63	k Ω
Fermi Wavelength	$\lambda_F = 2\pi/k_F$	40	112-35	nm
Mean Free Path	$l = v_F \tau$	$10^2 - 10^4$	37-118	nm
Phase Coherence Length ^b	$l_\phi = (D\tau_\phi)^{1/2}$	200-...	40-400	$\text{nm}(T/\text{K})^{-1/2}$
Thermal Length	$l_T = (\hbar D/k_B T)^{1/2}$	330-3300	70-220	$\text{nm}(T/\text{K})^{-1/2}$
Cyclotron Radius	$l_{\text{cycl}} = \hbar k_F / eB$	100	37-116	$\text{nm}(B/\text{T})^{-1}$
Magnetic Length	$l_m = (\hbar/eB)^{1/2}$	26	26	$\text{nm}(B/\text{T})^{-1/2}$
	$k_F l$	15.8-1580	2.1-21	
	$\omega_c \tau$	1-100	1	(B/T)
	$E_F/\hbar\omega_c$	7.9	1-10	(B/T) ⁻¹

Figure 1.11: Electronic properties of the 2DEG in GaAs-AlGaAs and Si inversion layers. From [10].

Chapter 2

Diffusive transport

2.1 Classical transport in diffusive regime

Boltzmann equation

According to classical physics, one can specify the coordinate \mathbf{r} and the momentum \mathbf{p} of the particle. Thus one can calculate the non-equilibrium distribution function, $f_{\mathbf{p}}(\mathbf{r}, t)$, the current density being

$$\mathbf{j}(\mathbf{r}, t) = e \int (d\mathbf{p}) \mathbf{v} f_{\mathbf{p}}(\mathbf{r}, t).$$

Here we denote $(d\mathbf{p}) \equiv d^d p / (2\pi\hbar)^d$. The distribution function is defined by the Boltzmann equation

$$\begin{aligned} \frac{df_{\mathbf{p}}(\mathbf{r}, t)}{dt} &\equiv \frac{\partial f}{\partial t} + \frac{\partial f}{\partial \mathbf{r}} \frac{d\mathbf{r}}{dt} + \frac{\partial f}{\partial \mathbf{p}} \frac{d\mathbf{p}}{dt} + I_{\text{coll}} \\ &= \frac{\partial f}{\partial t} + \mathbf{v} \frac{\partial f}{\partial \mathbf{r}} + \mathbf{F} \frac{\partial f}{\partial \mathbf{p}} + I_{\text{coll}} \\ &= 0 \end{aligned} \tag{2.1}$$

Here

$$\mathbf{F} = e \left(\mathbf{E} + \frac{1}{c} [\mathbf{v} \times \mathbf{H}] \right)$$

is the force acting upon the electrons, $\mathbf{v} \equiv \partial \epsilon_{\mathbf{p}} / \partial \mathbf{p}$ is the (group) electron velocity, while I_{coll} is the *collision operator*. It expresses the changes in the state due to quantum collisions and can be expressed through the transition probability W_{if} between the initial state (i) and the final state (f),

$$I_{\text{coll}}(f_{\alpha}) = \sum_{\alpha'} [W_{\alpha\alpha'} f_{\alpha} (1 - f_{\alpha'}) - W_{\alpha'\alpha} f_{\alpha'} (1 - f_{\alpha})]. \tag{2.2}$$

Here α denotes the electronic state (in our case $\alpha \equiv \{\mathbf{p}, s\}$).

In a stationary situation and in the absence of external fields the solution of the Boltzmann equation is the Fermi function. Substituting it into the collision operator we obtain a very important relation between the probabilities of the direct and reverse processes,

$$W_{\alpha\alpha'}e^{-\epsilon_{\alpha'}/kT} = W_{\alpha'\alpha}e^{-\epsilon_{\alpha}/kT}.$$

Drude formula

The simplest problem is to calculate the linear response to a small stationary electric field, \mathbf{E} . Since we assume E to be small, it is reasonable to search solution as

$$f_{\mathbf{p}}(\mathbf{r}) = f_0(\epsilon_{\mathbf{p}}) + f^{(1)}, \quad |f^{(1)}| \ll f_0.$$

Since $I_{\text{coll}}(f_0) = 0$ we come to the integral equation

$$I_{\text{coll}}(f^{(1)}) = -e\mathbf{E}\frac{\partial f_0(\epsilon_{\mathbf{p}})}{\partial \mathbf{p}} = e\mathbf{E}\mathbf{v}\left(-\frac{df_0(\epsilon_{\mathbf{p}})}{d\epsilon_{\mathbf{p}}}\right).$$

The linearized collision operator has the simplest form for elastic processes when $W_{\mathbf{p}\mathbf{p}'} = W_{\mathbf{p}'\mathbf{p}}$. Then,

$$I_{\text{coll}}(f^{(1)}) = \sum_{\mathbf{p}'} W_{\mathbf{p}\mathbf{p}'} \left(f_{\mathbf{p}}^{(1)} - f_{\mathbf{p}'}^{(1)} \right).$$

Since we are interested in the function odd in \mathbf{p} (to create a current) and it must be a scalar it is natural to assume that

$$f_{\mathbf{p}}^{(1)} \propto (\mathbf{p} \cdot \boldsymbol{\nu}), \quad \boldsymbol{\nu} \equiv \mathbf{E}/E.$$

Under such an assumption

$$I_{\text{coll}}(f^{(1)}) = \frac{f_{\mathbf{p}}^{(1)}}{\tau_{\text{tr}}}, \quad \frac{1}{\tau_{\text{tr}}} = \sum_{\mathbf{p}'} W_{\mathbf{p}\mathbf{p}'} \left(\frac{p_{\boldsymbol{\nu}} - p'_{\boldsymbol{\nu}}}{p_{\boldsymbol{\nu}}} \right).$$

The quantity τ_{tr} is called the transport relaxation time. If the material is isotropic then W is dependent only on the scattering angle θ between \mathbf{p} and \mathbf{p}' . From the simple geometrical construction shown in Fig. 2.1 we observe that

$$p'_{\boldsymbol{\nu}} = p' \cos \theta \cos \phi, \quad p_{\boldsymbol{\nu}} = p \cos \phi.$$

Consequently, we can express the relaxation time in the form

$$\frac{1}{\tau_{\text{tr}}} = g(\epsilon_{\mathbf{p}}) \frac{1}{2} \int_0^{\pi} d\theta \sin \theta (1 - \cos \theta) W(\theta). \quad (2.3)$$

Using the expression for the relaxation time we can write

$$f_{\mathbf{p}}^{(1)} = \tau_{\text{tr}} e(\mathbf{E} \cdot \mathbf{v}) \left(-\frac{df_0(\epsilon_{\mathbf{p}})}{d\epsilon_{\mathbf{p}}} \right) \rightarrow \mathbf{j} = e^2 \int (d\mathbf{p}) \mathbf{v}(\mathbf{E} \cdot \mathbf{v}) \tau_{\text{tr}}(\epsilon_{\mathbf{p}}) \left(-\frac{df_0(\epsilon_{\mathbf{p}})}{d\epsilon_{\mathbf{p}}} \right).$$

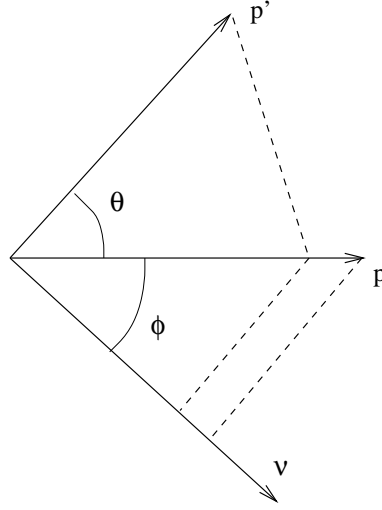


Figure 2.1: On the calculation of the transport relaxation time.

As a result, we arrive at the Ohm's law, $\mathbf{j} = \sigma \mathbf{E}$ with

$$\sigma = \int_0^\infty d\epsilon g(\epsilon) \langle v_{\mathbf{E}}^2 \tau_{\text{tr}} \rangle_\epsilon \left(-\frac{df_0(\epsilon)}{d\epsilon} \right). \quad (2.4)$$

Here $v_{\mathbf{E}}$ means the projection of the velocity on the direction of the electric field, while $\langle \dots \rangle_\epsilon$ means the average over the surface of a constant energy ϵ ,

$$\langle A(\mathbf{p}) \rangle_\epsilon \equiv \frac{\int (d\mathbf{p}) A(\mathbf{p}) \delta(\epsilon - \epsilon_{\mathbf{p}})}{\int (d\mathbf{p}) \delta(\epsilon - \epsilon_{\mathbf{p}})}.$$

The quantity

$$D = \langle v_{\mathbf{E}}^2 \tau_{\text{tr}} \rangle_\epsilon = \frac{1}{d} v^2 \tau_{\text{tr}} = \frac{1}{d} v \ell \quad (2.5)$$

has an explicit physical meaning. This is just the diffusion constant for the electrons with a given energy ϵ . Indeed, for low temperatures we get

$$\sigma = e^2 g(\epsilon_F) D(\epsilon_F). \quad (2.6)$$

On the other hand, the phenomenological expression for the current density in the presence of the density gradient reads as

$$\mathbf{j} = \sigma \mathbf{E} - eD \nabla n,$$

where D is the diffusion constant. In the equilibrium the current is zero and

$$eD \nabla n = eD g(\epsilon_F) \nabla \zeta = -\sigma \nabla \varphi.$$

At the same time, the electro-chemical potential $\zeta + \varphi/e$, must be constant and $\nabla \varphi = -e \nabla \zeta$. Substituting Eq. (2.6) we identify the quantity $D(\epsilon_F)$ with the diffusion constant. Eq. (2.6) is known as the Einstein relation.

2.2 Linear response in quantum mechanics

Let us find a linear response to the perturbation ¹

$$\mathcal{H}^{ex} = \lim_{\eta \rightarrow 0} \lambda e^{-i\omega t} \hat{A} e^{\eta t}. \quad (2.7)$$

According to time-dependent perturbation theory, the change in any quantity $\langle B \rangle$ in the Heisenberg representation can be written as

$$\begin{aligned} \delta \langle B(t) \rangle &= \frac{i}{\hbar} \int_{-\infty}^t dt' \langle g | [\mathcal{H}_H^{ex}(t'), B_H(t')] | g \rangle \\ &= \frac{i}{\hbar} \int_{-\infty}^t dt' \sum_n \{ \langle g | \mathcal{H}_H^{ex} | n \rangle \langle n | B_H | g \rangle - \langle g | B_H | n \rangle \langle n | \mathcal{H}_H^{ex} | g \rangle \}. \end{aligned} \quad (2.8)$$

Here $|n\rangle$ means a complete set of eigenstates for the unperturbed Hamiltonian \mathcal{H} , g stands for the ground state, while subscript H stands for Heisenberg representation with respect to non-perturbed Hamiltonian, \mathcal{H} . Going to the Schrödinger representation as,

$$\langle g | A_H | n \rangle = e^{i\omega_{gn}t} \langle g | A | n \rangle \equiv e^{i\omega_{gn}t} A_{gn}, \quad \hbar\omega_{gn} \equiv E_g - E_n$$

we find that $\delta B(t) = \delta B_\omega e^{-i\omega t}$ with

$$\delta B_\omega = \lim_{\eta \rightarrow 0} \frac{\lambda}{\hbar} \sum_n \left\{ -\frac{\langle g | A | n \rangle \langle n | B | g \rangle}{\omega + \omega_{ng} + i\eta} + \frac{\langle g | B | n \rangle \langle n | A | g \rangle}{\omega - \omega_{ng} + i\eta} \right\}. \quad (2.9)$$

Defining linear response as $\delta B_\omega = \chi_{BA}(\omega)\lambda$ we find

$$\chi_{BA} = \lim_{\eta \rightarrow 0} \frac{1}{\hbar} \sum_n \left\{ -\frac{A_{gn} B_{ng}}{\omega + \omega_{ng} + i\eta} + \frac{B_{gn} A_{ng}}{\omega - \omega_{ng} + i\eta} \right\}. \quad (2.10)$$

Let us use this general formula for the response of a dipole moment density $e\mathbf{r}/\mathcal{V}$ in the direction β to the electric field \mathbf{E} directed in the direction α . Here \mathcal{V} is the volume of the sample. Since the perturbation Hamiltonian is $e\mathbf{E} \cdot \mathbf{r}$ we find

$$\chi_{\beta\alpha} = \frac{e^2}{\hbar\mathcal{V}} \lim_{\eta \rightarrow 0} \sum_n \left\{ -\frac{\mathbf{r}_{gn}^\alpha \mathbf{r}_{ng}^\beta}{\omega + \omega_{ng} + i\eta} + \frac{\mathbf{r}_{gn}^\beta \mathbf{r}_{ng}^\alpha}{\omega - \omega_{ng} + i\eta} \right\}. \quad (2.11)$$

Since the complex dielectric function is

$$1 + 4\pi\chi(\omega) = 1 + 4\pi i\sigma(\omega)/\omega$$

we obtain

$$\sigma_{\beta\alpha}(\omega) = i\omega \frac{e^2}{\mathcal{V}\hbar} \lim_{\eta \rightarrow 0} \sum_n \left\{ \frac{\mathbf{r}_{gn}^\alpha \mathbf{r}_{ng}^\beta}{\omega + \omega_{ng} + i\eta} - \frac{\mathbf{r}_{gn}^\beta \mathbf{r}_{ng}^\alpha}{\omega - \omega_{ng} + i\eta} \right\}. \quad (2.12)$$

¹ Here I partly follow the derivation given in Ref. [4].

In particular,

$$\Re \sigma_{\beta\alpha}(\omega) = \frac{e^2 \omega \pi}{\mathcal{V} \hbar} \sum_n [\delta(\omega + \omega_{ng}) \mathbf{r}_{gn}^\alpha \mathbf{r}_{ng}^\beta - \delta(\omega - \omega_{ng}) \mathbf{r}_{gn}^\beta \mathbf{r}_{ng}^\alpha] \quad (2.13)$$

Now we can generalize the presentation for finite temperature doing inverse Fourier transform. Since $\delta(\omega) = \int dt \exp(-i\omega t)$ we can write

$$\begin{aligned} \Re \sigma_{\beta\alpha}(\omega) &= \frac{\omega e^2}{2\mathcal{V} \hbar} \int_{-\infty}^{\infty} dt \langle g | [\mathbf{r}^\alpha(0), \mathbf{r}^\beta(t)] | g \rangle e^{-i\omega t} \\ &\rightarrow \frac{\omega e^2}{2\mathcal{V} \hbar} \int_{-\infty}^{\infty} dt \langle [\mathbf{r}^\alpha(0), \mathbf{r}^\beta(t)] \rangle_T e^{-i\omega t}. \end{aligned} \quad (2.14)$$

Here we have replaced ground state average by the thermal one to allow for finite temperatures.

Fluctuation-dissipation theorem

Our derivation allows to obtain an important *fluctuation-dissipation theorem* relating fluctuations in the system with the dissipation. Let us characterize fluctuations by the factor

$$S_{\beta\alpha}(\omega) = \int_{-\infty}^{\infty} dt \langle \mathbf{r}^\alpha(0) \mathbf{r}^\beta(t) \rangle_T e^{i\omega t} = \sum_{g,n} \mathbf{r}_{gn}^\alpha \mathbf{r}_{ng}^\beta \delta(\omega - \omega_{ng}) P_g$$

where P_g is the thermal weight of the state g . Using equilibrium thermal weights² for Fermi particles, $P_g = f_0(E_g)[1 - f_0(E_n)]$, where $f_0(E)$ is the equilibrium Fermi distribution, we obtain

$$\Re \sigma_{\beta\alpha}(\omega) = \frac{e^2 \omega \pi}{\mathcal{V} \hbar} S_{\beta\alpha}(\omega) [1 - e^{-\hbar\omega/kT}] \quad (2.15)$$

This theorem is often used in some other form which can be obtained using the relations between the operators $\mathbf{v} = \dot{\mathbf{r}}$. Assuming $\hbar\omega \ll kT$ we get

$$\Re \sigma_{xx}(\omega) = \frac{e^2}{2\mathcal{V} kT} \int_{-\infty}^{\infty} dt \langle v^x(0) v^x(t) \rangle_T e^{i\omega t} \quad (2.16)$$

Writing $\langle v^x(0) v^x(t) \rangle_T$ as a Fourier transform of velocity fluctuations, $S_v(\omega)$, we get

$$\frac{e^2 S_v(\omega)}{\mathcal{V}} = \frac{kT}{\pi} \Re \sigma(\omega)$$

which is just the famous Nyquist-Johnson relationship between the current noise spectrum and the conductivity.

²Here we actually assume the transport through the device to be *incoherent*.

At finite temperature using the expression for P_g we get

$$\frac{e^2 S_v(\omega)}{\mathcal{V}} = \frac{\hbar\omega}{\pi} \left(\frac{1}{2} + \frac{1}{e^{\beta\hbar\omega} - 1} \right) \Re \sigma(\omega) \quad (2.17)$$

Finally, since the contribution of an electron to the current is ev/L ,

$$S_I(\omega) = \frac{\hbar\omega}{2\pi} \coth \left(\frac{\hbar\omega}{2kT} \right) \Re G(\omega).$$

Here $G(\omega) \equiv \sigma\mathcal{A}/L$ is the *conductance* of the system (\mathcal{A} is the area, while L is its length).

Derivation of Drude formula

Now we can derive the Drude formula explicitly. Coming back to the expression (2.14) and introducing velocity operators we get

$$\Re \sigma_{\alpha\beta}(\omega) = \frac{e^2}{2} \int dE g(E) \frac{f_0(E) - f_0(E + \hbar\omega)}{\hbar\omega} \int_{-\infty}^{\infty} dt e^{-i\omega t} \langle v^\alpha(0) v^\beta(t) \rangle_E. \quad (2.18)$$

Here $g(E)$ is the density of states while subscript E means that the average is calculated over all the states with given energy E .

The quantity

$$D_{\alpha\beta}(E) = \frac{1}{2} \int_{-\infty}^{\infty} dt e^{-i\omega t} \langle v^\alpha(0) v^\beta(t) \rangle_E \quad (2.19)$$

is nothing else than *diffusion constant*. Indeed, assume that we have a small gradient in electron density, $n(x) = n_0 + cx$. Then the particle current is

$$\begin{aligned} j_x &= \lim_{\Delta t \rightarrow 0} \langle v_x(t=0) n[x(t = -\Delta t)] \rangle = \lim_{\Delta t \rightarrow 0} c \langle v_x(0) x(-\Delta t) \rangle \\ &= -c \lim_{\Delta t \rightarrow 0} \int_0^{\Delta t} dt \langle v_x(0) v_x(-t) \rangle. \end{aligned}$$

In this way we obtain the classical expression for diffusion constant. Finally, at $\hbar\omega \ll \mu$ we arrive at the formula

$$\Re \sigma_{\alpha\beta} = e^2 \int dE g(E) \left(-\frac{\partial f}{\partial E} \right) D_{\alpha\beta}(E).$$

Substituting

$$D_{\alpha\beta}(E) = \frac{\langle v_\alpha^2 \rangle}{2} \int_{-\infty}^{\infty} e^{-i\omega t - |t|/\tau_{\text{tr}}} dt = \frac{v^2}{d} \frac{\tau_{\text{tr}}}{1 + (\omega\tau_{\text{tr}})^2}$$

(where d is dimensionality of the electron motion) we finally arrive at the Drude formula.

2.3 Linear response in magnetic field. Shubnikov-de Haas effect

Transport coefficients depend both on the density of states (DOS) and on the scattering probability. The behavior of DOS in magnetic field was discussed in Chapter 1. We have seen that DOS oscillates because of the energy quantization. The scattering probability, in its term, is also dependent on the density of states, as well on the scattering matrix element. Consequently, it also oscillates in magnetic field, and it appears that the last contribution is the most important. The quantum oscillations of conductivity is called the *Shubnikov-de Haas effect*. Quantum oscillations of transport coefficients are widely used for investigation of the properties of metals and semiconductors.

Let us outline main principles of these effects. To take the electric field into account one should analyze the Schrödinger equation in crossed electric and magnetic field ($\mathbf{H} \parallel \mathbf{z}$, $\mathbf{E} \parallel \mathbf{x}$)

$$-\frac{\hbar^2}{2m} \frac{\partial^2 \psi}{\partial x^2} + \frac{1}{2m} \left(\frac{\hbar}{i} \frac{\partial}{\partial y} + \frac{e}{c} Hx \right)^2 \psi - \frac{\hbar^2}{2m} \frac{\partial^2 \psi}{\partial z^2} + (eEx - \varepsilon) \psi = 0.$$

Here we use the gauge $\mathbf{A} = (0, Hx, 0)$. In this case we can search the solution as

$$\varphi(x) \exp(ik_y y + ik_z z).$$

The equation for φ has the form

$$-\frac{\hbar^2}{2m} \frac{d^2 \varphi}{dx^2} + \left[\frac{1}{2m} \left(\frac{eH}{c} \right)^2 x^2 + \left(\frac{\hbar e H}{mc} k_y + eE \right) x + \frac{\hbar^2 (k_y^2 + k_z^2)}{2m} - \varepsilon \right] \varphi = 0.$$

The result can be expressed just in the same way as for the case $E = 0$ with the additional terms

$$\varepsilon_\nu^E = \varepsilon_N + \frac{\hbar^2 k_z^2}{2m} + \delta\varepsilon, \quad \delta\varepsilon = -a_H^2 e E k_y - \frac{mc^2}{2} \left(\frac{E}{H} \right)^2$$

for the energy and

$$x_0^E = x_0 + \delta x_0, \quad x_0 = -a_H^2 k_y, \quad \delta x_0 = -\frac{e E a_H^2}{\hbar \omega_c}.$$

for the oscillator center x_0 .

Now we introduce the following concept. Assume that the electron in the state ν is situated at the point x_0^E . The electric current is

$$j_x = -e \sum_{\nu, \nu'}^I \{ f_0(\varepsilon_\nu^E) [1 - f_0(\varepsilon_{\nu'}^E)] W_{\nu\nu'}^E - f_0(\varepsilon_{\nu'}^E) [1 - f_0(\varepsilon_\nu^E)] W_{\nu'\nu}^E \}.$$

The prime over the sum means that the state ν has $x_0^E < 0$, while the state ν' has $x_0^E > 0$. Then we expand the expression up to the linear in E term and get

$$\sigma_{xx} = e^2 \sum_{\nu, \nu'} \left(-\frac{\partial f_0(\varepsilon_\nu)}{\partial \varepsilon_\nu} \right) \frac{(x_0 - x_0')^2}{2} W_{\nu\nu'}.$$

This formula has an explicit physical meaning. Indeed, the quantity

$$\frac{(x_0 - x_0')^2}{2} W_{\nu\nu'}$$

is just the contribution of the states ν, ν' to the 2D diffusion coefficient in the plane (x, y) . Thus we come to the old formula

$$\sigma = e^2 \int d\varepsilon g(\varepsilon) D(\varepsilon) \left(-\frac{\partial f_0}{\partial \varepsilon} \right)$$

where both $g(\varepsilon)$ and $D(\varepsilon)$ should be calculated with the help of quantum mechanics:

$$g(\varepsilon) = \sum_{\nu} \delta(\varepsilon - \varepsilon_\nu), \quad D(\varepsilon) = \frac{1}{g(\varepsilon)} \sum_{\nu, \nu'} \delta(\varepsilon - \varepsilon_\nu) \frac{(x_0 - x_0')^2}{2} W_{\nu\nu'}.$$

One can see that the result is strongly dependent on the scattering mechanism and oscillates in the case of the Fermi statistics.

2.4 Weak localization

Consider noninteracting electrons having $p_F \ell \gg \hbar$ and passing between the points A and B through scattering media. The probability is

$$W = \left| \sum_i A_i \right|^2 = \sum_i |A_i|^2 + \sum_{i \neq j} A_i A_j^*. \quad (2.20)$$

Here A_i is the propagation *amplitude* along the path i . The first item – classical probability, the second one – *interference* term.

For the majority of the trajectories the phase gain,

$$\Delta\varphi = \hbar^{-1} \int_A^B \mathbf{p} \cdot d\mathbf{l} \gg 1, \quad (2.21)$$

and interference term vanishes. Special case - trajectories with self-crossings. For these parts, if we change the direction of propagation, $\mathbf{p} \rightarrow -\mathbf{p}$, $d\mathbf{l} \rightarrow -d\mathbf{l}$, the phase gains are the same, and

$$|A_1 + A_2|^2 = |A_1|^2 + |A_2|^2 + 2A_1 A_2^* = 4|A_1|^2.$$

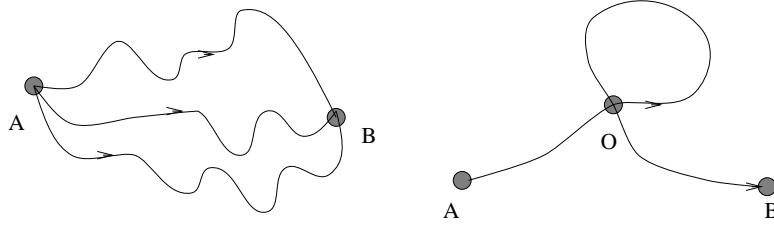


Figure 2.2: Feynman paths responsible for weak localization

Thus quantum effects double the result. As a result, the total scattering probability at the scatterer at the site O *increases*. As a result, conductance *decreases* - predecessor of localization.

Probability of self-crossing. The cross-section of the site O is in fact de Broglie electron wave length, $\lambda \sim \hbar/p_F$. Moving diffusively, it covers the distance $\sqrt{x_i^2} \sim \sqrt{Dt}$, covering the volume $(Dt)^{d/2}b^{3-d}$. Here d is the dimensionality of the system, while b is the “thickness” of the sample. To experience interference, the electron must enter the interference volume, the probability being

$$\frac{v\lambda^2 dt}{(Dt)^{d/2}b^{3-d}}.$$

Thus the relative correction is

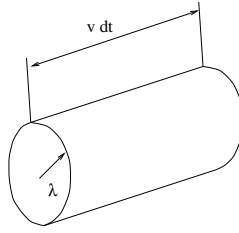


Figure 2.3: On the calculation of the probability of self-crossing.

$$\frac{\Delta\sigma}{\sigma} \sim - \int_{\tau}^{\tau_{\varphi}} \frac{v\lambda^2 dt}{(Dt)^{d/2}b^{3-d}} \quad (2.22)$$

The upper limit is the so-called *phase-breaking time*, τ_{φ} . Physical meaning – it is the time during which the electron remains coherent. For example, any inelastic or spin-flip scattering gives rise to phase breaking.

3d case

In a 3d case,

$$\frac{\Delta\sigma}{\sigma} \sim - \frac{v\lambda^2}{D^{3/2}} \left(\frac{1}{\sqrt{\tau}} - \frac{1}{\sqrt{\tau_{\varphi}}} \right) \sim - \left(\frac{\lambda}{\ell} \right)^2 + \frac{\lambda^2}{\ell L_{\varphi}}. \quad (2.23)$$

Here we have used the notations

$$D \sim v\ell, \quad \tau \sim \ell/v, \quad L_\varphi = \sqrt{D\tau_\varphi}. \quad (2.24)$$

On the other hand, one can rewrite the Drude formula as

$$\sigma \sim \frac{n_e e^2 \tau}{m} \sim \frac{n_e e^2 \ell}{p_F} \sim \frac{e^2 p_F^2 \ell}{\hbar^3}.$$

In this way, one obtains

$$\Delta\sigma \sim -\frac{e^2}{\hbar\ell} + \frac{e^2}{\hbar L_\varphi}. \quad (2.25)$$

Important point: The second item, though small, is of the most interest. Indeed, it is temperature-dependent because of inelastic scattering. There are several important contributions:

- Electron-electron scattering:

$$\tau_\varphi \sim \hbar\epsilon_F/T^2.$$

Thus

$$\frac{\sigma(T) - \sigma(0)}{\sigma(0)} \sim \left(\frac{\lambda}{\ell}\right)^{3/2} \left(\frac{T}{\epsilon_F}\right).$$

It is interesting that at low temperatures this quantum correction can exceed the classical temperature-dependent contribution of e - e -scattering which is $\propto T^2$. It is also important to note that the above estimate is obtained for a clean system. It should be revised for disordered systems where electron-electron interaction appears more important (see later).

- Electron-phonon-interaction. In this case,³

$$\tau_\varphi \sim \frac{\hbar^2 \omega_D^2}{T^3},$$

and

$$\frac{\sigma(T) - \sigma(0)}{\sigma(0)} \sim \left(\frac{\lambda}{\ell}\right)^{3/2} \left(\frac{T}{\epsilon_F}\right)^{1/2} \left(\frac{T}{\hbar\omega_D}\right).$$

Thus there is a cross-over in the temperature dependencies. To obtain the dominating contribution one has to compare τ_φ^{-1} . Consequently, at low temperatures e - e -interaction is more important than the e - ph one, the crossover temperature being

$$T_0 \sim (\hbar\omega_D^2/\epsilon_F) \sim 1 \text{ K}.$$

³Under some limitations.

Low-dimensional case

If the thickness b of the sample is small ⁴, then the interference volume $\lambda^2 v dt$ has to be related to $(Dt)^{d/2} b^{3-d}$. For a film $d = 2$, while for a quantum wire $d = 1$. As a result,

$$\frac{\Delta\sigma}{\sigma} \sim -\frac{v\lambda^2}{D} \begin{cases} b^{-1} \ln(\tau_\varphi/\tau), & d = 2 \\ b^{-2} L_\varphi, & d = 1 \end{cases} . \quad (2.26)$$

It is convenient to introduce *conductance* as

$$G \equiv \sigma b^{3-d} .$$

We have,

$$\Delta G \sim -\frac{e^2}{\hbar} \begin{cases} \ln(L_\varphi/\ell), & d = 2 \\ L_\varphi, & d = 1 \end{cases} . \quad (2.27)$$

Important note: In low-dimensional systems the main mechanism of the phase breaking is different. It is so-called low-momentum-transfer electron-electron interaction which we do not discuss in detail

2.5 Weak localization in external magnetic field

In a magnetic field one has to replace $\mathbf{p} \rightarrow \mathbf{p} + (e/c)\mathbf{A}$ (remember - we denote electronic charge as $-e$). Thus the product AA^* acquires an additional phase

$$\Delta\varphi_H = \frac{2e}{c\hbar} \oint \mathbf{A} d\mathbf{l} = \frac{2e}{c\hbar} \oint \text{curl } \mathbf{A} d\mathbf{S} = 4\pi \frac{\Phi}{\Phi_0} \quad (2.28)$$

where Φ is the magnetic flux through the trajectory while $\Phi_0 = 2\pi\hbar c/e$ is the so-called *magnetic flux quantum*. Note that it is 2 times greater than the quantity used in the theory of superconductivity for the flux quantum.

Thus magnetic field behaves as an additional *dephasing mechanism*, it “switches off” the localization correction, increases the conductance. In other words, we observe *negative magnetoresistance* which is very unusual.

To make estimates, introduce the typical dephasing time, t_H , to get $\Delta\varphi_H \sim 2\pi$ for the trajectory with $L \sim \sqrt{Dt_H}$. In this way,

$$t_H \sim \Phi_0/(HD) \sim l_H^2/D, \quad l_H = \sqrt{c\hbar/eH} . \quad (2.29)$$

The role of magnetic field is important at

$$t_H \leq \tau_\varphi \quad \rightarrow \quad H \geq H_0 \sim \Phi_0/(D\tau_\varphi) \approx \hbar c/L_\varphi^2 .$$

⁴The general form of the criterion depends on the relationship between the film thickness, b , and the elastic mean free path ℓ . The result presented is correct at $b \ll \ell$. At $L \gg b \gg \ell$ one can replace the lower limit τ of the integral (2.22) by $\tau_b = b^2/D$.

Note that at $H \approx H_0$

$$\omega_c \tau \sim \hbar / (\epsilon_F \tau \varphi) \ll 1$$

that means the absence of classical magnetoresistance. *Quantum effects manifest themselves in extremely weak magnetic fields.*

To get quantitative estimates one has to think more carefully about the geometry of diffusive walks. Let consider the channel of 2DEG with width W . The estimates given above are valid for $\ell, L_\varphi \ll W$, exact formulas could be found, e. g. in Ref. [10]. Usually H_0 is very weak, at $L_\varphi = 1 \mu\text{m}$ $H_0 \approx 1 \text{ mT}$. The suppression of weak localization is complete at $H \geq \hbar/e\ell^2$, still under conditions of classically weak magnetic field, $\omega_c \tau \ll 1$.

The situation is a bit different at $W \leq L_\varphi$, this case can be mentioned as one-dimensional for the problem in question, see Fig. 2.4. Then a typical enclosed area is

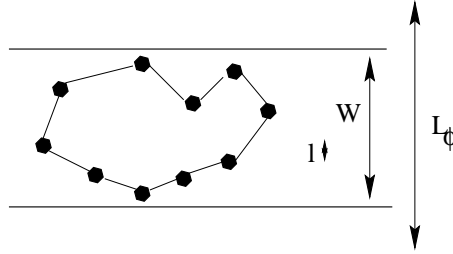


Figure 2.4: On quasi 1D weak localization.

$S \sim WL_\varphi$, and the unit phase shift takes place at

$$t_H \sim L_H^4 / DW^2, \quad \rightarrow \quad H_0 \sim \hbar c / eWL_\varphi.$$

Some experimental results on magnetoresistance of wide and narrow channels are shown in Fig. 2.5.

There are also several specific effects in the interference corrections:

- anisotropy of the effect with respect of the direction of magnetic field (in low-dimensional cases);
- spin-flip scattering acts as a dephasing time;
- oscillations of the longitudinal conductance of a hollow cylinder as a function of magnetic flux. The reason – typical size of the trajectories.

2.6 Aharonov-Bohm effect

Magnetoconductance corrections are usually aperiodic in magnetic field because the interfering paths includes a continuous range of magnetic flux values. A *ring* geometry, in contrast, encloses a continuous well-defined flux Φ and thus imposes a fundamental periodicity,

$$G(\Phi) = G(\Phi + n\Phi_0), \quad \Phi_0 = 2\pi\hbar c/e.$$

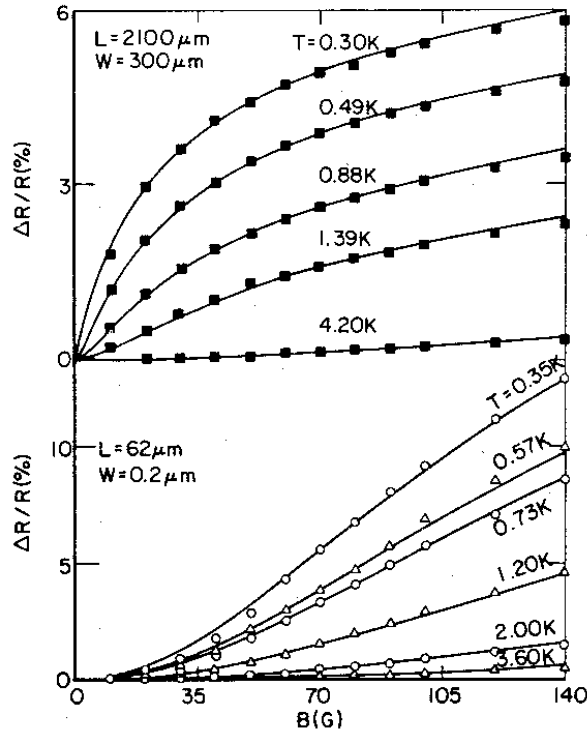


Figure 2.5: Experimental results on magnetoresistance due to 2D weak localization (upper panel) and due to 1D weak localization in a narrow channel (lower panel) at different temperatures. Solid curves are fits based on theoretical results. From K. K. Choi *et al.*, Phys. Rev. B. **36**, 7751 (1987).

Such a periodicity is a consequence of gauge invariance, as in the originally thought experiment by Aharonov and Bohm (1959). The fundamental periodicity

$$\Delta B = \frac{2\pi\hbar c}{eS}$$

comes from interference of the trajectories which make one half revolution along the ring, see Fig. 2.6. There is an important difference between hc/e and $hc/2e$ oscillations. The first ones are sample-dependent and have random phases. So if the sample has many rings in series or in parallel, then the effect is mostly averaged out. Contrary, the second oscillations originate from time-reversed trajectories. The proper contribution leads to a minimum conductance at $H = 0$, thus the oscillations have the same phase. This is why $hc/2e$ -oscillations survive in long hollow cylinders. Their origin is a periodic modulation of the weak localization effect due to coherent backscattering. Aharonov-Bohm oscillations in long hollow cylinders, Fig. 2.7, were predicted by Altshuler, Aronov and Spivak [20] and observed experimentally by Sharvin and Sharvin [21]. A rather simple estimate for the magnitude of those oscillations can be found in the paper by Khmelnitskii [22].

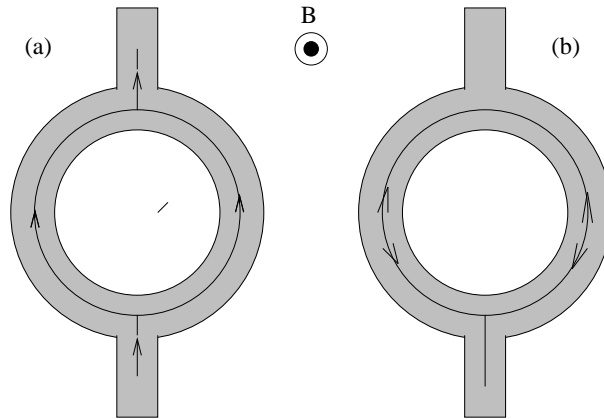


Figure 2.6: Illustration of Aharonov-Bohm effect in a ring geometry. (a) Trajectories responsible for hc/e periodicity, (b) trajectories of the pair of time-reversed states leading to $hc/2e$ -periodicity.

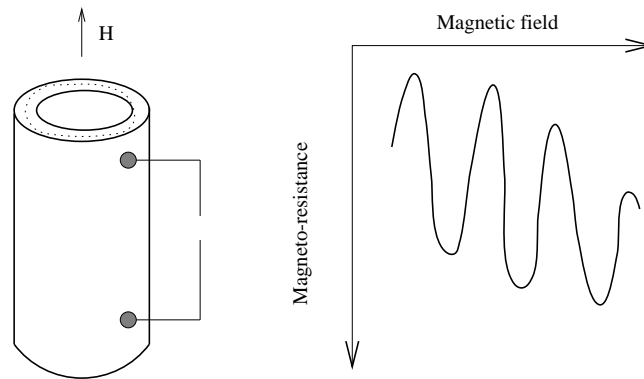
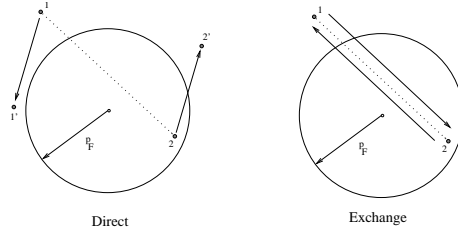


Figure 2.7: On the Aharonov-Bohm oscillations in a long hollow cylinder.

2.7 Electron-electron interaction in a weakly disordered regime

Let us discuss the effect of the $e - e$ interaction on the density of states. Let us concentrate on the exchange interaction, shown in a right panel of Fig. 2.8

$$\Delta\epsilon = - \int_{|\mathbf{p}-\hbar\mathbf{k}|\leq p_F} g(\mathbf{k}) \frac{d^3k}{(2\pi\hbar)^3}. \quad (2.30)$$

Figure 2.8: On the calculation of $e - e$ interaction.

Here $g(\mathbf{k})$ is the Fourier component of the interaction potential, the sign “-” is due to exchange character of the interaction. In the absence of screening $g(k) = 4\pi e^2/k^2$, and

$$\begin{aligned}
 \Delta\epsilon &= -4\pi e^2 \int_{|\mathbf{p}-\hbar\mathbf{k}|\leq p_F} k^{-2} \frac{d^3k}{(2\pi)^3} \\
 &= -4\pi e^2 \hbar^2 \int_{p' < p_F} \frac{1}{|\mathbf{p}-\mathbf{p}'|^2} \frac{d^3p'}{(2\pi\hbar)^3} \\
 &= -\frac{e^2}{\pi\hbar} \left(p_F - \frac{p^2 - p_F^2}{2p} \ln \frac{p + p_F}{p - p_F} \right). \tag{2.31}
 \end{aligned}$$

To obtain this formula it is convenient to use spherical coordinates - $(dp') = 2\pi p'^2 dp' d(\cos\phi)$ and auxiliary integral

$$\int_{-1}^1 \frac{d(\cos\phi)}{p^2 + p'^2 - 2pp' \cos\phi} = \frac{1}{pp'} \ln \left[\frac{p + p'}{p - p'} \right]. \tag{2.32}$$

At small $p - p_F$ it is convenient to introduce $\xi = v(p - p_F) \ll \epsilon_F$ to get (omitting the irrelevant constant)

$$\Delta\epsilon = -(e^2/\pi\hbar v)\xi \ln(2p_F v/\xi). \tag{2.33}$$

Screening can be allowed for by the replacement $k^{-2} \rightarrow (k^2 + \kappa^2)^{-1}$ that replaces $p \pm p'$ in the argument of the logarithm in Eq. (2.32) by $\sqrt{(p \pm p')^2 + (\hbar\kappa)^2}$. As a result,

$$\Delta\epsilon = -(e^2/\pi\hbar v)\xi \ln(2p_F/\hbar\kappa) \quad \text{at} \quad \hbar\kappa \ll p_F. \tag{2.34}$$

This is a simple-minded estimate because it ignores the interference of the states. Indeed, if the two states differ in the energy by $|\xi|$ the coherence time is $\hbar/|\xi|$. If the electron returns back for this time, then the effective interaction constant increases by

$$\alpha_\xi = \int_\tau^{\hbar/|\xi|} \frac{v\lambda^2 dt}{(Dt)^{d/2} b^{3-d}}. \tag{2.35}$$

Thus

$$e_{eff}^e = e^2(1 + \alpha_\xi).$$

In a similar way

$$\frac{\Delta v}{v} = \frac{\Delta g}{g} = \frac{e^2}{\hbar v} \alpha_\xi.$$

Here g is the density of electronic states. Consequently, since $\sigma \propto \nu$, we arrive to a specific correction to conductance. Comparing this correction with the interference one we conclude that interaction dominates in 3d case, has the same order in 2d case and not important in 1d case. Another important feature is that the interaction effects are limited by the coherence time $\hbar/|\xi| \approx \tau_T = \hbar/k_B T$ rather than by τ_φ . Usually, $\tau_\varphi \gg \tau_T$. Consequently, the interference effects can be destroyed by weaker magnetic fields than the interaction ones (important for separation of the effects).

2.8 Few words about Anderson localization

If we come back to the interference correction for $d = 2, 1$ we observe that it *increases* with τ_φ , or at $T \rightarrow 0$. Thus the corrections becomes not small. We can also prepare the samples with different values of the mean free path ℓ .

What happens if the corrections are not small? Anderson (1958) suggested localization of electronic states at $T = 0$. This suggestion has been later proved for an infinite 1d system, as well as for an infinite wire of finite thickness (Thouless, 1977). Later it has been shown that

$$G \propto \exp(-L/L_{\text{loc}})$$

where $L_{\text{loc}} \sim \ell$ in the first case and $(bp_F/\hbar)^2 \ell$ for the second one (exponential localization). It seems that such a law is also the case for a metallic *film* (rigorous proof is absent).

Very simple-minded explanation - over-barrier reflection + *interference* of incoming and reflected waves. Because of the interference the condition $T = 0$ is crucial (no phase breaking). This explanation is good for one-dimensional case.

A little bit more scientific discussion. Consider interference corrections to the conductance at $T \rightarrow 0$. In this case one has to replace

$$\tau_\varphi \rightarrow L^2/D, \quad L_\varphi \rightarrow L.$$

One can conclude that in 3d case the relative correction is $\sim (\hbar/p_F \ell)^2 \ll 1$ (usually). However, at $d = 1, 2$ it *increases* with the size.

At what size $\Delta\sigma \approx \sigma$?

$$L_c = \begin{cases} \ell \exp(p_F^2 b \ell / \hbar^2), & d = 2 \\ \ell (p_F \ell / \hbar)^2, & d = 1 \end{cases}. \quad (2.36)$$

We can conclude that in 3d case localization takes place at $p_F \ell \sim \hbar$, while in 1d and 2d case it takes place at any concentration of impurities.

Scaling hypothesis – According to the “gang of 4” (Abrahams, Anderson, Licciardello and Ramakrishnan)

$$G(qL) = f[q, G(L)]. \quad (2.37)$$

Assuming $q = 1 + \alpha$, $\alpha \ll 1$, we can iterate this equation in α :

$$\begin{aligned} G(L) &= f[1, G(L)]; \\ \alpha L G'(L) &= \alpha (\partial f / \partial q)_{q=1}. \end{aligned} \quad (2.38)$$

Denoting

$$G^{-1}(\partial f/\partial q)_{q=1} \equiv \beta(G)$$

we re-write the scaling assumption through the Gell-Mann & Low function, $\beta(G)$:

$$\partial \ln G / \partial \ln L = \beta(G).$$

At very large G we can expect that the usual theory is valid:

$$G = \sigma \begin{cases} S_{\perp}^2/L = L, & d = 3; \\ bL_{\perp}/L = b, & d = 2; \\ b^2/L, & d = 1 \end{cases} \quad (2.39)$$

Thus, in the zero approximation,

$$\beta(G) = d - 2.$$

Then we can use the weak localization approximation to find next corrections. One can get

$$\beta(G) \approx d - 2 - \alpha_d G_0/G, \quad (2.40)$$

where

$$G_0 = e^2/(\pi^2 \hbar), \quad \alpha_d \sim 1.$$

Indeed, for $d = 3$

$$\ln G = \ln[(\sigma + \Delta\sigma)L] \approx \ln \sigma L + (\Delta\sigma)/\sigma \approx \ln[(\sigma + \Delta\sigma|_{L=\infty})L] + \hbar^2/(p_F^2 \ell L).$$

Thus

$$\beta(G) = \frac{\partial \ln G}{\partial \ln L} = 1 - \frac{\hbar^2}{p_F^2 \ell L} = 1 - \frac{\hbar^2 \sigma}{p_F^2 \ell G} = 1 - \alpha_3 \frac{G_0}{G}.$$

At small G one can suggest exponential localization:

$$G \sim G_0 \exp(-L/L_c) \quad \rightarrow \quad \beta(G) \sim \ln(G/G_0).$$

Thus we have the scenario shown in Fig. 2.9. Believing in such a scenario we get localization for 1d case ($\beta(G) < 0$ - conductance *increases* with the length). At $d = 3$ we have a fixed point at G_c , which is *unstable* (β changes sign). Under the simplest assumptions

$$\begin{aligned} \beta(G) &\approx \gamma(\ln G - \ln G_c) \approx \gamma(G/G_c - 1), \\ G &= G^{(0)} \quad \text{at } L = L_0 \text{ (initial condition)} \end{aligned}$$

($G^{(0)}$ is close to G_c) we obtain

$$\frac{G}{G_c} \approx \left(\frac{G^{(0)}}{G_c} \right)^{(L/L_0)^\gamma}. \quad (2.41)$$

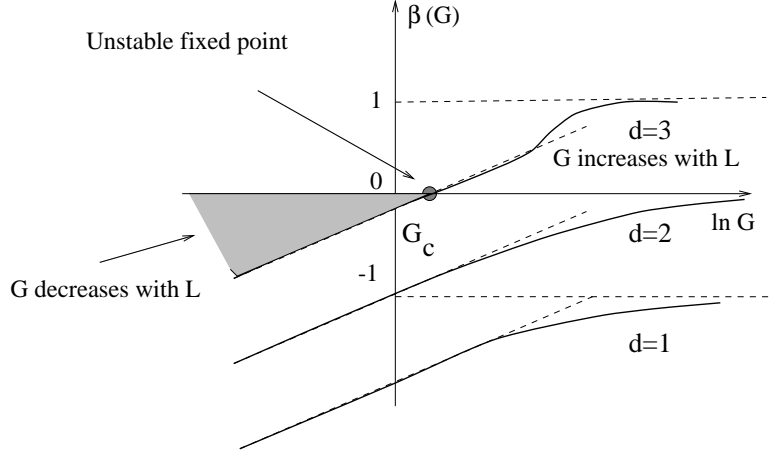


Figure 2.9: Flow curves for Anderson localization.

From Eq. (2.41) one can find important dependencies near the critical point. It is natural to choose $L_0 \approx \ell$ and to suggest that at this size

$$\sigma_0 \sim e^2 p_F^2 \ell / \hbar^3 \quad \rightarrow \quad G_0 = \sigma_0 L = (e^2 / \hbar) (p_F \ell / \hbar)^2.$$

Now we can assume that we can control some parameter (say, impurity content, x , which effects the mean free path ℓ), and that G_0 is regular in this parameter. Then, at small x $G^{(0)} = G_c(1 + x)$. At $L_0 = \ell$ we obtain

$$G = G_c(1 + x)^{(L/\ell)^\gamma} \approx G_c \exp[x(L/\ell)^\gamma].$$

Of course, such an assumption valid only at

$$x \ll 1, \quad L/\ell \gg 1.$$

Thus at $x < 0$ we obtain exponential localization with the characteristic length

$$L_{\text{loc}} \sim \ell |x|^{-1/\gamma}, \quad x < 0.$$

However, at $x > 0$ G grows with L . In a spirit of the concept of phase transitions we can treat the quantity $L_c = \ell x^{-1/\gamma}$ as a *correlation length*. At the scales of the order of L_c the properties of conducting and insulator phases are similar. The above law can be valid only in the vicinity of $G_0 \sim G_c$. Then we match the usual Ohm's law, $G = \sigma L$. Consequently, the conductivity can be estimated as

$$\sigma \sim \frac{G_0}{L_c} \sim \left(\frac{G_0}{\ell} \right) x^{1/\gamma}, \quad x > 0.$$

Thus, we predict *power law*. Experiments on the dielectric constant ($\kappa_0 \propto L_c^2$) support the value

$$\gamma = 0.6 \pm 0.1.$$

Don't forget that we discuss the case $T = 0$, and the conductance is supposed at zero frequency. The range of applicability is given by the inequalities

$$L_c \ll L_\varphi, L_\omega = \sqrt{D\omega}.$$

This is almost impossible to meet these conditions, so usually people *extrapolate* experimental curves to $T = 0$, $\omega = 0$. It is a very subtle point because, as it was shown, the conductance at $L \leq L_\varphi$ is not a *self-averaging* quantity with respect to an ensemble of samples. More precise, the fluctuations between the samples *cannot be described* by the Gaussian law, their distribution being much wider. Then,

- have all these scaling assumptions any sense?
- Why they reasonably agree with the experiment?

The answer is positive because both the scaling predictions and the experiment are valid as an extrapolation from the region $L \geq L_\varphi$.

As the temperature grows, fluctuations decrease and the conductance tends to the Ohm's law.

Role of $e - e$ interaction

Nobody can consider both disorder and interaction acting together. To get some understanding of the role of $e - e$ interaction let us consider a *clean* metallic conductor. Assume that under some external perturbation (say, pressure) the band overlap changes. In this way we control the Fermi level (number of electrons and holes). One can consider them as free ones as their kinetic energy $p_F^2/2m^*$ exceeds the potential energy $e^2/(\kappa_0\bar{r})$. In this way we come to the condition

$$\frac{e^2}{\kappa_0\hbar v} \leq 1.$$

Otherwise electrons and hole form complexes - Wannier-Mott excitons. This state is insulating because excitons are neutral. This is only one of possible scenario. In general, the problem is a front end of modern condensed matter physics.

Chapter 3

Ballistic transport

3.1 Landauer formula

We start this chapter by a description of a very powerful method in physics of small systems - so-called *Landauer approach*.

The main principle of this approach is the assumption that the system in question is coupled to large reservoirs where all inelastic processes take place. Consequently, the transport through the systems can be formulated as a quantum mechanical *scattering problem*. Thus one can reduce the non-equilibrium transport problem to a quantum mechanical one.

Another important assumption is that the system is connected to reservoirs by *ideal quantum wires* which behave as waveguides for the electron waves. We start our analysis from the discussion of the properties of an ideal quantum wire.

Ideal quantum wire

Consider 2 large reservoirs of electron gas reservoirs having the difference δn in the electron density and separated by a pure narrow channel. For small δn one can assume that there is a difference in a chemical potential, $\delta\mu = \delta n/g(\epsilon_F)$. In the following we shall use the Fermi level of non-biased system as the origin for the chemical potentials. So the difference between the chemical potential in α -th reservoir will be denoted as μ_α .

If the channel is long and uniform, then the total current carried by the state characterized by a transverse mode n and a given direction of spin which propagates without scattering is

$$J_n = e \int \frac{dk_z}{2\pi\hbar} \frac{\partial \varepsilon_n(k_z)}{\partial k_z} = \frac{2}{2\pi\hbar} \int_{\epsilon_F + \mu_\alpha}^{\epsilon_F + \mu_\beta} d\varepsilon \frac{\partial \varepsilon_n(k_z)/\partial k_z}{|\partial \varepsilon_n(k_z)/\partial k_z|} = \frac{2}{h} \delta\mu.$$

If we take into account electron spin and N transverse modes are open, then the conductance is given by the expression $G = \frac{2e^2}{h} N$.

We come to a very important conclusion: an *ideal* quantum wire has *finite* resistance $h/2e^2 N$ which is independent of the length of the wire.

As we have seen, even an ideal quantum wire has a finite resistance. That means a finite heat generation even in the absence of any inelastic processes inside the wire. Below we will discuss the physical picture of heat release by a current-carrying nanostructure (here we follow the considerations of Ref. [23]).

First of all let us specify what heat release is. It will be convenient to consider an isolated system. Therefore we will have in mind the following physical situation. There is a capacitor which is discharged through the conductor of interest. The product RC of the whole system, R and C being the resistance and capacitance respectively, is much bigger than any relaxation time characterizing the electron or phonon system of the conductor. This means that for all the practical purposes the conduction process can be looked upon as a stationary one. The total energy of the system, \mathcal{U} , is conserved, while its total entropy, $\hat{\mathcal{S}}$, is growing. The rate of heat generation is expressed through $T\partial\hat{\mathcal{S}}/\partial t$, where T is the temperature, i.e. through the applied voltage and characteristics of the nanostructure itself. This means that the result is independent of the assumption that the considered system is isolated, which is made only for the sake of derivation. This thermodynamically defined heat is generated in the classical reservoirs over the length having a physical meaning of the electron mean free path. That is the same mean free path that enters the Drude formula, which determines the conductivity of the reservoirs themselves, the amount of heat generated per second in both reservoirs being the same.

It is interesting to indicate that even purely elastic collisions can result in a heat generation although they of course cannot establish full equilibrium. This has a clear physical meaning. The amount of order in the electron distribution resulting in electric current can bring about mechanical work. For instance, one can let the current flow through a coil, and a magnetic rod can be drawn into the coil. In such a way the electrons transferring the current can execute a work on the rod. As a result of scattering, the amount of order in the electrons' distribution diminishes, and this means dissipation of mechanical energy into the heat. It has been shown that the heat release is symmetric in both reservoirs even if the scatterers in the system are asymmetric.

All the above considerations do not mean that the collisions that give the main contribution to the heat release, also establish *full equilibrium*. What equilibrium needs is inelastic collisions which transfer the energy of electrons taking part in charge transfer to other degrees of freedom, such as to other electrons and phonons. In particular, a *local equilibrium electron distribution* is established over the length scale determined by *electron-electron* interaction. Such a distribution can be characterized by a local electro-chemical potential and sometimes an electron temperature. The latter can in principle be measured by optical methods. On the other hand, the *equilibrium with respect to the lattice* is established at the scales of *electron-phonon* and *phonon-phonon* mean free paths. Only over those distances from the channel one can treat the results in terms of the true local temperature.

Resistance of a quantum resistor

Consider a system shown in Fig. 3.1 consisting of a barrier connected to reservoirs by ideal quantum wires. If there is some reflection only a part of the current is transmitted. In this

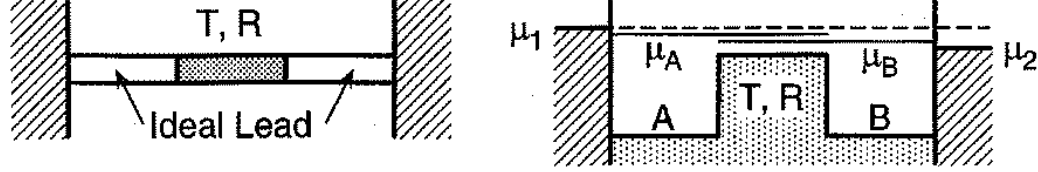


Figure 3.1: On the resistance of a quantum resistor.

case one can introduce the transmission probability of the mode n , T_n , to obtain (including spin degeneracy)

$$J = \frac{2}{h} \delta\mu \sum_{n=1}^N T_n.$$

As a result,

$$G = \frac{2e^2}{h} \sum_{n=1}^N T_n = \frac{2e^2}{h} \text{Tr } \mathbf{t} \mathbf{t}^\dagger. \quad (3.1)$$

Here \mathbf{t} is the matrix of *scattering amplitudes* while the expression is called *two-terminal* Landauer formula.

This very important and looking simple formula was confusing during a long period. Indeed, this is the conductance which is measured between two reservoirs. Having in mind that the resistance of the connecting ideal wires (per one conducting mode) is $h/2e^2$ we can ascribe to the scattering region the resistance

$$\frac{h}{2e^2} \left[\frac{1}{T} - 1 \right] = \frac{h}{2e^2} \frac{R}{T},$$

where R is the reflection coefficient. Consequently, in the original formulation the quantum resistance was described as

$$G = \frac{2e^2}{h} \sum_{n=1}^N \frac{T_n}{1 - T_n}. \quad (3.2)$$

However, the quantity which is usually measured is given by Eq. (3.1).

Now we derive the Landauer formula for finite-temperature and so-called multichannel case when the leads have several transverse modes. Consider ideal wires which lead to a general elastic scattering system. Let each lead has the cross section A and have N_\perp transverse channels characterized by wave vectors k_i so that,

$$E_i + \frac{\hbar^2 k_i^2}{2m} = E_F.$$

The incoming channels are fed from the electron baths with the same temperature and chemical potentials μ_1, μ_2, \dots . The outgoing channels are fed up to *thermal equilibrium population*. We shall assume that the particles are absorbed in the outgoing baths. The sources are assumed to be *incoherent*, the differences $\mu_1 - \mu_2$ are also assume small to yield linear transport. We introduce the scattering amplitudes t_{ij} for the transmission from j th incoming to i th outgoing channel. Reflection amplitudes r_{ij} are introduces in a similar way for reflection into the i th incoming channel. If we replace the incoming and outgoing channels, we denote the proper amplitudes by primes. In this way it is convenient to introduce $2N_{\perp} \times 2N_{\perp}$ scattering matrix as

$$S = \begin{pmatrix} r & t' \\ t & r' \end{pmatrix}.$$

From the current conservation we must require unitarity while from time reversal symmetry $S = \tilde{S}$. Thus we have also $SS^* = I$ where star stays for complex conjugation while tilde for transposition. In a magnetic field the Onsager relation requires $S(H) = \tilde{S}(-H)$.

It one defines the total transmission and reflection into i th channel as

$$T_i = \sum_j |t_{ij}|^2, \quad R_i = \sum_j |r_{ij}|^2.$$

then from unitarity condition we get

$$\sum_i T_i = \sum_i (1 - R_i).$$

Since the densities of states in each channel are 1D like, $g_i(E) = (\pi\hbar v_i)^{-1}$ we write the current through outgoing channels as

$$\begin{aligned} I &= \frac{e}{\pi\hbar} \sum_i \int dE [f_1(E)T_i(E) + f_2(E)R'(E) - f_2(E)] \\ &= \frac{(\mu_1 - \mu_2)e}{\pi\hbar} \int dE \left(-\frac{\partial f}{\partial E} \right) \sum_i T_i(E). \end{aligned}$$

Thus the conductance becomes

$$G = \frac{2e^2}{h} \int dE \left(-\frac{\partial f}{\partial E} \right) \text{Tr } \mathbf{t} \mathbf{t}^\dagger.$$

This is the *two-terminal* conductance measured between the *outside* reservoirs which includes contact resistances.

Multiterminal resistance

For simplicity we shall discuss the case of zero temperature. Let us introduce the total transmission probability from the bath α to the bath β ,

$$T_{\alpha \rightarrow \beta} = \sum_{n=1}^{N_\alpha} \sum_{m=1}^{N_\beta} |t_{\beta\alpha, mn}|^2.$$

Here N_i is the number of propagating modes in each lead connected to i th reservoir. Counting all the chemical potentials from the Fermi level, we see that the reservoir α injects the current $(2e/h)N_\alpha\mu_\alpha$ into the lead α . The fraction $T_{\alpha\rightarrow\beta}/N_\alpha$ is transmitted to the reservoir β while the fraction $T_{\alpha\rightarrow\alpha}/N_\alpha = R_\alpha/N_\alpha$ is reflected back into reservoir α . The net current I_α is given by the following set of equation,

$$\frac{h}{2e}I_\alpha + (N_\alpha - R_\alpha)\mu_\alpha - \sum_{\beta\neq\alpha} T_{\beta\rightarrow\alpha}\mu_\beta. \quad (3.3)$$

Introducing vectors \vec{I} and $\vec{\mu}$ with components I_α and μ_α , respectively, we can write

$$\vec{I} = \hat{G}\vec{\mu}, \quad (3.4)$$

where the conductance matrix \hat{G} is defined as

$$\begin{aligned} G_{\alpha\beta} &= \frac{2e^2}{h} [(N_\alpha - R_\alpha)\delta_{\alpha\beta} - T_{\beta\rightarrow\alpha}(1 - \delta_{\alpha\beta})] \\ &= \frac{2e^2}{h} [N_\alpha\delta_{\alpha\beta} - T_{\beta\rightarrow\alpha}]. \end{aligned} \quad (3.5)$$

Here we use the relation $T_{\alpha\rightarrow\alpha} = R_\alpha$. The sum of rows of this matrix is zero because of current conservation, the sum of the elements of each row also vanishes because if one changes all the chemical potentials by the same amount no current will be induced. Thus

$$N_\alpha - R_\alpha = \sum_{\beta\neq\alpha} T_{\beta\rightarrow\alpha} = \sum_{\beta\neq\alpha} T_{\alpha\rightarrow\beta}.$$

The equations (3.4) and (3.5) are called often the *Landauer-Büttiker formalism*. They

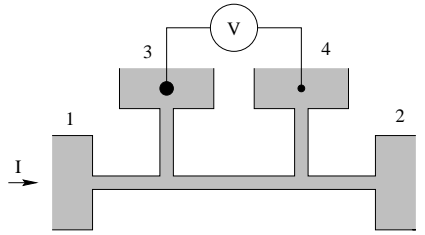


Figure 3.2: On the resistance of 4-terminal device.

allow find, e. g. 4-terminal resistance. Indeed, we can put $I_1 = -I_2 = I$, $I_3 = I_4 = 0$. Then $\vec{I} = I\vec{j}$ where

$$\vec{j} = I \begin{pmatrix} 1 \\ -1 \\ 0 \\ 0 \end{pmatrix}.$$

Thus

$$\mathcal{R}_{34} = \frac{\mu_4 - \mu_3}{I} = \left(\hat{G}^{-1}\vec{j} \right)_4 - \left(\hat{G}^{-1}\vec{j} \right)_3.$$

Having in mind the properties of the scattering amplitudes we have,

$$T_{\alpha \rightarrow \beta}(H) = T_{\beta \rightarrow \alpha}(-H)$$

that results in the *reciprocity relation*

$$\mathcal{R}_{\alpha\beta,\gamma\delta}(H) = \mathcal{R}_{\gamma\delta,\alpha\beta}(-H).$$

Here $\mathcal{R}_{\alpha\beta,\gamma\delta}$ stands for the resistance measured for voltage contacts γ, δ while the current passes through the contacts α, β . Note that this relation works even in the case when the concept of local conductivity is not applicable. What we only need is linear response and absence of inelastic scattering inside the device under consideration.

One can easily generalize the above expressions for the case of finite temperatures by replacement of the element of \hat{G} -matrix by their thermal averages,

$$\langle A \rangle_T = \frac{\int_0^\infty dE g(E) (\partial f_0 / \partial E) A(E)}{\int_0^\infty dE g(E) (\partial f_0 / \partial E)}.$$

3.2 Application of Landauer formula

Point ballistic contact

The most clean system is the so-called quantum point contact (QPC) - short and narrow constrictions in 2d electron gas. A sketch of QPC is shown in Fig. 3.3 The conductance of

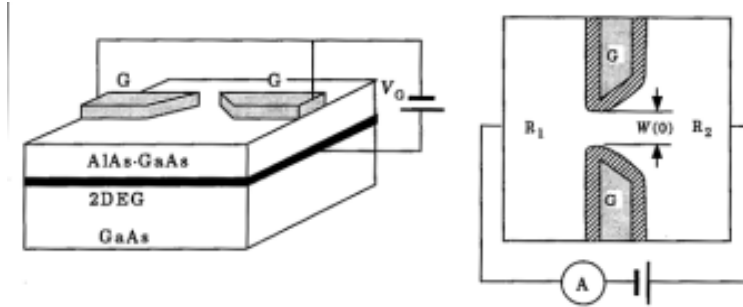


Figure 3.3: A sketch of QPC formed by splitted gates.

QPC is quantized in the units of $2e^2/h$. The quantization is not that accurate as in quantum Hall effect (about 1%) because of non-unit transparencies T_n and finite temperature. It is interesting to compare quantum and classical behavior of QPC. In a classical picture one can write

$$J = W(\delta n)v_F \int_{-\pi/2}^{\pi/2} \frac{d\alpha}{2\pi} \cos \alpha = \frac{1}{\pi} W v_F (\delta n).$$

Thus the “diffusion constant” is

$$D_{eff} = \frac{J}{\delta n} = \frac{1}{\pi} W v_F \quad \rightarrow \quad G = e^2 g(\epsilon_F) D_{eff} = \frac{2e^2}{h} \frac{k_F W}{\pi}.$$

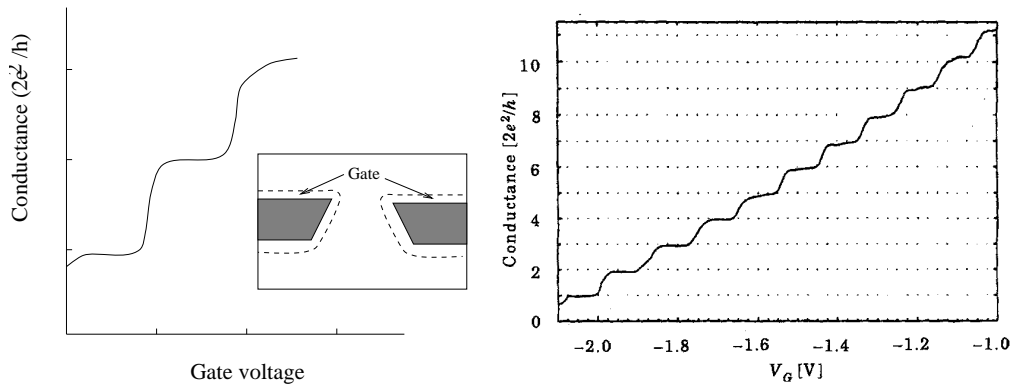


Figure 3.4: Quantization of conductance of a point contact: Schematic picture (left) and experimental result (right).

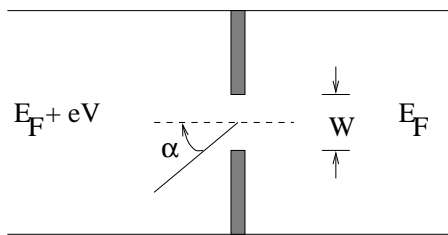


Figure 3.5: On the classical conductance of a point contact.

Note that the integer part of the quantity $k_F W / \pi$ is just the number of occupied modes according to quantum mechanics.

Series addition of quantum resistors

Assume that we have two obstacles in series. Let the wave with unit amplitude is incident to the region, the amplitude of the reflected wave is A while D is the amplitude the wave transmitted through device. The obstacles are connected by an ideal conductor, the phase shift of the wave along which being ϕ . Let the wave emerging from the obstacle

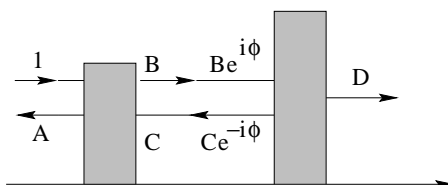


Figure 3.6: On series of quantum resistors.

1 is $B \exp(kx - \omega t)$. It reaches the obstacle 2 gaining the phase ϕ , having the complex amplitude $B \exp(i\phi)$. The reverse wave C gains the phase $-\phi$. In this way we get the

following set of equations,

$$\begin{aligned} A &= r_1 + t_1 C, & B &= t_1 + r'_1 C \\ C e^{-i\phi} &= r_2 B e^{i\phi}, & D &= t_2 B e^{i\phi} \end{aligned}$$

Solving this equation we obtain,

$$D = \frac{e^{i\phi} t_1 t_2}{1 - e^{2i\phi} r_2 r'_1},$$

that yields for the total transmittance:

$$T = |D|^2 = \frac{T_1 T_2}{1 + R_1 R_2 - 2\sqrt{R_1 R_2} \cos \theta} \quad (3.6)$$

where $\theta = 2\phi + \arg(r_2 r'_1)$. The ratio between reflection and transmission which should be understood as a reduced resistance (in units $h/2e^2$) of the system excluding wires is

$$\mathcal{G}^{-1} \equiv \frac{R}{T} = \left| \frac{A}{D} \right|^2 = \frac{R_1 + R_2 - 2\sqrt{R_1 R_2} \cos \theta}{T_1 T_2}, \quad \mathcal{G} \equiv \frac{hG}{2e^2}. \quad (3.7)$$

This is a very strange formula. Assume that we made an ensemble of the systems which differ only by the distance between the obstacles, i. e. by the phase ϕ . Let the distribution of ϕ will be constant in the interval $(0, 2\pi)$. The averaging over ϕ we get

$$\langle \mathcal{G}^{-1} \rangle = \frac{R_1 + R_2}{(1 - R_1)(1 - R_2)},$$

while the Ohm's law will provide

$$\mathcal{G}^{-1} = \frac{R_1}{1 - R_1} + \frac{R_2}{1 - R_2}.$$

As a result the Ohm's law survives only at small reflections.

Let us construct a chain of n resistors with very small reflections. Then the total reflection first increases linearly in n . Finally the total transmission becomes substantially less than 1. Now let us add a very good conductor to this chain. We get

$$\langle \mathcal{G}^{-1} \rangle_{n+1} = \frac{R_n + R}{T_n} = \langle \mathcal{G}^{-1} \rangle_n + \frac{R}{T_n}.$$

Thus an addition a good conductor increases the resistance by $R/T_n > R$. Such a behavior can be formulated as a “renormalization group”

$$\frac{1}{R} \frac{d}{dn} \langle \mathcal{G}^{-1} \rangle_n = \langle \mathcal{G}^{-1} \rangle_n + 1.$$

Thus the average resistance grows exponentially with the length which has something to do with 1D localization. This considerations are not fully satisfactory because resistance

is not the proper quantity to be averaged. Following Anderson, the proper quantity to be averaged is $\ln(1 + \mathcal{G}^{-1})$. Indeed,

$$1 + \mathcal{G}^{-1} = 1 + R/T = 1/T \quad \rightarrow \ln(1 + \mathcal{G}^{-1}) = -\ln T.$$

The quantity $-\ln T$ plays the role of extinction exponent and it should be additive to successive scatterers if the relative phases are averaged out. We get this relation using

$$\int_0^{2\pi} d\theta \ln(a + b \cos \theta) = \pi \ln \frac{1}{2} \left[a + \sqrt{a^2 - b^2} \right].$$

So the exact scaling is given by the relation

$$\langle \ln(1 + \mathcal{G}_n^{-1}) \rangle = n(Rh/2e^2).$$

Parallel addition of quantum resistors.

Let us now discuss the parallel addition of two single-channeled quantum resistors. The geometry of the problem is shown in Fig. 3.7. All the phases and scattering effects along

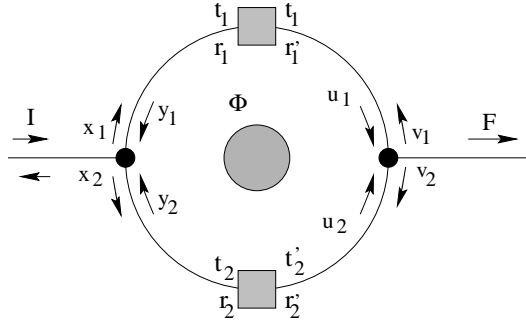


Figure 3.7: On the parallel addition of quantum resistances.

the branches are absorbed by the scattering parameters. Time-reversal symmetry requires $t_i = t_i'$ while the current conservation requires

$$-t_i/t_i'^* = r_i/r_i'^*.$$

In the presence of Aharonov-Bohm flux Φ through the loop, following from the gauge invariance the scattering amplitudes are renormalized as

$$t_1 \rightarrow t_1 e^{-i\theta}, \quad t_1' \rightarrow t_1' e^{+i\theta}, \quad t_2 \rightarrow t_2 e^{+i\theta}, \quad t_2' \rightarrow t_2' e^{-i\theta}, \quad r_i \rightarrow r_i, \quad r_i' \rightarrow r_i'.$$

Here $\theta = \pi\Phi/\Phi_0$.

This point needs some more explanation. An Aharonov-Bohm flux Φ through the opening can be represented as $\oint \mathbf{A} \cdot d\mathbf{l}$ along the path circulating the opening. Here \mathbf{A} is the vector potential. One can eliminate this flux by a gauge transform

$$\psi' = \psi \exp \left[\frac{ie}{\hbar c} \sum_j \chi_j(\mathbf{r}_j) \right],$$

where χ is defined as $A_l = \nabla\chi$. The transformed Schrödinger equation has $A_l = 0$. However, the price for this is that the transformed wave function, ψ' , does not satisfy periodic boundary conditions. When the electron coordinate is rotated once around the ring the phase of χ' is changed by $\delta\chi = 2\pi\Phi/\Phi_0$. In our calculation this phase shift is absorbed into the expressions for the transition amplitudes.

To find the transmitted wave one has to determine 10 unknown amplitudes, $x_1, x_2, y_1, y_2, u_1, u_2, v_1, v_2, F, \dots$. It can be done solving the set of matching equations at the scatterers and the triple connections. It is assumed that the connections do not introduce additional scattering and can be described by the unitary scattering matrix

$$S = \begin{pmatrix} 0 & -1/\sqrt{2} & -1/\sqrt{2} \\ -1/\sqrt{2} & 1/2 & -1/2 \\ -1/\sqrt{2} & -1/2 & 1/2 \end{pmatrix}.$$

Here S_{ii} denote the reflection amplitude of the i th channel while off-diagonal elements S_{ij} are the transition amplitudes from the channel i to j . The subscript 1 is used for left incoming channel and right outgoing channel. After rather long algebra made originally in Ref. [24] we arrive at the solution,

$$T \equiv |F|^2 = 4 \frac{\alpha + \beta \cos 2\theta}{\gamma + \delta \cos 2\theta + \epsilon \cos 4\theta}, \quad (3.8)$$

where $\alpha, \beta, \gamma, \delta, \epsilon$ are rather complicated functions of the scattering amplitudes,

$$\begin{aligned} \alpha &= |A|^2 + |B|^2, \quad \beta = 2 \Re(AB^*), \quad \gamma = |D|^2 + |E|^2, \\ \delta &= 2 \Re(DC^* + EC^*), \quad \epsilon = 2 \Re(DE^*), \\ A &= t_1^2 t_2 + t_2(r_1 - 1)(1 - r'_1), \quad B = t_2^2 t_1 + t_1(r_2 - 1)(1 - r'_2), \\ D &= E = t_1 t_2 \quad C = t_1^2 + t_2^2 - (2 - r_1 - r_2)(2 - r'_1 - r'_2). \end{aligned}$$

This expression describes a rich physical picture. Even in the absence of magnetic field, $\theta = 0$ the transmittance can be strongly dependent on the phases of the complex scattering amplitude. If we make one branch fully non-conducting, $t_1 = 0$, still the appropriate choice of phases of the reflection amplitudes r_1 and r'_1 can result either in $T = 0$ or $T = 1$. Indeed, in this case,

$$\begin{aligned} A &= t_2(r_1 - 1)(1 - r'_1), \quad B = D = E = 0, \quad C = t_2^2 - (2 - r_1 - r_2)(2 - r'_1 - r'_2), \\ \alpha &= |t_2|^2 |(r_1 - 1)(1 - r'_1)|^2, \quad \beta = 0, \quad \gamma = |t_2^2 - (2 - r_1 - r_2)(2 - r'_1 - r'_2)|^2, \\ \delta &= \epsilon = 0. \end{aligned}$$

As a result we get

$$T = \frac{|t_2|^2 |(r_1 - 1)(1 - r'_1)|^2}{|t_2^2 - (2 - r_1 - r_2)(2 - r'_1 - r'_2)|^2}.$$

Putting $r_1 = 1$ we obtain $T = 0$. Thus we observe that non-conducting branch can influence the total conductance strongly.

Of course, all the discussed effects are due to interference. If the size of the system exceeds L_φ we come back to classical laws.

3.3 Additional aspects of ballistic transport

Adiabatic point contacts

The results of first observations of conductance quantization were surprising. Indeed, from quantum mechanics it is well known that any sharp potential barrier produces oscillations in the transmission coefficient as a function of the energy. However, the experimental steps were more or less rectangular. An explanation of such a behavior was given in Ref. [25]. The authors showed that if the point contact has a smooth profile, i. e. if its width d depends on the longitudinal coordinate x in a smooth way, then the $T(E)$ dependence is very close to a perfect step. To make the results simple, let us consider a channel with rectangular confinement. Let us assume that we can separate the variables in an adiabatic way, $\Psi_n(x, y) = \psi_n(x)\varphi_{n,x}(y)$, and first solve the Schrödinger equation for a given width d . In this way we get the transverse wave functions

$$\varphi_{n,x}(y) = \sqrt{\frac{2}{d(x)}} \sin \left[\pi n \frac{2y + d(x)}{d(x)} \right].$$

The Schrödinger equation for the longitudinal motion has the form

$$-\frac{\hbar^2}{2m} \frac{d^2\psi}{dx^2} + \epsilon_n(x)\psi = E\psi, \quad \epsilon_n(x) = \frac{\pi^2 n^2 \hbar^2}{2m[d(x)]^2}.$$

If the variation $d(x)$ is smooth at the scale of de Broglie wave length, k_F^{-1} , the potential $\epsilon_n(x)$ is semiclassical. Then one can use the semiclassical scheme for scattering problem and choose

$$\psi_n(x) = \sqrt{\frac{p_n(\infty)}{p_n(x)}} \exp \left[\frac{i}{\hbar} \int_0^x p_n(x') dx' \right], \quad p_n(x) = \sqrt{2m[E - \epsilon_n(x)]}.$$

The transmittance step depends occurs when the Fermi energy crosses the maximum of

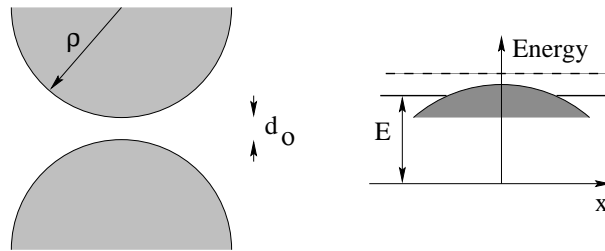


Figure 3.8: On the adiabatic quantum point contact.

the potential $\epsilon_n(x)$ for the upper transverse mode, see Fig. 3.8. Expanding the potential near its maximum we get

$$\epsilon_n(x) = \epsilon_n(0) \left[1 - \left(\frac{\partial^2 d(x)}{\partial x^2} \right)_{x=0} \frac{x^2}{d} \right].$$

Since $\partial^2 d / \partial x^2 = 2/\rho$ where ρ is the curvature radius of the center of constriction, we get the barrier as

$$U(x) = \epsilon_n(0) \left[1 - \frac{2x^2}{d\rho} \right].$$

The transmission through a parabolic barrier is known,

$$T(E) = \frac{1}{1 + \exp[-\pi^2(kd_0/\pi - n_0)\sqrt{2\rho/d_0}]}. \quad (3.9)$$

Here d_0 is the minimal width of the constriction, n_0 is the number of upper level, while $k = \hbar^{-1}\sqrt{2mE}$. We observe that the shape of the step is almost n independent, the transition being sharp at $\rho \geq d_0$. It is important that the numerical factor $\pi^2\sqrt{2}$ makes the transitions sharp even at $R \sim d_0$. The same numerical factor helps for the semiclassical condition to be valid. This criterion reads $\pi^2\sqrt{2\rho/d_0} \gg 1$. To make the motion through the contact ballistic the elastic mean free path should exceed $\sqrt{\rho d_0}$.

3.4 Electron-electron interaction in ballistic systems

The case of pure 3D metal. Concept of Fermi liquid

Let us begin with the estimate of the electron-electron scattering in a Fermi gas. Suppose that we have a particle 1 outside the Fermi sea, see Fig. 3.9. If this particle interacts with

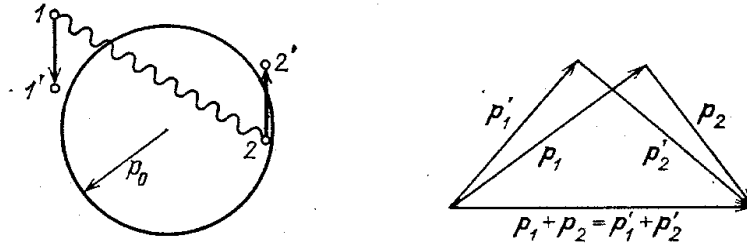


Figure 3.9: Scattering processes for electron-electron interaction.

another one, 2, inside the Fermi sea both final states should be outside the Fermi sea (Pauli principle!). According to the momentum conservation law,

$$\mathbf{p}_1 + \mathbf{p}_2 = \mathbf{p}'_1 + \mathbf{p}'_2,$$

and, as we have seen,

$$p_1, p'_1, p'_2 > p_F; \quad p_2 < p_F.$$

The momentum conservation law is shown graphically in the right panel of Fig. 3.9. One should keep in mind that the planes $(\mathbf{p}_1, \mathbf{p}_2)$ and $(\mathbf{p}'_1, \mathbf{p}'_2)$ are not the same, they are

shown together for convenience. To get the escape probability for the particle 1 one should integrate over the intermediate momenta

$$W \propto \int \delta(\varepsilon_1 + \varepsilon_2 - \varepsilon'_1 - \varepsilon'_2) (dp_2) (dp'_1)$$

(\mathbf{p}'_2 is fixed by the momentum conservation). The energy conservation law actually determines the angle between \mathbf{p}'_1 and \mathbf{p}'_2 for given absolute values of these vectors. Consequently, the rest is to integrate over $p_2 = |\mathbf{p}_2|$ and $p'_1 = |\mathbf{p}'_1|$.

Let p_1 be close to p_F . It means that all the momenta are close to p_F and the angles with the vector $\mathbf{p}_1 + \mathbf{p}_2$ are almost the same. So let us assume cosines to be the same and from the relation between the projections write down

$$p'_1 \approx p_1 + p_2 - p'_2.$$

Now let us recall that $p'_2 > p_F$. Consequently, $p'_1 < p_1 + p_2 - p_F$. But at the same time, $p'_1 > p_F$. Thus

$$p_1 + p_2 - p_F > p_F, \text{ or } p_2 > 2p_F - p_1.$$

But from the Pauli principle, the upper limit for p_2 is p_F . As a result, we come to the following chain of inequalities

$$0 > p_2 - p_F > p_F - p_1, \quad 0 < p'_1 - p_F < (p_1 - p_F) + (p_2 - p_F).$$

Finally,

$$\int dp_2 dp'_1 = \int_{-\alpha_1}^0 d\alpha_2 \int_0^{\alpha_1 + \alpha_2} d\alpha'_1 = \frac{\alpha_1^2}{2}$$

where we have introduced $\alpha_i = p_i - p_F$. Now we should remember that $\varepsilon - \varepsilon_F = v_F(p - p_F)$. So $W \propto (\varepsilon - \varepsilon_F)^2$. The simplest way to estimate τ is to use dimensionality approach. Indeed, the average potential and kinetic energies are of the order of ε_F . Consequently, the only quantity which is proportional to $(\varepsilon - \varepsilon_F)^2$ and has the time dimensionality is

$$\tau \sim \frac{\hbar \varepsilon_F}{(\varepsilon - \varepsilon_F)^2}.$$

We came to important conclusion: if one is interested in quasiparticles near the Fermi level, $|\varepsilon - \varepsilon_F| \ll \varepsilon_F$, he can treat them as to near classical ones provided

$$\frac{\hbar}{(\varepsilon - \varepsilon_F)\tau} \approx \frac{\varepsilon - \varepsilon_F}{\varepsilon_F} \ll 1.$$

The typical value for the quasiparticle energy is $k_B T$. This is why the electron-electron interaction can be treated in the leading approximation in a self-consistent approximation. The estimates above based on the conservation laws provide background of the theory of *Fermi liquid*. The essence of this concept is that the excitations in the vicinity of the the Fermi surface can be treated as *quasiparticles* which behave as particles with renormalized velocity. Consequently, the effects of electron-electron interaction are not crucially important in pure 3D systems.

One-dimensional systems. Tomonaga-Luttinger liquid

For 1D interacting systems the above considerations are not valid because for a single branch linear dispersion near the Fermi points the energy spectrum is close to linear, $E - E_F \approx v(p - p_F)$. That means that the energy and momentum conservation laws are actually the same, and this is why they are not restrictive as in a 3D case. For this reason, the perturbative corrections describing even weak electron-electron interaction are divergent. A proper model for interactive 1D electrons is the so-called Tomonaga-Luttinger model. According to this model, collective electron modes (plasmons) with linear spectra are described by new, *boson* modes. Creation of a real electron in this model is equivalent to excitation an infinite number of plasmons. Because of that, the space and time dependence of density (and spin) correlation functions are substantially different from the ones for non-interacting systems. That manifests itself in various kinetic quantities. For example, the Drude conductivity is predicted to vary as power law with temperature.

The *Luttinger liquid* model which was previously used for 1D organic conductors now became important for high-mobility quantum wires, as well as for edge states under conditions of quantum Hall effect (see below). One can find a good review of this model in Ref. [16].

A 1D quantum wire is appropriately characterized by a conductance. In the absence of interactions, the conductance of an ideal single-mode quantum wire, adiabatically connected to leads, is quantized, $G = 2e^2/h$. In the presence of a scatterer, the conductance drops to $G = 2e^2T/h$, where T is the transmission coefficient.

The electron-electron interaction modifies dramatically the low-energy excitations in a quantum wire that leads to striking predictions for the transport. The new features manifest itself only if there is one (or several) scatterers inside the quantum wire - otherwise the correlation effects are canceled out at the contacts between the interacting quantum wire and non-interacting reservoirs. All that together leads to a rich and very interesting physical picture.

To get a flavor of the theory ¹ let us consider a spinless electrons hopping on 1D lattice with the Hamiltonian

$$\mathcal{H} = -t \sum_j c_j^\dagger c_{j+1} + \frac{V}{2} \sum_j c_j^\dagger c_j c_{j+1}^\dagger c_{j+1} + h.c. . \quad (3.10)$$

When the interaction $V = 0$ this Hamiltonian can be diagonalized as $E_k = -t \cos k$, $|k| < \pi$. The low-energy excitation exist near $\pm k_F$. Consider a single particle excitation near $+k_F$ where we remove one electron with $k < k_F$ and place it into a free state with $k + q > k_F$. Then the energy of excitation is $\hbar\omega_k = \hbar q v_F$. Adding a similar state near $-k_F$ we have a situation similar to phonons in one dimension. When the interaction is turned on this dispersion law remains, however the velocity is renormalized.

Linear spectrum implies a boson-like description. Mathematically in can be done using

¹Here we follow Ref. [16].

(Jordan-Wigner) canonical transform,

$$c_j = \exp\left(i\pi \sum_{k>j} c_k^\dagger c_k\right) b_j,$$

that keeps the Hamiltonian (3.10) in the same form with replacement $c \rightarrow b$. One can check that the b operators at different lattice points *commute*, and therefore they are *bosons*. Now, the boson operators can be approximately decoupled as $b_j \rightarrow \sqrt{n_j} \exp(i\phi_j)$, $n_j \equiv c_j^\dagger c_j$. Then we can proceed to continuum limit, focusing on scales long compared to the lattice constant. In this way we replace

$$\phi_j \rightarrow \phi(x), \quad n_j \rightarrow \tilde{\rho}(x).$$

Extracting from the total electron density its average value, $\rho_0 = k_F/\pi$ and introducing the “displacement” operator, θ , as $\tilde{\rho} - \rho_0 = \partial_x \theta(x)/\pi$ we arrive at the phonon-like commutation rule,

$$[\phi(x), \theta(x')] = \frac{i\pi}{2} \delta(x - x').$$

We observe that $\partial_x \phi$ is the momentum conjugate to θ . As a result, we arrive at the effective Hamiltonian,

$$\mathcal{H} = \frac{v}{2\pi} [g(\partial_x \phi)^2 + g^{-1}(\partial_x \theta)^2]. \quad (3.11)$$

From the commutation relations it can be seen that the Hamiltonian leads to the equation of motion

$$\partial_t^2 \theta = v^2 \partial_x^2 \theta$$

and a similar equation for ϕ . The velocity v , as well as an additional dimensionless constant g depend on the strength of interaction. For non-interacting electrons, $v = v_F$ and $g = 1$.

It is convenient to expand the original Fermion operator into two parts corresponding to the motion around the points $\pm k_F$,

$$\phi(x) \approx \psi_R + \psi_L = e^{k_F x} e^{i\Phi_R} + e^{-k_F x} e^{i\Phi_L},$$

where $\Phi_{R/L} \equiv \phi \pm \theta$. These two fields commute with one another and satisfy the relations,

$$[\Phi_R(x), \Phi_R(x')] = -[\Phi_L(x), \Phi_L(x')] = i\pi \operatorname{sgn}(x - x').$$

The right and left moving electron densities can be reconstructed as

$$N_{B/L} = \pm \partial_x \Phi_{R/L}.$$

Then we can rewrite the Hamiltonian (3.11) as

$$\mathcal{H} = \pi v_0 [N_R^2 + N_L^2 + 2\lambda N_R N_L] \quad (3.12)$$

with

$$v_0 = \frac{v}{2} \left(g + \frac{1}{g} \right), \quad \lambda = \frac{1 - g^2}{1 + g^2}.$$

This Hamiltonian describes interacting system of right and left moving electrons. We identify v_0 to v_F , the case $g < 1$ corresponds to $\lambda > 0$ (repulsion) while $g > 1$ corresponds to attraction.

It is not straightforward how one can relate the parameters v and g with the original lattice model because we have only the effective theory for low-energy excitations. There are analytical expressions only for some models, e. g. for the case of long-range interaction comparing to the scale k_F^{-1} .

A very important point is that the parameter g has a physical meaning of dimensionless (in units e^2/h per spin) conductance of an infinite ideal Luttinger liquid. That can be traced introducing new variables, $\phi_{R/L} = g\phi \pm \theta$, that diagonalize the Hamiltonian (3.10) as

$$\mathcal{H} = \frac{\pi v}{g} (n_R^2 + n_L^2), \quad n_{R/L} = \pm \frac{1}{2\pi} \partial_x \phi_{R/L}. \quad (3.13)$$

The operators $n_{R/L}$ correspond to the densities of right and left moving *interacting* electrons. The Hamiltonian allows chiral general solutions $f(x \pm vt)$. Now we can raise the chemical potential of right chiral mode n_R by an amount μ_R . Then $\delta\mathcal{H} = -e\mu_R n_R$, and minimizing (3.13) we get $n_R = (ge/2\pi v)\mu_R$. Since the additional current to the right is $I_R = en_R v$ we get

$$G = g \frac{e^2}{h}. \quad (3.14)$$

As is was already mentioned, in a quantum wire it is impossible to couple only to one chiral mode. As a result, the d.c. conductance of a finite Luttinger liquid wire coupled to noninteracting leads appears the same as for noninteracting case. However, interaction effects can be revealed in a.c. experiments, as well as in the presence of some scatterers. Because of long-range correlations, the scatterers “undress” the excitations of interacting systems. As a result, may interesting and important effects can be observed. In particular, the interaction leads to a strong renormalization of density of states near an obstacle. For example, if the Luttinger liquid wire has a large barrier with low transmission coefficient T_0 one can employ the results for the density of states in a semi-infinite liquid. That results in the nonlinear current-voltage curve at low temperatures.

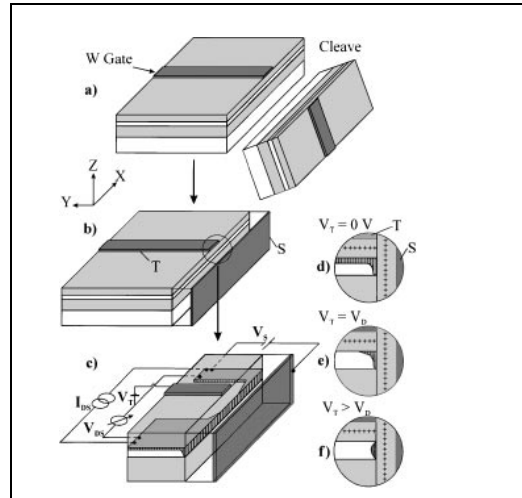
$$I \propto T_0 |V|^{2(g-1)/g} V \rightarrow G(V) \equiv \frac{dI}{dV} \propto T_0 |V|^{2(g-1)/g}.$$

Thus, got the repulsive case the linear conductance is *zero*. At finite temperature it does exist. However it is proportional to $T^{2(g-1)/g}$. In the case of weak scattering the results are substantially different.

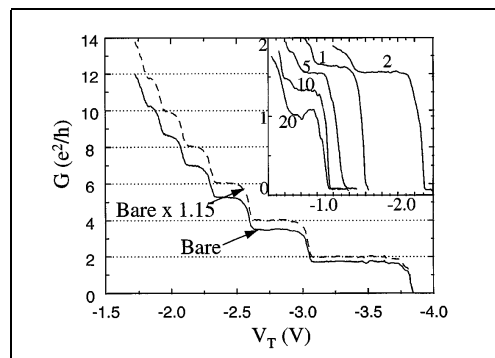
There are several experiments where some deviations from the predictions of single-electron theory were observed, such as unusual conductance quantization and anomalous temperature dependences. Unfortunately, the electron-electron correlations are effectively

destroyed by disorder and electron-phonon scattering. Therefore, to observe the interaction effect one needs extremely pure samples and low temperatures. The results of such experiment is demonstrated in Fig. 3.10.

The concept of Luttinger liquid is specifically important for quantum Hall effect systems. We shall see that near the edges of a Hall bar a specific edge states appear which can be described by the above mentioned model. This system is much more pure than quantum wires, and interaction effects are crucially important. We are going to discuss quantum Hall systems later.



(a) Wire preparation by cleaved edge overgrowth of GaAs-AlGaAs by MBE. The wire is fabricated by cleaving the specimen [see also panel (b)]. Edge states (d) form the quantum wire. Panels (e) and (f) show different charge distributions for different top voltages. The panel (c) shows a blowup of critical device region. The mean free path is estimated as $10 \mu\text{m}$, the length of the channel is about $2 \mu\text{m}$.



Linear response conductance of a $2 \mu\text{m}$ log wire in a 25 nm quantum well vs. the top-gate voltage (V_T) measured at a temperature 0.3 K . Solid line is the measured conductance. The dashed curve is the measured conductance multiplied by an empirical factor 1.15 . Inset: Linear response conductance of the last plateau for wires of different lengths fabricated consecutively along the edge of a single 25 nm cleaved edge overgrowth specimen. The numbers denote the wire lengths in microns.

Figure 3.10: Non-universal Conductance Quantization in Quantum wires [From A. Yacoby, *et al.*, Physical Review Letters, **77**, 4612 (1996).]

Chapter 4

Tunneling and Coulomb blockage

4.1 Tunneling

Modern technology allows to fabricate various structures involving tunneling barriers. One of the ways is a split-gate structure. Such a system can be considered as a specific example

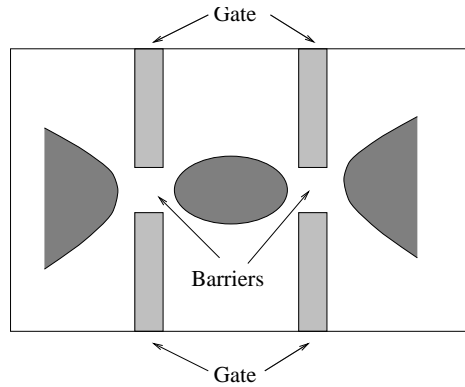


Figure 4.1: Split-gate structure allowing resonant tunneling.

of series connection of two obstacles. The complex amplitude of the wave transmitted through the whole system is

$$D = \frac{t_1 t_2 e^{i\phi}}{1 - e^{2i\phi} r_2 r_1'} = \frac{t_1 t_2 e^{i\phi}}{1 - e^{\theta} \sqrt{R_1 R_2}}, \quad (4.1)$$

where $\theta = 2\phi + \arg(r_2 r_1')$. It is clear that the transmittance

$$T = \frac{T_1 T_2}{1 + R_1 R_2 - 2\sqrt{R_1 R_2} \cos \theta} \quad (4.2)$$

is maximal at some specific value of θ where $\cos \theta = 1$, the maximal value being

$$T_{\max} = \frac{T_1 T_2}{(1 - \sqrt{R_1 R_2})^2}. \quad (4.3)$$

This expression is specifically simple at $T_1, T_2 \ll 1$,

$$T_{\max} = \frac{4T_1T_2}{(T_1 + T_2)^2}. \quad (4.4)$$

Thus we observe that two low-transparent barriers in series can have a unit transmittance if they have the same partial transparencies, $T_1 = T_2 = T$. The reason of this fact in quantum interference in the region between the barriers which makes wave functions near the barriers very large to overcome low transmittance of each barrier.

An important point is that the phase θ gained in the system is a function of the electron energy. Thus near a particular value $E^{(r)}$ defined by the equality

$$\cos \theta(E^{(r)}) = 0 \rightarrow \theta(E_k^{(r)}) = 2\pi k$$

one can expand $\cos \theta$ as

$$1 - \frac{1}{2} \left(\frac{\partial \theta}{\partial E} \right)^2 (E - E^{(r)})^2.$$

Thus at low transmittance we arrive at a very simple formula of a Breit-Wigner type,

$$\begin{aligned} T &\approx \frac{T_1T_2}{(T_1 + T_2)^2/4 + (\theta')^2 (E - E^{(r)})^2} \\ &= \frac{\Gamma_1\Gamma_2}{(\Gamma_1 + \Gamma_2)^2/4 + (E - E^{(r)})^2}. \end{aligned} \quad (4.5)$$

Here we denote $\theta' \equiv (\partial\theta/\partial E)_{E=E^{(r)}}$ and introduce $\Gamma_i = T_i/|\theta'|$.

The physical meaning of the quantities Γ_i is transparent. Let us assume that all the phase shift is due to ballistic motion of an electron between the barriers. Then,

$$\theta = 2ka = 2ah^{-1}\sqrt{2mE} \rightarrow \theta' = \frac{a}{\hbar} \sqrt{\frac{2m}{E}} = \frac{2a}{\hbar v}$$

where v is the electron velocity. As a result, the quantity Γ_i can be rewritten as $\Gamma = \hbar\nu_a T_i$, where $\nu_a = v/2d$ is the frequency of oscillations inside the inter-barrier region, the so-called *attempt frequency*. Thus it is clear that Γ_i are the escape rates through i -th barrier.

To specify the transition amplitudes let us consider a 1D model for a particle in a well between two barriers. We are interested in the scattering problem shown in Fig. 4.2. To find a transmission probability one has to match the wave functions and their gradients at the interfaces 1-4 between the regions **A-C**. They have the following form

$$\begin{array}{ll} e^{ikx} + re^{-ikx} & \text{in the region A;} \\ a_1 e^{\kappa_B x} + a_2 e^{-\kappa_B x} & \text{in the region B;} \\ b_1 e^{ikx} + b_2 e^{-ikx} & \text{in the region C;} \\ c_1 e^{\kappa_D x} + c_2 e^{-\kappa_D x} & \text{in the region D;} \\ te^{ikx} & \text{in the region E} \end{array} .$$

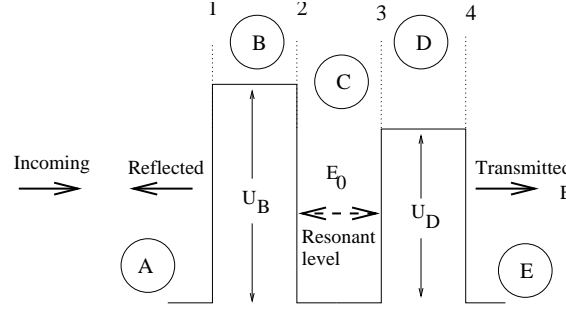


Figure 4.2: On the resonant tunneling in a double-barrier structure.

Here

$$k = \hbar^{-1}\sqrt{2mE}, \quad \kappa_i = \sqrt{\kappa_{0i}^2 - k^2}, \quad \kappa_{0i} = \hbar^{-1}\sqrt{2mU_i}.$$

The transmission amplitude is given by the quantity t while the reflection amplitude – by the quantity r . In fact we have 8 equations for 8 unknowns (r, t, a_i, b_i, c_i), so after some tedious algebra we can find everything. For a single barrier one would get

$$T(E) = \frac{4k^2\kappa^2}{\kappa_0^4 \sinh^2(\kappa d) + 4k^2\kappa^2} \approx \frac{k^2\kappa^2}{\kappa_0^4} e^{-2\kappa d}.$$

Here d is the barrier's thickness. So the transparency exponentially decays with increase of the product κd . The calculations for a double-barrier structure is tedious, so we consider a simplified model of the potential

$$U(x) = U_0 d [\delta(x) + \delta(x - a)].$$

In this case we have 3 regions,

$$\begin{aligned} e^{ikx} + r e^{-ikx} & \quad x < 0. \\ A \sin kx + B \cos kx & \quad 0 < x < a, \\ t e^{ik(x-a)} & \quad x > a \end{aligned} \quad (4.7)$$

The matching conditions for the derivatives at the δ -functional barrier has the form

$$\psi'(x_0 + 0) - \psi'(x_0 - 0) = \kappa^2 d \psi(x_0). \quad (4.8)$$

Here $\kappa^2 = 2mU_0/\hbar^2$. One can prove it by integration of the Schrödinger equation

$$(\hbar^2/2m)\nabla^2\psi + U_0 d \delta(x - x_0)\psi = E\psi$$

around the point x_0 . Thus we get the following matching conditions

$$\begin{aligned} B &= 1 + r, \\ kA - ik(1 - r) &= \kappa^2 a(1 + r), \\ A \sin ka + B \cos ka &= t, \\ ikt - k(A \cos ka - B \sin ka) &= t\kappa^2 a. \end{aligned}$$

First one can easily see that there is a solution with *zero reflectance*, $r = 0$. Substituting $r = 0$ we get the following requirement for the set of equation to be consistent

$$k = k_0, \quad \tan k_0 a = -\frac{2k_0}{\kappa^2 d}. \quad (4.9)$$

We immediately observe that at that $k |t| = 1$ (total transmission). At strong enough barrier, $\kappa d \gg 1$, this condition means

$$k_0 a = \pi(2s + 1), \quad s = 0, \pm 1, ..$$

Physically, that means that an electron gains the phase $2\pi s$ during its round trip (cf. with optical interferometer). Thus two barriers in series can have perfect transparency even if the transparency of a single barrier is exponentially small. The physical reason is *quantum interference*.

The condition (4.9) defines the energy

$$E_0 = \frac{\hbar^2 k_0^2}{2m}$$

where the transparency is maximal. Near the peak one can expand all the quantities in powers of

$$k - k_0 \approx \frac{E - E_0}{(\partial E / \partial k)_{k_0}} \approx k_0 \frac{E - E_0}{2E_0}.$$

The result for a general case can be expressed in the Breit-Wigner form

$$T(E) = \frac{\Gamma_L \Gamma_R}{(E - E_0)^2 + \frac{1}{4}(\Gamma_L + \Gamma_R)^2}.$$

Here $\Gamma_{L(R)}/\hbar$ are the *escape rates* for the electron inside the well to the left(right) lead. They are given by the attempt frequency $v_0/2a = \hbar k_0/2ma$ times the transparency of a given barrier.

Of course, if voltage across the system is zero the total number of electrons passing along opposite directions is the same, and the current is absent. However, in a biased system we obtain the situation shown in Fig. 4.3. *Negative* differential conductance, $dJ/dV \leq 0$, allows one to make a generator. One can also control the system moving the level E_0 with respect to the Fermi level by the gate voltage. In this way, one can make a *transistor*.

Commercial resonant tunneling transistors are more complicated than the principle scheme described above. A schematic diagram of a real device is shown in Fig. 4.4. In this device resonant tunneling takes place through localized states in the barrier. There exist also transistors with two quantum wells where electrons pass through the resonant levels in two quantum wells from the emitter to collector if the levels are aligned. The condition of alignment is controlled by the collector-base voltage, while the number of electrons from emitter is controlled by the base-emitter voltage.

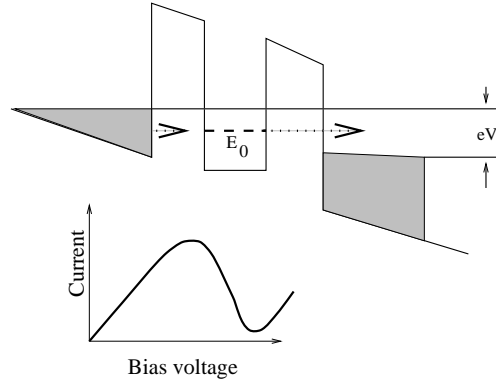


Figure 4.3: Negative differential conductance in double-barrier resonant-tunneling structure.

4.2 Coulomb blockade

Now let us discuss a specific role of Coulomb interaction in a mesoscopic system. Consider a system with a dot created by a split-gate system (see above).

If one transfers the charge Q from the source to the grain the change in the energy of the system is

$$\Delta E = QV_G + \frac{Q^2}{2C}.$$

Here the first item is the work by the source of the gate voltage while the second one is the energy of Coulomb repulsion at the grain. We describe it by the effective capacitance C to take into account polarization of the electrodes. The graph of this function is the parabola with the minimum at

$$Q = Q_0 = -CV_G,$$

So it can be tuned by the gate voltage V_G . Now let us remember that the charge is transferred by the electrons with the charge $-e$. Then, the energy as a function of the number n of electrons at the grain is

$$\Delta E(n) = -neV_G + \frac{n^2 e^2}{2C}.$$

Now let us estimate the difference

$$\Delta E(n+1) - \Delta E(n) = -eV_G + n\frac{e^2}{C}.$$

We observe that at certain values of V_G ,

$$V_{Gn} = n\frac{e}{C}, \quad (4.10)$$

the difference vanishes. It means that only at that values of the gate voltage resonant transfer is possible. Otherwise one has to pay for the transfer that means that only inelastic

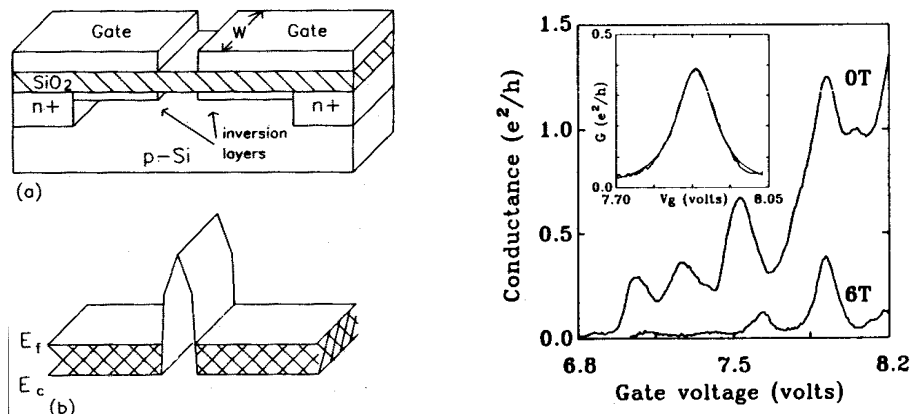


Figure 4.4: Schematic diagram of a Si MOSFET with a split gate (a), which creates a potential barrier in the inversion layer (b). In the right panel oscillations in the conductance as a function of gate voltage at 0.5 K are shown. They are attributed to resonant tunneling through localized states in the barrier. A second trace is shown for a magnetic field of 6 T. From T. E. Kopley *et al.*, Phys. Rev. Lett. **61**, 1654 (1988).

processes can contribute. As a result, at

$$k_B T \leq \frac{e^2}{2C}$$

the linear conductance is exponentially small if the condition (4.10) is met. This phenomenon is called the Coulomb blockade of conductance.

As a result of the Coulomb blockade, electron tunnel *one-by-one*, and the conductance vs. gate voltage dependence is a set of sharp peaks. That fact allows one to create a so-called *single-electron transistor* (SET) which is now the *most sensitive* electrometer. Such a device (as was recently demonstrated) can work at room temperature provided the capacitance (size!) is small enough.

Coulomb blockade as a physical phenomenon has been predicted by Kulik and Shekhter [26]. There are very good reviews [13, 14, 15] about single-charge effects which cover both principal and applied aspects. Below we shall review the simplest variant of the theory, so called “orthodox model”.

A simple theory of single charge tunneling

For simplicity, let us ignore discrete character of energy spectrum of the grain and assume that its state is fully characterized by the number n of excess electrons with respect to an electrically neutral situation. To calculate the energy of the systems let us employ the equivalent circuit shown in Fig. 4.5. The left (emitter) and right (collector) tunnel junctions are modeled by partial resistances and capacitances.

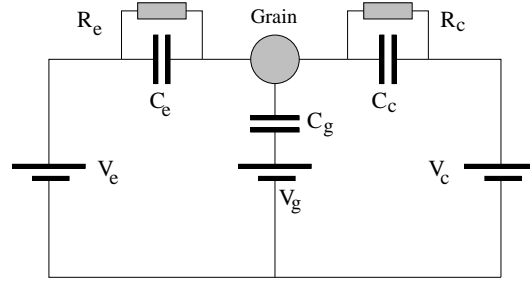


Figure 4.5: Equivalent circuit for a single-electron transistor. The gate voltage, V_g , is coupled to the grain via the gate capacitance, C_g . The voltages V_e and V_c of emitter and collector are counted from the ground.

The charge conservation requires that

$$\begin{aligned} -ne &= Q_e + Q_c + Q_g \\ &= C_e(V_e - U) + C_c(V_c - U) + C_g(V_g - U), \end{aligned} \quad (4.11)$$

where U is the potential of the grain. The effective charge of the grain is hence

$$Q = CU = ne + \sum_{i=e,c,g} C_i V_i, \quad C \equiv \sum_i C_i.$$

This charge consists of 4 contributions, the charge of excess electrons and the charges induced by the electrodes. Thus, the electrostatic energy of the grain is

$$E_n = \frac{Q^2}{2C} = \frac{(ne)^2}{2C} + \frac{ne}{C} \sum_i C_i V_i + \frac{1}{2C} \left(\sum_i C_i V_i \right)^2. \quad (4.12)$$

The last item is not important because it is n -independent. In the stationary case, the currents through both junctions are the same. Here we shall concentrate on this case. In the non-stationary situation, an electric charge can be accumulated at the grain, and the currents are different, see Appendix D.

To organize a transport of one electron one has to transfer it first from emitter to grain and then from grain to collector. The energy cost for the first transition,

$$E_{n+1} - E_n = \frac{(2n+1)e^2}{2C} + \frac{e}{C} \sum_i C_i V_i \quad (4.13)$$

must be less than the voltage drop eV_e . In this way we come to the criterion

$$E_n - E_{n+1} + eV_e \geq 0. \quad (4.14)$$

In a similar way, to organize the transport from grain to collector we need

$$E_{n+1} - E_n - eV_c \geq 0. \quad (4.15)$$

The inequalities (4.15) and (4.14) provide the relations between V_e , V_c and V_g to make the current possible. For simplicity let us consider a symmetric system, where

$$G_e = G_c = G, \quad C_e = C_c \approx C/2 \quad (C_g \ll C), \quad V_e = -V_c = V_b/2$$

where V_b is bias voltage. Then we get the criterion,

$$V_b \geq (2n + 1)|e|/C - 2(C_g/C)V_g.$$

We observe that there is a threshold voltage which is necessary to exceed to organize transport. This is a manifestation of *Coulomb blockade*. It is important that the threshold linearly depends on the gate voltage which makes it possible to create a transistor. Of course, the above considerations are applicable at zero temperature.

The current through the emitter-grain transition we get

$$I = e \sum_n p_n [\Gamma_{e \rightarrow g} - \Gamma_{g \rightarrow e}]. \quad (4.16)$$

Here p_n is the stationary probability to find n excess electrons at the grain. It can be determined from the balance equation,

$$p_{n-1}\Gamma_{n-1}^n + p_{n+1}\Gamma_{n+1}^n - (\Gamma_n^{n-1} + \Gamma_{n+1}^n) p_n = 0. \quad (4.17)$$

Here

$$\Gamma_{n-1}^n = \Gamma_{e \rightarrow g}(n-1) + \Gamma_{c \rightarrow g}(n-1); \quad (4.18)$$

$$\Gamma_{n+1}^n = \Gamma_{g \rightarrow e}(n+1) + \Gamma_{g \rightarrow c}(n+1). \quad (4.19)$$

The proper tunneling rates can be calculated from the golden rule expressions using tunneling transmittance as perturbations. To do that, let us write down the Hamiltonian as

$$\begin{aligned} \mathcal{H}_0 &= \mathcal{H}_e + \mathcal{H}_g + \mathcal{H}_{\text{ch}} + \mathcal{H}_{\text{bath}}; \\ \mathcal{H}_{e,c} &= \sum_{\mathbf{k}\sigma} \epsilon_{\mathbf{k}} c_{\mathbf{k}\sigma}^\dagger c_{\mathbf{k}\sigma}, \\ \mathcal{H}_g &= \sum_{\mathbf{q}\sigma} \epsilon_{\mathbf{q}} c_{\mathbf{q}\sigma}^\dagger c_{\mathbf{q}\sigma}, \\ \mathcal{H}_{\text{ch}} &= (\hat{n} - Q_0)/2C, \quad \hat{n} = \sum_{\mathbf{q}\sigma} c_{\mathbf{q}\sigma}^\dagger c_{\mathbf{q}\sigma} - N^+. \end{aligned}$$

Here $\mathcal{H}_{\text{bath}}$ is the Hamiltonian for the thermal bath. We assume that emitter and collector electrodes can have different chemical potentials. N^+ is the number of positively charged ions in the grain. To describe tunneling we introduce the tunneling Hamiltonian between, say, emitter and grain as

$$\mathcal{H}_{e \leftrightarrow g} = \sum_{\mathbf{k}, \mathbf{q}, \sigma} T_{\mathbf{k}\mathbf{q}} c_{\mathbf{k}\sigma}^\dagger c_{\mathbf{q}\sigma} + \text{h.c.}$$

Applying the golden rule we obtain

$$\Gamma_{e \rightarrow g}(n) = \frac{G_e}{e^2} \int_{-\infty}^{\infty} d\epsilon_k \int_{-\infty}^{\infty} d\epsilon_q f_e(\epsilon_k) [1 - f_g(\epsilon_q)] \delta(E_{n+1} - E_n - eV_e).$$

Here we have introduced the tunneling conductance of $e - g$ junction as

$$G_e = (4\pi e^2/\hbar) g_e(\epsilon_F) g_g(\epsilon_F) \mathcal{V}_e \mathcal{V}_g \langle |T_{\mathbf{k}\mathbf{q}}|^2 \rangle.$$

along the Landauer formula, $\mathcal{V}_{e,g}$ being the volumes of the lead and grain, respectively. In this way one arrives at the expressions

$$\Gamma_{e \rightarrow g}(n, V_e) = \Gamma_{g \rightarrow e}(-n, -V_e) = \frac{2G_e}{e^2} \mathcal{F}(\Delta_{+,e}); \quad (4.20)$$

$$\Gamma_{g \rightarrow c}(n, V_c) = \Gamma_{c \rightarrow g}(-n, -V_c) = \frac{2G_c}{e^2} \mathcal{F}(\Delta_{-,c}). \quad (4.21)$$

Here

$$\mathcal{F}(\epsilon) = \frac{\epsilon}{1 + \exp(-\epsilon/kT)} \rightarrow \epsilon \Theta(\epsilon) \text{ at } T \rightarrow 0,$$

while

$$\Delta_{\pm,\mu}(n) = E_n - E_{n\pm 1} \pm eV_\mu = \frac{1}{C} \left[\frac{e^2}{2} \mp en \mp e \sum_i C_i V_i \right] \pm eV_\mu$$

is the energy cost of transition. The temperature-dependent factor arise from the Fermi occupation factor for the initial and final states, physically they describe thermal activation over Coulomb barrier. The results of calculation of current-voltage curves for a symmetric transistor structure are shown in Fig. 4.6. At low temperatures and low bias voltages,

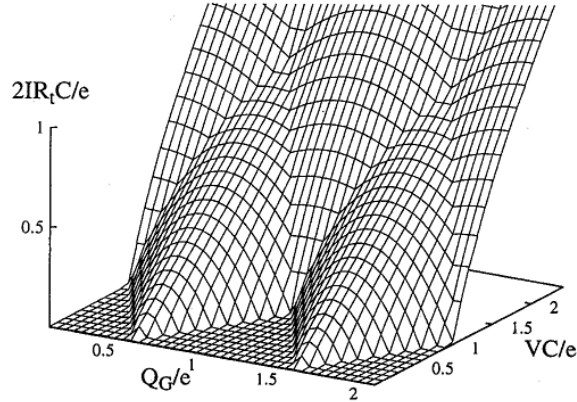


Figure 4.6: The current of a symmetric transistor as a function of gate and bias voltage at $T = 0$ (from the book [5]).

$VC/e < 1$, only two charge states play a role. At larger bias voltage, more charge states are involved. To illustrate this fact, a similar plot is made for symmetrically biased transistor, $V_e = -V_g = V/2$, for different values of Q_0 , Fig. 4.7.

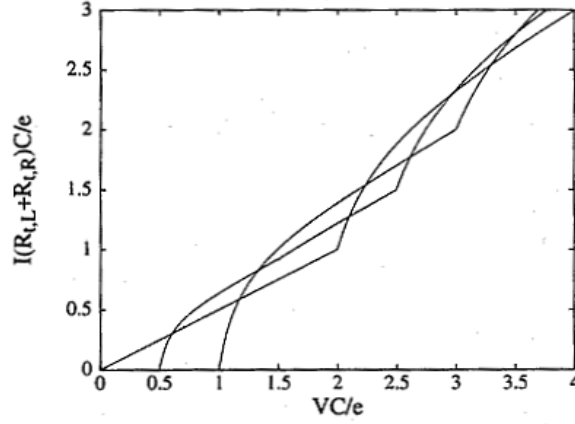


Figure 4.7: The current of asymmetric transistor, $G_e = 10G_c$, as a function of bias voltage at $T = 0$ and different $Q_0/e = 0, 0.25$ and 1 (from the book [5]). At $Q_0 = 0$ the Coulomb blockade is pronounced, while at $Q_0/e = 0.5$ the current-voltage curve is linear at small bias voltage. The curves of such type are called the *Coulomb staircase*.

Cotunneling processes

As we have seen, at low temperature the sequential tunneling can be exponentially suppressed by Coulomb blockade. In this case, a higher-order tunneling process transferring electron charge coherently through two junctions can take place. For such processes the excess electron charge at the grain exists only virtually.

A standard next-order perturbation theory yields the rate

$$\Gamma_{i \rightarrow f} = \frac{2\pi}{\hbar} \left| \sum_{\psi} \frac{\langle i | \mathcal{H}_{\text{int}} | \psi \rangle \langle \psi | \mathcal{H}_{\text{int}} | i \rangle}{E_{\psi} - E_i} \right|^2 \delta(E_i - E_f).$$

Two features are important.

- There are 2 channel which add coherently: (i) $e \rightarrow g, g \rightarrow c$ with the energy cost $\Delta_{-,e}(n+1)$, and (ii) $g \rightarrow c, e \rightarrow g$ with the energy cost $\Delta_{+,c}(n-1)$.
- The leads have macroscopic number of electrons. Therefore, with overwhelming probability the outgoing electron will come from a different state than the one which the incoming electron occupies. Hence, after the process an *electron-hole excitation* is left in the grain.

Transitions involving different excitations are added incoherently, the result being

$$\begin{aligned} \Gamma_{\text{cot}} &= \frac{\hbar G_e G_c}{2\pi e^4} \int_e d\epsilon_k \int_g d\epsilon_q \int_g d\epsilon_{q'} \int_c d\epsilon_{k'} f(\epsilon_k) [1 - f(\epsilon_q)] f(\epsilon_{q'}) [1 - f(\epsilon_{k'})] \\ &\times \left[\frac{1}{\Delta_{-,e}(n+1)} + \frac{1}{\Delta_{+,c}(n-1)} \right]^2 \delta(eV + \epsilon_k - \epsilon_q + \epsilon_{q'} - \epsilon_{k'}). \end{aligned}$$

At $T = 0$ the integrals can be done explicitly, and one obtains

$$\Gamma_{\text{cot}} = \frac{\hbar G_e G_c}{12\pi e} \left[\frac{1}{\Delta_{-,e}(n+1)} + \frac{1}{\Delta_{+,c}(n-1)} \right]^2 V^3 \quad \text{for } eV \ll \Delta_i.$$

As a result, the current appears proportional to V^3 that was observed experimentally. The situation is not that simple for the degenerate case when $\Delta_i = 0$. In that case the integrals are divergent and the divergence must be removed by a finite life time of a state. A detailed treatment of that case is presented in the book [5].

There is also a process when an electron tunnels through the system leaving no excitations in the grain. The probability of such *elastic cotunneling* has a small factor $(g_g \mathcal{V}_g)^{-1}$. However, it leads to the current, proportional to V , thus it can be important at very low bias voltage.

Concluding remarks

There are many experiments where Coulomb-blockaded devices are investigated. Probably most interesting are the devices where tunneling takes place through a small quantum dot with discrete spectrum. An example of such device is shown in Fig. 4.8. The linear conductance of such a structure as a function of the gate electrode C is shown in Fig. 4.9. An important point is that at present time the devices can be fabricated so small that the criterion $kT \leq e^2/C$ can be satisfied at room temperatures. Now several room temperature operating Coulomb blockade devices were reported. Among them are devices consisting of large molecules with the probes attached in different ways. This is probably a starting point for new extremely important field - *molecular electronics*. Such devices are extremely promising both because they are able to operate at room temperatures and because they will allow high integration. This is one of important trends. Another one concerns with single-electron devices which include superconducting parts. There is a lot of interesting physics regarding transport in such systems.

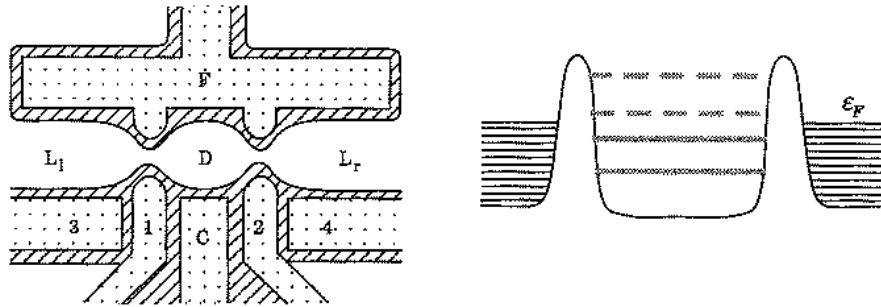


Figure 4.8: (a) A typical structure of a quantum dot. The depleted (shaded) areas are controlled by electrodes 1-4, C, and F. Electrode C also controls the electrostatic potential in the dot. (b) a model of a quantum dot. From [7].

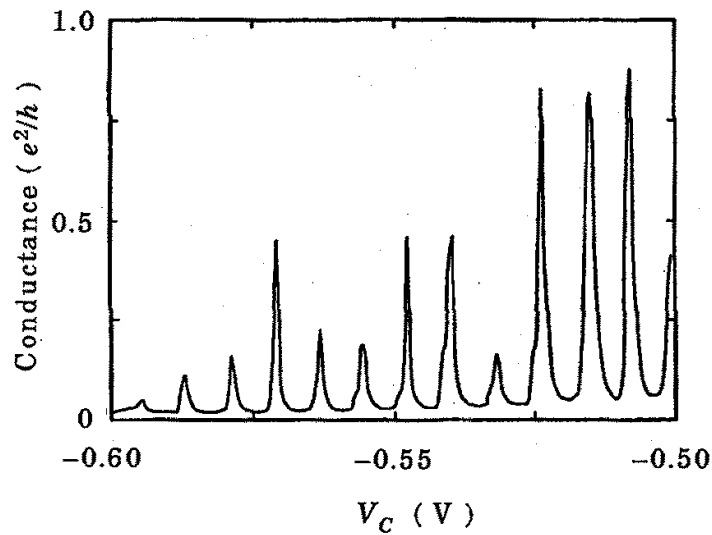


Figure 4.9: Conductance of a quantum dot vs. the voltage of gate electrode C. From L. P. Kouwenhoven *et al.*, *Z. Phys. B* **85**, 367 (1991).

Chapter 5

Conductance Fluctuations. Mesoscopics

5.1 General considerations

We have mentioned that fluctuations between the values of conductance of different samples become very large in low-dimensional systems. However, the samples still contain many atoms. According to the estimates, one can expect a very specific behavior in the sample with the size $\sim 10^{-4}$ cm at $T = 0.1$ K. So,

- where is the difference between *macroscopic* and *microscopic* systems?
- What is going on in between, in such a so-called *mesoscopic* region?

It is very important that one can observe mesoscopic behavior even in a given sample monitoring its properties as a function of an external parameter, say magnetic field. The reason is that these effects are manifestations of quantum interference. External magnetic field effects the phase gains along the trajectories which behave as almost random quantities. So (with some restrictions) one can consider a sample in a given field as a separate representation of the ensemble of samples. Experimentally, mesoscopic fluctuations manifest themselves as fluctuations in the resistance as a function of magnetic field. They look random. However, they are “fingerprints” of a sample, they are reproduced at any experimental run.

Now we discuss mesoscopic fluctuations in more detail.

5.2 Universal conductance fluctuations

As we have already mentioned, in 2D case the Drude conductance for a single spin direction (and a single valley) can be written as

$$G = \frac{e^2}{h} \frac{\pi \ell}{2L} N, \quad N \equiv \frac{k_F W}{\pi}.$$

Here L is the length of the sample, W is its width, while ℓ is the elastic mean free path. The number N is just the number of subbands that are occupied at the Fermi energy in a conductor with width W .

Let us have in mind the Landauer picture of two reservoirs with some disordered region in between.¹ For simplicity let us assume that the latter region is connected to reservoirs by ideal quantum wires.

If $L \gg \ell$ then the modes have the same average transmission probability, $\pi\ell/2L$, that we can establish comparing Drude and Landauer formulas. We are interested in the fluctuations around this average. For that let us come back to the multichannel Landauer formula (for one spin)

$$G = \frac{e^2}{h} \sum_{\alpha,\beta=1}^N |t_{\alpha\beta}|^2.$$

For the ensemble average transmission coefficient we get

$$\langle |t_{\alpha\beta}|^2 \rangle = \pi\ell/2NL.$$

We are interested in the quantity

$$\text{Var}(G) \equiv \langle (G - \langle G \rangle)^2 \rangle.$$

An important point that while doing such an average one should keep track of the correlation in transmission probabilities $|t_{\alpha\beta}|^2$ for different pairs of incident and outgoing channels. The reason is that the transmission takes place via many scattering events, and they may involve the same scatterers. On the other hand, the *reflections* are dominated only by few scattering events, so they can be considered as uncorrelated. These considerations definitely need a rigorous derivation which has been given first by Altshuler [28]. Taking this concept for granted, we get

$$\sum_{\alpha,\beta=1}^N |t_{\alpha\beta}|^2 = N - \sum_{\alpha,\beta=1}^N |r_{\alpha\beta}|^2 \quad (5.1)$$

so the variance of the conductance is

$$\text{Var}(G) = \left(\frac{e^2}{h}\right)^2 \text{Var}\left(\sum_{\alpha,\beta=1}^N |r_{\alpha\beta}|^2\right) = \left(\frac{e^2}{h}\right)^2 N^2 \text{Var}(|r_{\alpha\beta}|^2), \quad (5.2)$$

assuming reflections to be *uncorrelated*. There are different Feynman paths for reflection, so we can write the variance

$$\text{Var}(|r_{\alpha\beta}|^2) = \langle |r_{\alpha\beta}|^4 \rangle - \langle |r_{\alpha\beta}|^2 \rangle^2$$

¹Here we follow the arguments by Lee [27].

using summation over the paths,

$$\begin{aligned}
\langle |r_{\alpha\beta}|^4 \rangle &= \sum_{i,j,k,l=1}^M \langle A^*(i)A(j)A^*(k)A(l) \rangle \\
&= \sum_{i,j,k,l=1}^M [\langle |A(i)|^2 \rangle \langle |A(k)|^2 \rangle \delta_{ij} \delta_{kl} + \langle |A(i)|^2 \rangle \langle |A(j)|^2 \rangle \delta_{il} \delta_{jk}] \\
&= 2 \langle |r_{\alpha\beta}|^2 \rangle^2 .
\end{aligned} \tag{5.3}$$

Here we neglected the terms smaller by a factor $1/M \ll 1$. Therefore

$$\text{Var} (|r_{\alpha\beta}|^2) = \langle |r_{\alpha\beta}|^2 \rangle^2 .$$

Since the average

$$\langle |r_{\alpha\beta}|^2 \rangle = \frac{1}{N} \left[1 - \mathcal{O} \left(\frac{\ell}{L} \right) \right]$$

that follows from the averaging of (5.1), we come to the conclusion that $\text{Var} (G) = (e^2/h)^2$ *independently* of ℓ and L in the diffusive limit $\ell \ll L$. This is why the called the *universal conductance fluctuations* (UCF).

The general formula reads as

$$\delta G = \sqrt{\text{Var} (G)} = \frac{g_s g_v}{2\sqrt{\beta}} C \frac{e^2}{h} .$$

Here g_i are degeneracy factors, C depends on the sample geometry (actually, of its effective dimensionality), while $\beta = 1$ in zero magnetic field and 2 when the magnetic field breaks time-reversal symmetry (see later).

5.3 Temperature effects

The thermal effects are a bit complicated because of finite phase coherence length $L_\varphi = \sqrt{D\tau_\varphi}$ and of thermal averaging characterized by the thermal length $L_T = \sqrt{\hbar D/kT}$. Both effects tend to restore self-averaging. We discuss the situation in a semi-qualitative way for the geometry of a narrow channel in a 2DEG, namely at

$$W \ll L_\varphi \ll L .$$

At $L_\varphi \ll L_T$ one can neglect the effects of thermal average and think only about coherence. Then one can divide the sample into uncorrelated segments with the length L_φ , each of which has a fluctuation of order e^2/h . All the segments are in series, so their resistances should be added according to the Ohm's law. Denoting the resistance of each segment by R_φ we get

$$\text{Var} (R_\varphi) \approx \langle R_\varphi \rangle^4 \text{Var} (1/R_\varphi) = \langle R_\varphi \rangle^4 (e^2/h)^2 .$$

The average resistance is $\langle R \rangle = (L/L_\varphi)\langle R_\varphi \rangle$. Thus the variance of the resistance is

$$\text{Var}(R) = (L/L_\varphi) \text{Var}(R_\varphi) = (L/L_\varphi)\langle R_\varphi \rangle^4 (e^2/h)^2.$$

Coming back to conductance, we get

$$\text{Var}(G) = \langle R \rangle^4 \text{Var}(R) \approx (L_\varphi/L)^3 (e^2/h)^2.$$

Finally

$$\delta G = \text{constant} \times \frac{e^2}{h} \left(\frac{L_\varphi}{L} \right)^3. \quad (5.4)$$

Now let us discuss the role of thermal average. Consider two Feynman paths with the energies different by δE . They can be considered as uncorrelated after a time t_1 if the acquired phase difference $\delta\varphi = (\delta E)t_1/\hbar$ is of the order unity. In this time the electron diffuses a distance $L_1 = \sqrt{Dt_1} \approx \sqrt{\hbar D/(\delta E)}$. Now we can define the correlation energy at which the phase difference following diffusion at the distance L_1 is unity,

$$E_c(L_1) \equiv \hbar D/L_1^2. \quad (5.5)$$

Equating $E_c = kT$ we obtain the expression for L_T . If $L_\varphi \gg L_T$, then the total energy interval kT near the Fermi level is divided into subintervals of the width $E_c(L_\varphi) = \hbar/\tau_\varphi$ in which the phase coherence is maintained. These intervals can be assumed as uncorrelated,² their number being $N \approx kT/E_c(L_\varphi)$. As a result, the fluctuations are suppressed by the factor $N^{-1/2} = L_T/L_\varphi$. There exists a very useful interpolation formula (see, e. g. Ref. [10])

$$\delta G = \frac{g_s g_v \sqrt{12}}{2\sqrt{\beta}} \frac{e^2}{h} \left(\frac{L_\varphi}{L} \right)^{3/2} \left[1 + \frac{9}{2\pi} \left(\frac{L_\varphi}{L_T} \right)^2 \right]^{-1/2}. \quad (5.6)$$

5.4 Magnetoconductance fluctuations

In real experiments, people change either Fermi energy (by gates) or magnetic field H rather than impurity configuration. It is conventionally assumed that sufficiently large changes in the Fermi energy or in magnetic field is equivalent to a complete change of impurity configuration (the so-called ergodic hypothesis³). The reason is that there exist characteristic values of the correlation energy E_c or magnetic field, H_c . That provides a possibility to study ensemble averages without changing the sample. The magnetoconductance correlation function is defined as

$$F(\Delta H) \equiv \langle [\delta G(H) - \langle G(H) \rangle] [\delta G(H + \Delta H) - \langle G(H + \Delta H) \rangle] \rangle.$$

Thus the previous correlation function is just $F(0)$ while the correlation field H_c is defined as $F(H_c) = F(0)/2$.

To understand what is going on let us take into account that the correlation function contains the product of 4 Feynman path amplitudes, $A(i, H), A^*(j, H), A(k, H +$

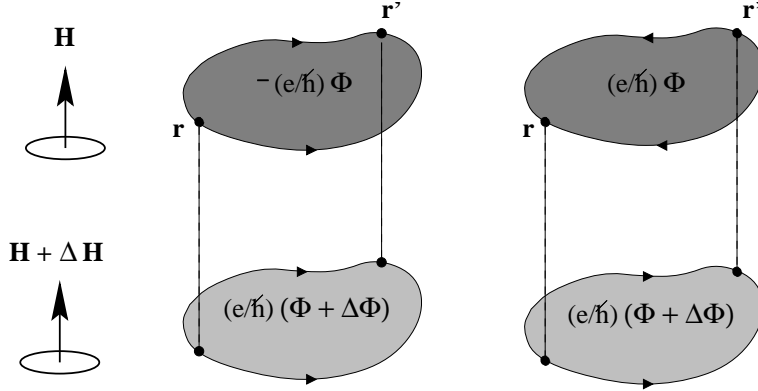


Figure 5.1: Illustration of the influence of magnetic field on the diffuson (left) and cooperon (right) contributions.

ΔH), $A^*(l, H + \Delta H)$ along various paths between the points \mathbf{r} and \mathbf{r}' , see Fig. 5.1. The term for which $i = l$, $j = k$, i. e.

$$A(i, H)A^*(j, H) \times A^*(i, H + \Delta H)A(j, H + \Delta H)$$

is called the *diffuson*. The physical meaning of this term is comes from the understanding that $A(i, H)$, $A^*(i, H)$ is just the classical probability for a diffusion from the point \mathbf{r} to the point \mathbf{r}' . The phase of this term in a magnetic field is

$$-\frac{e}{c} \oint \mathbf{A} \cdot d\mathbf{l} + \frac{e}{c} \oint (\mathbf{A} + \Delta\mathbf{A}) \cdot d\mathbf{l} = \frac{e}{\hbar} \Delta\Phi.$$

It contains only the increment of the flux, $\Delta\Phi = A \cdot \Delta H$ and does not contain the flux $A \cdot H$ itself.

For the *cooperon* which is the product

$$A_-(i, H)A_-(j, H)A_+(j, H + \Delta H)A_+(i, H + \Delta H)$$

where the $-$ sign refers to the trajectory from \mathbf{r}' to \mathbf{r} (i. e. time-reverted) while $+$ sign refers to the trajectory from \mathbf{r} to \mathbf{r}' , the phase is

$$\frac{e}{c} \oint \mathbf{A} \cdot d\mathbf{l} + \frac{e}{c} \oint (\mathbf{A} + \Delta\mathbf{A}) \cdot d\mathbf{l} = \frac{e}{\hbar} (2\Phi + \Delta\Phi).$$

In contrast to the diffuson, the cooperon is sensitive to the total flux Φ through the loop and therefore can be suppressed by a weak magnetic field.

We conclude that at $B \geq B_c$ only the diffuson contributes to the magnetoconductance fluctuations. The combined effect of magnetic field and inelastic scattering on the diffuson can be allowed for by the replacement $\tau_\varphi \rightarrow \tau_{\text{eff}}$ with

$$\tau_{\text{eff}}^{-1} = \tau_\varphi^{-1} + t_{\Delta H/2}^{-1}.$$

Here $t_{\Delta H/2}$ corresponds to the magnetic relaxation time t_H obtained for weak localization with substitution $H \rightarrow \Delta H/2$.

²This is actually true only at $W \ll L_\varphi$.

5.5 $I - V$ -curve of a metallic wire: Fluctuations

Let us consider an example - current-voltage curve of a small (but macroscopic) metallic wire with

$$\ell \ll b \ll L \ll L_\varphi.$$

Let us estimate the phase difference between the electrons which have the difference in energies $\delta\varepsilon$ and had a *total path* S within the sample:

$$\Delta\varphi_c \sim \frac{S[p(\varepsilon + \delta\varepsilon) - p(\varepsilon)]}{\hbar} \sim \frac{S\delta\varepsilon}{\hbar v}.$$

The electronic states can interfere if $\Delta\varphi_c \leq 1$. On the other hand, for a diffusive motion $S \sim vt \sim vL^2/D$. Thus

$$\delta\varepsilon \sim \frac{\hbar v}{S} \sim \frac{\hbar D}{L^2}.$$

As a result, $I - V$ curve must fluctuate at the voltage scale

$$V_c \sim \hbar D/(eL^2).$$

What is the *scale* of the fluctuations in current? To estimate it let us take into account that only the electrons within the layer eV near the Fermi level are important (at $T = 0$). However, the fluctuations within the strips having the width V_c are statistically independent, the number of such intervals being V/V_c (at $V \gg V_c$). Each interval contributes to the current as

$$\Delta\left(\frac{V_c}{R}\right) = \Delta\left(\frac{V_c}{L/\sigma b^2}\right) = \frac{V_c}{L} b^2 (\Delta\sigma) \sim \frac{V_c e^2}{\hbar}.$$

Here we have assumed 1d formula $\Delta\sigma b^2 \sim (e^2/\hbar)L$. Making use of statistical independence of fluctuations, we obtain

$$I_c \sim \frac{e^2}{\hbar} \sqrt{VV_c}.$$

Here we used the similarity to the diffusive motion:

$$x \sim \sqrt{Dt} \sim \sqrt{vt\ell} \sim \sqrt{S\ell}$$

with the mapping

$$S \rightarrow V, \quad \ell \rightarrow V_c.$$

It is interesting that

$$\frac{I_c}{V_c} \sim \frac{e^2}{\hbar} \frac{\sqrt{VV_c}}{V_c} \sim \frac{e^2}{\hbar} \sqrt{\frac{V}{V_c}}.$$

It *increases* with V . This one can face negative differential conductance and corresponding instabilities at

$$\frac{V}{V_c} > \left(\frac{\hbar}{e^2 R_0}\right)^2.$$

As we have seen, the interference interval is crucially important. At finite temperature, the energy spread T plays the same role as the interval eV above. Consequently, we have $T/(\delta\varepsilon)$ independent intervals, the summary effect being proportional to $\sqrt{T\delta\varepsilon}$. Thus the average manifestation of the interference goes as

$$\frac{\sqrt{T\delta\varepsilon}}{T} \sim \sqrt{\frac{\delta\varepsilon}{T}}.$$

Requesting $\delta\varepsilon \geq T$ we get

$$L \leq L_T \sim \sqrt{\hbar D/T}.$$

Thus in general (with some restrictions) one has to require $L \leq L_\varphi, L_T$ to observe mesoscopic phenomena.

5.6 Random matrix theory

Universal conductance fluctuations (UCF) can be described by a very different approach based on on statistical theory of energy levels in complex systems, developed originally in atomic physics (see [17] for a review). The approach was initially suggested by Altshuler and Shklovskii [29] and Imry [30]. The starting point is the Thouless formula for the dimensionless conductance $\mathcal{G} = G/G_0$, $G_0 = e^2/h$,

$$\mathcal{G} = E_c/\Delta, \tag{5.7}$$

where E_c is a typical shift of the discrete levels in a finite sample induced by changing the boundary conditions, say, from periodic to antiperiodic, while $\Delta = [g(\epsilon_F)L^d]^{-1}$ is a typical interlevel spacing at the Fermi energy.

The physical meaning of Eq. (5.7) can be understood having in mind that E_c is just the quantum mechanical uncertainty associated with the time required to move through the sample. Thus, for the diffusive system,

$$E_c = \hbar D/L^2, \tag{5.8}$$

where D is the diffusion constant. By the contrast, if the states are localized, E_c decays exponentially with the sample length L , $E_c \sim \exp(-L/\xi)$ where ξ is the localization length. If we formally introduce the *scale-dependent* diffusion constant, $D(L)$, then we come from Eq. (5.7) to a generalized Einstein relation,

$$\mathcal{G}(L) \sim hg(\epsilon_F)D(L)L^{d-2}$$

which is just the Drude formula for $D = (1/d)v_F\ell$.

According to Eq. (5.7), the reduced conductance \mathcal{G} equals to the number of levels, N_c , within the band of width E_c at the Fermi level. In metallic regime, $N_c \gg 1$. One could expect that that the variance of the quantity N_c defined as

$$\text{Var } N_c \equiv \langle N_c^2 \rangle - \langle N_c \rangle^2,$$

is of the order N_c . However from the microscopic theory it follows that

$$\text{Var } N_c \approx 1. \quad (5.9)$$

From this point of view, the fluctuations are anomalously *small*, though they are much larger than the thermodynamical ones.

The basic reason for that is that interlevel spacings are *correlated*. To quantitative treatment of the correlation the *Wigner-Dyson approach* is usually used. The approach assumes that the energy eigenvalues of complex systems may be approximated by those of random matrices \mathcal{H} for their Hamiltonians.

For pedagogical reasons, let us first discuss the case 2×2 symmetric random matrices,

$$\mathcal{H} = \begin{pmatrix} h_{11} & h_{12} \\ h_{12} & h_{22} \end{pmatrix}$$

with 3 independent random parameters h_{11}, h_{12}, h_{22} . The eigenvalues are

$$\begin{aligned} E_{\pm} &= (h_{\pm} \pm s)/2; \\ h_{\pm} &= h_{11} \pm h_{22}, \\ s &= \sqrt{h_{12}^2 + 4h_{12}^2}. \end{aligned}$$

Let us find the distribution of the eigenvalues, $p(E_+, E_-)$, assuming known the distributions of random matrix elements, $\mathcal{P}(h_{11}, h_{12}, h_{22})$. We have

$$\begin{aligned} p(E_+, E_-) &= \int dh_{11} dh_{22} dh_{12} \mathcal{P}(h_{11}, h_{12}, h_{22}) \\ &\quad \times \delta(E_+ - h_+/2 - s/2) \delta(E_- - h_+/2 + s/2). \end{aligned}$$

Since

$$dh_{11} dh_{22} = 2dh_+ dh_- \quad \text{and} \quad dh_+ ds = dE_+ dE_-$$

we get

$$p(E_+, E_-) \propto \int_{-s}^s dh_- \left| \frac{\partial h_{12}}{\partial s} \right| \dots \propto \frac{s}{2} \int_{-s}^s \frac{dh_-}{\sqrt{s^2 - h_-^2}} \propto \frac{\pi(E_+ - E_-)}{2}.$$

Thus we conclude that the probability to find two eigenvalues vanishes as $|E_2 - E_1|$ for close levels. This is the so-called *quantum level repulsion*.

The original Wigner-Dyson (WD) prescription which allows to prove several important theorems for the so-called *Gaussian orthogonal ensemble* is

$$p(\mathcal{H}) \propto \exp\left(-\frac{N}{\lambda_0^2} \text{Tr}(\mathcal{H}^2)\right),$$

where N is the matrix range while λ_0 is a numerical parameter. Using this assumption we obtain

$$p(E_+, E_-) = \frac{\pi(E_+ - E_-)}{2} \exp\left(-\frac{2(E_+^2 + E_-^2)}{\lambda_0^2}\right).$$

The probability for the interlevel spacing s is thus

$$p(s) = \frac{1}{2} \int_{-\infty}^{\infty} dh_+ p(E_+, E_-) \propto s \exp\left(-\frac{s^2}{\lambda_0^2}\right).$$

This is the famous *WD surmise* for the spacing distribution. It is exact for 2×2 matrices, but also tends to be true for any N . Indeed, for 2 very close levels the problem is effectively reduced to a 2×2 matrix, and we arrive at the expression

$$p(s) = \int dh_- \int dh_{12} \delta\left(s - \sqrt{h_-^2 + 4h_{12}^2}\right) \dots$$

which is proportional to s at small s .

Now let us turn to the case when the time-reversal symmetry is broken (say, by an external magnetic field). Then the corresponding Hamiltonian is complex (and Hermitian) rather than real symmetric, and the level spacing is

$$s = \sqrt{h_-^2 + (2\Re h_{12})^2 + (2\Im h_{12})^2}.$$

Now *three* parameters must vanish simultaneously for an accidental degeneracy $s = 0$. As a result, at small s

$$p(s) \propto s^2.$$

The general expression for the eigenvalue distribution can be constructed as

$$p(E_1 < E_2 \dots < E_n) \propto \prod_{i>j} (E_i - E_j)^\beta \exp\left(-\frac{\beta N}{\lambda_0^2} \sum_{-} E_i^2\right).$$

Here $\beta = 1, 2$ and 4 for the so-called orthogonal, unitary and symplectic ensembles.³

To prove the adequacy of the description one should calculate the conductance variance and compare it with microscopic derivation. To calculate the variance the Dyson-Mehta theorem can be used. It states that the variance of any random variable of the form⁴

$$A = \sum_i a(E_i)$$

can be expressed as

$$\text{Var } A = \frac{1}{\pi^2 \beta} \int_0^\infty t dt \left| \int dE e^{iEt} a(E) \right|^2.$$

For our purpose of evaluating N_c we assume

$$a(E) = 1 - \Theta(|E| - E_c/2). \quad (5.10)$$

³A symplectic matrix is a unitary matrix with real quaternion elements.

⁴This expression is called the *linear statistics* because it does not intermix different eigenvalues.

Applying the Dyson-Mehta theorem we find that the expression for $\text{Var } N_c$ diverges at small t unless the integral is cut off at $t \approx \Delta^{-1}$. As a result,

$$\text{Var } N_c = \frac{2}{\pi^2 \beta} \ln \frac{E_c}{\Delta} = \frac{2}{\pi^2 \beta} \ln \langle N_c \rangle.$$

This formula shows strong depression of fluctuations. However it differs from the microscopic derivation by a large logarithm. The discrepancy was analyzed by Altshuler and Shklovskii who pointed out that the above expression is actually valid for a *closed* system. In an *open* system the levels are broadened by the amount of the order E_c itself. To incorporate this broadening one can replace Eq. (5.10) by a smooth-edge expression

$$a(E) = (1 + E^2/E_c^2)^{-1}$$

to obtain $\text{Var } N_c = 1/4\beta$. Unfortunately, the numerical factor here depends on the particular shape of $a(E)$ and not universal. A generalization which yields the exact numerical factors exists only in 1D case (see [17] for a review). This is the case of 2-terminal resistance between the leads 1 and 2 which is given by the Landauer formula

$$\mathcal{G} = 2\text{Tr } S_{21} S_{21}^\dagger.$$

The matrix $S_{21} S_{21}^\dagger$ is Hermitian and positive, it has N transverse eigenvalues corresponding to N transverse modes with $0 \leq T_i \leq 1$. The result for the average distribution function for the parameters $\lambda_i \equiv (1 - T_i)/T_i$ has the form

$$p(\lambda) = \frac{2N\ell/L}{4\sqrt{\lambda(1+\lambda)}},$$

where it is assumed that $N\ell \gg L \gg \ell$.

Chapter 6

Quantum Hall Effect and Adiabatic Transport

6.1 Ordinary Hall effect

In a magnetic field electrons' trajectories are curved because of Lorentz force. As a result,

$$\mathbf{j} = \sigma_0 (\mathbf{E} + [\mathbf{j} \times \mathbf{H}]/nec), \quad \sigma_0 = ne^2\tau/m.$$

One can solve this vector equation to obtain the resistivity tensor

$$\hat{\rho} = \begin{bmatrix} \rho_0 & H/enc \\ -H/enc & \rho_0 \end{bmatrix}, \quad \rho_0 = 1/\sigma_0.$$

The inversion of this tensor gives the *conductivity tensor* with the components (in 2d case)

$$\sigma_{xx} = \frac{\sigma_0}{1 + (\omega_c\tau)^2}, \quad \sigma_{xy} = \frac{nec}{H} + \frac{1}{\omega_c\tau}\sigma_{xx}. \quad (6.1)$$

There is a striking similarity between the quantization of the conductance of a ballistic channel in units of e^2/h and of the Hall conductance.

6.2 Integer Quantum Hall effect - General Picture

In the quantum case one faces the Landau levels. We have seen that the number of states per unit area for a filled Landau level is

$$n_H = 1/2\pi a_H^2 = eH/ch.$$

Usually the *filling factor*

$$\nu = n/n_H$$

for a fractionally filled level is introduced. If one substitutes to the expression for the Hall component of the conductivity tensor and assumes $\omega_c\tau \rightarrow \infty$ he obtains $\sigma_{xy} = \nu e^2/h$.

This result seems very fundamental. Indeed, according to the electrodynamics, one can eliminate the electric field on a *spatially-homogeneous* system by assuming a drift velocity

$$\mathbf{v} = c[\mathbf{E} \times \mathbf{H}]/H^2.$$

Thus, the result seems fundamental independently whether classical or quantum mechanics is discussed.

Experimentally, the following picture was observed. It is clear that only violation of

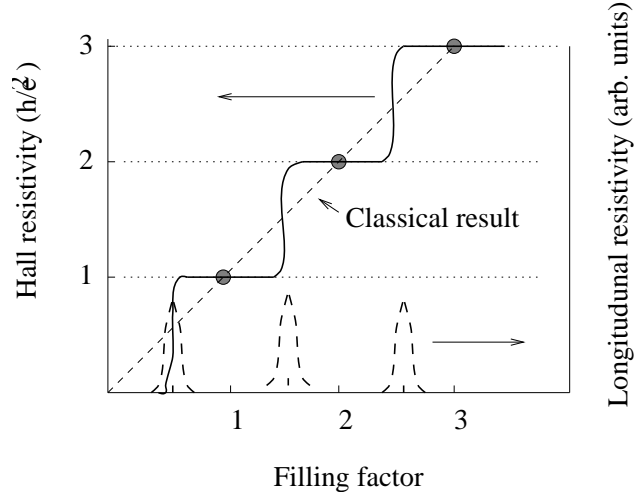


Figure 6.1: Schematic dependence of Hall resistance on filing factor.

the translational invariance can lead to such a picture. Thus one has to consider either impurities, or edges.

The generally accepted picture is as follows. Impurities violate the translational invariance. As a result, p_y is not a good quantum number any more, and Landau levels smear into sub-bands. The crucial point that the most of the states are *localized* and cannot carry the current.

To make the analysis as simple as possible let us discuss a 2d electrons in crossed electric and magnetic fields ($\mathbf{E} \parallel \mathbf{x}$, $\mathbf{H} \parallel \mathbf{z}$) and a single impurity at the point $\mathbf{r}_0 = \{x_0, y_0\}$. As we have seen (see *Shubnikov-de Haas effect*), the weak electric field leads to the energy shift $p_y v$ where $v = cE/H$ is the drift velocity in y -direction, as well as to the shift in the center-of-motion co-ordinate is shifted in x -direction by v/ω_c . Using the corresponding states as a basis, we can now expand the exact wave function as

$$\Psi = \sum_{np_y} c_{np_y} \psi_{np_y}(\mathbf{r}).$$

We get

$$\sum_{np_y} c_{np_y} [\hat{\mathcal{H}}_0 + V] \psi_{np_y} = \sum_{np_y} c_{np_y} [E_{np_y} + V] \psi_{np_y} = E \sum_{np_y} c_{np_y} \psi_{np_y}.$$

Because $V \propto \delta(\mathbf{r} - \mathbf{r}_0)$ one can write

$$c_{np_y} = \lambda \frac{\psi_{np_y}^*(\mathbf{r}_0) \Psi(\mathbf{r}_0)}{E - E_{np_y}}.$$

Now we recall that $\sum_{np_y} c_{np_y} \psi_{np_y}(\mathbf{r}_0) = \Psi(\mathbf{r}_0)$. Substituting the previous expression into this equation, we get the exact condition for eigen energy

$$\frac{1}{\lambda} = \sum_{n,p_y} \frac{|\psi_{n,p_y}(\mathbf{r}_0)|^2}{E - E_{n,p_y}}.$$

The right hand side of this equation as a function of the energy is shown below. One can

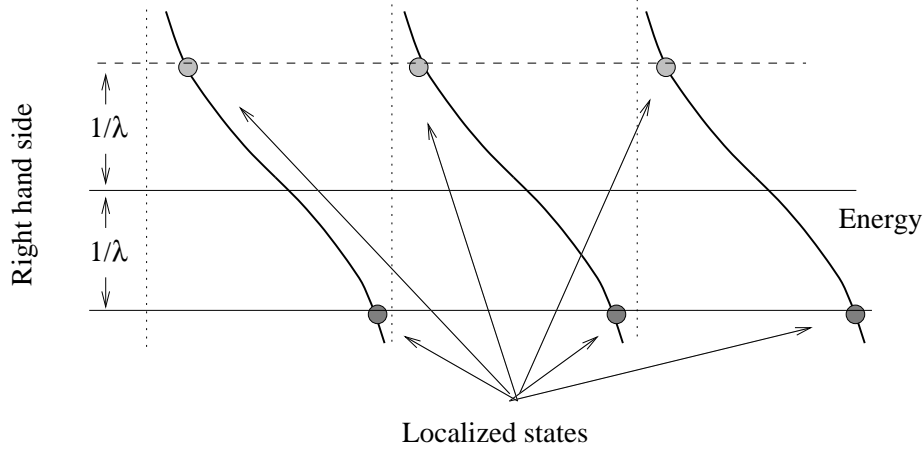


Figure 6.2: Formation of localized states in 2DEG in magnetic field.

find from this equation one completely localized state for each Landau level, its energy shift being proportional to λ . The lowest such state can be represented as (for $\mathbf{r}_0 = 0$)

$$\psi_{\text{loc}} \sim \exp \left[\frac{ixy}{2a_H^2} - \frac{x^2 + y^2}{4a_H^2} \right].$$

The other levels are almost unperturbed and extended.

Now let us take into account only the lowest Landau level which we assume to be completely filled. We have one localized state and $N-1$ extended ones where $N = A/2\pi a_H^2$, which we can label by the discrete quantum number k as

$$k = \frac{p_y L_y}{2\pi \hbar}.$$

Each mode behaves just as the transverse mode in a quantum channel, and the current is given as

$$I = -\frac{2}{h} \sum_{nk} (E_{n,k+1} - E_{nk}) = -\frac{2}{h} \sum_{nk} (E_{n,k_{\text{max}}} - E_{n,k_{\text{min}}}).$$

It is not trivial to prove this equation. It was done by R. Prange using gauge considerations.

Proof :

The main procedure is as follows. We have specified periodic boundary conditions along y -axis. Consider the system as a cylinder and introduce an auxiliary constant vector-potential along y axis as $2\pi\alpha/L_y$. The vector-potential of such a type can be eliminated by the gauge transform

$$\psi \rightarrow \exp(2\pi\alpha y/L_y)\psi.$$

This function can satisfy periodic boundary conditions only if α is integer. Thus the extended states which extend from 0 to L_y must depend on α .

The current operator can be written as $\hat{I} = (-e/h)d\mathcal{H}/d\alpha$, while the average current is

$$I = \langle \hat{I} \rangle = -\frac{e}{h} \frac{d}{d\alpha} \sum_{nk} E_{nk}(\alpha).$$

According to the construction of the quantum number k the introduction of the vector-potential leads to the replacement $k \rightarrow k + \alpha$. Thus

$$E_{n,k}|\alpha=1 = E_{n,k+1}|\alpha=0.$$

Replacing the derivative by the average value we get the result given above.

Thus we come to the following picture. as the Fermi level passes the regions of the

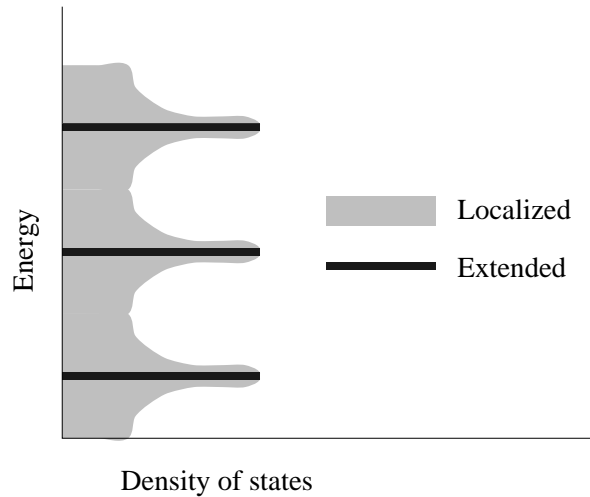


Figure 6.3: Density of states in 2DEG in magnetic field.

extended states the steps in Hall resistance and peaks at the longitudinal resistance occur. As we have shown, the current is *independent* of the density of states, only the number of occupied extended states is important.

Now we have to remember that the state with $k_{\max}(k_{\min})$ correspond to the upper (lower) edge of the sample if we map the quantum number k to the centers of gravity of the states. Thus we come in a natural way to edge states.

6.3 Edge Channels and Adiabatic Transport

The quantization of the conductance of the ballistic channel arises from the finite number of *propagating modes* each of which can carry only a very specific current. Thus it is tempting to consider the modes of an ideal finite system embedded into an external magnetic field. In this simplified picture we can obtain some understanding concerning the nature of localized and extended states.

Let us start from a *ideal* electron system confined by the potential $V(x)$ in the presence of the magnetic field $\mathbf{H} \parallel \mathbf{z}$. For a single spin component we have the Hamiltonian

$$\mathcal{H} = \frac{p_x^2}{2m} + \frac{[p_y + (eH/c)x]^2}{2m} + V(x).$$

It is natural to look for a solution in the form (\mathcal{H} commutes with p_y !)

$$|n, k\rangle = \psi_{nk}(x)e^{iky}$$

where $\hbar k$ is the eigenvalue of p_y . The average velocity for such a state is

$$v_n(k) = \left\langle n, k \left| \frac{p_y + (eH/c)x}{m} \right| n, k \right\rangle = \left\langle n, k \left| \frac{\partial \mathcal{H}}{\partial p_y} \right| n, k \right\rangle = \frac{1}{\hbar} \frac{dE_n(k)}{dk}.$$

It is easy to calculate such a velocity for a parabolic confinement,

$$V(x) = \frac{1}{2}m\omega_0^2 x^2.$$

The result is

$$v(k) = \frac{\hbar k}{M} = \frac{\hbar k}{m} \frac{1}{1 + (\omega_c/\omega_0)^2}.$$

To understand what is going on let us consider a classical orbit with the center (X, Y) . Then one can write

$$x = X + v_y/\omega_c, \quad y = Y - v_x/\omega_c.$$

The quantity $r_c = v/\omega_c$ is the cyclotron radius of the orbit. We have two constants of motion, the energy E and X . In a long strip of width W the trajectories can be classified as a cyclotron orbits, skipping orbits, or traversing trajectory. In the (X, E) space such trajectories are separated by the line

$$(X \pm W/2)^2 = r_c^2.$$

According to quantum mechanics, the motion is quantized, and we come to the following picture of quantum terms. The cyclotron orbits (solid lines) correspond to Landau level, and they have zero group velocity. We have not shown traversing trajectories which correspond to higher energies. Dashed lines reproduce two sets of edge states (corresponding to skipping orbits). These sets carry the currents in opposite directions.

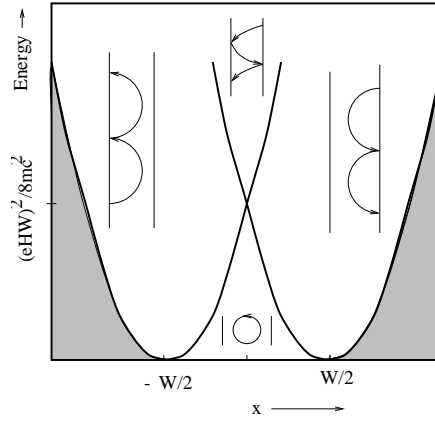


Figure 6.4: Typical electron trajectories in a 2D strip in magnetic field.

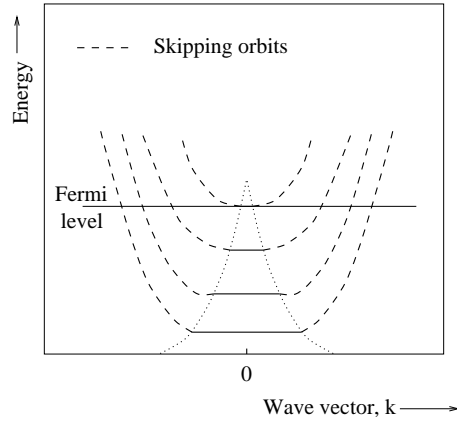


Figure 6.5: Electron terms in a 2D strip in magnetic field.

If the Fermi level is situated *between* the Landau levels, only the edge states can contribute to the current. Their dispersion law can be obtained (approximately) from the Bohr-Sommerfeld quantization condition,

$$h^{-1} \oint p_x dx + \gamma = 2\pi n, \quad n = 1, 2, \dots$$

One can show that for the rigid boundary the phase shift of the skipping orbit $\gamma = \pi/2$, while

$$p_x = mv_x = (eH/c)(Y - y).$$

Thus,

$$\frac{1}{a_H^2} \oint (Y - y) dx = 2\pi \frac{\Phi}{\Phi_0} = 2\pi \left(n - \frac{\gamma}{2\pi} \right).$$

Consider an electron at the Fermi level. Its energy consists of $(n - 1/2)\hbar\omega_c$ (+ spin contribution which I do not discuss now), as well the the part

$$E_G = \epsilon_F - (n - 1/2)\hbar\omega_c$$

due to electrostatic potential created by the edges, as well as by disorder. In an external potential, the center of the orbit moves with the drift velocity

$$v_d(\mathbf{R}) = \frac{c}{eH} [\nabla V(\mathbf{R}) \times \mathbf{H}]$$

which is parallel to the equipotentials. That can be easily shown from classical mechanics in a magnetic field. The typical spread of the wave function along the guiding center is spread within the range of magnetic length a_H . Now we can map the classical picture to quantum mechanics according to $\hbar k \rightarrow -x(eH/c)$. Thus, if the typical scale of the random potential of the disorder is greater than the magnetic length, we arrive at the picture.



Figure 6.6: Electron terms in the presence of long-range disorder.

Assume that the edges are in a local equilibrium. Thus if there is a difference $\delta\zeta$ chemical potentials *between the edges*, then each channel contributes $(e/h)\delta\zeta$ to the current in the *Hall direction*. The system appears robust because to obtain an inter-channel exchange one needs tunneling with exponentially low probability. Actually we have an almost ideal ballistic conductor and the only difference with the systems discussed earlier is that the edge channels with different directions of the current do not overlap in space.

In a typical realistic situation, the contacts are out of local equilibrium and the measured resistance depends on the properties of contacts. Consider for example, a situation when the edge channel at the lower edge are in equilibrium at chemical potential E_F , while the edge channel at the upper edge are not in local equilibrium. Then the current at the upper edge is not equipartitioned between N modes. Let f_n is the fraction of the total current I that is carried by states above E_F in the n th channel at the upper edge, $I_n = f_n I$. The voltage contact at the upper edge will measure a chemical potential which depends on how it is coupled to each of the edge channels. The transmission probability T_n is the fraction of the current I_n that is transmitted through the voltage probe to a reservoir at chemical potential $E_F + \delta\zeta$. The incoming current

$$I_{\text{in}} = \sum_n^N T_n f_n I, \quad \text{with} \quad \sum_n f_n = 1, \quad (6.2)$$

has to be balanced by an outgoing current,

$$I_{\text{out}} = \frac{e}{h} \delta\zeta (N - R) = \frac{e}{h} \delta\zeta \sum_n T_n, \quad (6.3)$$

since the voltage probe draws no net current. Thus the Hall resistance,

$$R_h = \frac{\delta\zeta}{eI} = \frac{h}{e^2} \left(\sum_n T_n f_n \right) \left(\sum_n T_n \right)^{-1}. \quad (6.4)$$

The Hall conductance remains quantized only if $f_n = 1/N$, or at $T_n = 1$. The first case corresponds to local equilibrium, while the second case corresponds to an ideal contact. The Landauer-Büttiker formalism forms the basis on which anomalies in the QHE due to absence of local equilibrium in combination with non-ideal contacts can be treated theoretically.

This is a simplified picture of the integer quantum Hall effect in the random potential. The real life is much more complicated. In particular, there exists an extremely interesting *fractional* quantum Hall effect, which manifests itself at fractional values of the filling factor. We do not discuss this effect in the present course.

Role of localization

As we have seen, at $H = 0$ a 2D system with disorder should have its states localized at all energies. However, only extended states are sensitive to the flux and can provide the QHE. At the same time, ranges of energies with only localized states are needed to pin E_F there and have finite plateaus. Thus, introduction of magnetic field must *delocalize some states*. As we have seen, extended modes appear near edges. However, extended states in a magnetic field are present also in the bulk of the conductor.

To discuss this phenomenon let us recall the main relevant quantities. First, let us note that the condition

$$\omega_c \tau \gg 1, \quad \text{or} \quad r_c \ll \ell, \quad r_c = v_F / \omega_c$$

for cyclotron motion is fully classical. In terms of quantum mechanical length, $a_H = \sqrt{c\hbar/eH}$ the classical cyclotron radius r_c can be written as

$$r_c \sim k_F a_H^2 \sim a_H \sqrt{E_F \hbar \omega_c} \sim a_H \sqrt{N}$$

where N is the number of full Landau levels. The *weak localization regime* corresponds to the inequality

$$a_H \ll \ell,$$

while the intermediate regime where $a_H \ll r_c$ while r_c can be comparable with ℓ also exists.

Strong magnetic field, $\omega_c \tau \gg 1$, $r_c \ll \ell$.

As we have discussed, in a uniform electric field the drift velocity directed along $[\mathbf{E} \times \mathbf{H}]$ appears, $v_d = c(E/H)$. This concept can be generalized for the case of a smooth random potential $V(x)$ which does not change a lot on the scale of cyclotron motion. Then, if r_c is much less than the correlation length d of the random potential, the guiding center moves along the equipotential line $V(\mathbf{r}) = V$. If its orbit is closed and embeds the area $A(V)$, then the typical frequency is

$$\frac{\omega_d}{2\pi} = \left[\oint \frac{dl}{v_d} \right]^{-1} = \frac{2c}{H} \left[\int \frac{dl dx_\perp}{dV} \right]^{-1} = \frac{2c}{H} \frac{\Delta V}{\Delta A},$$

where dx_\perp is an element of length in the direction of the potential gradient. Such a slow motion can be quantized for any Landau levels into locally equidistant levels with the separation $\hbar\omega_d$. The area between two quantized orbits is given by the relation

$$H \Delta A = \frac{\hbar c}{e} = \Phi_0; \quad \Delta A = 2\pi a_H^2.$$

Thus the flu of H in the area per state in a given Landau level corresponds to a flux quantum, as for free electron.

Let us assume that the amplitude of the random potential is much less than $\hbar\omega_c$, so there is no inter-Landau-level mixing. Then the potential energy of a properly quantized levels should be added to $\hbar\omega_c(j + 1/2)$ for j th Landau band. The levels correspond to the orbits running around the potential “hills”, or inside potential “lakes”. Both kinds of states are localized. There is one and only one energy, E_c , (in 2D case) at which the equipotential curves span the whole system (imagine filling up of the potential $V(\mathbf{r})$ “terrain” with water). The characteristic size of the orbit, ξ_p , may be defined by the r.m.s. of the area enclosed by the equipotential contours for the localized states. It must blow up at $E \rightarrow E_c$,

$$\xi_p \sim |E - E_c|^{-\nu_p}, \quad \nu_p \gtrsim 1.$$

Such an orbit provides the way to transfer an electron between the edges.

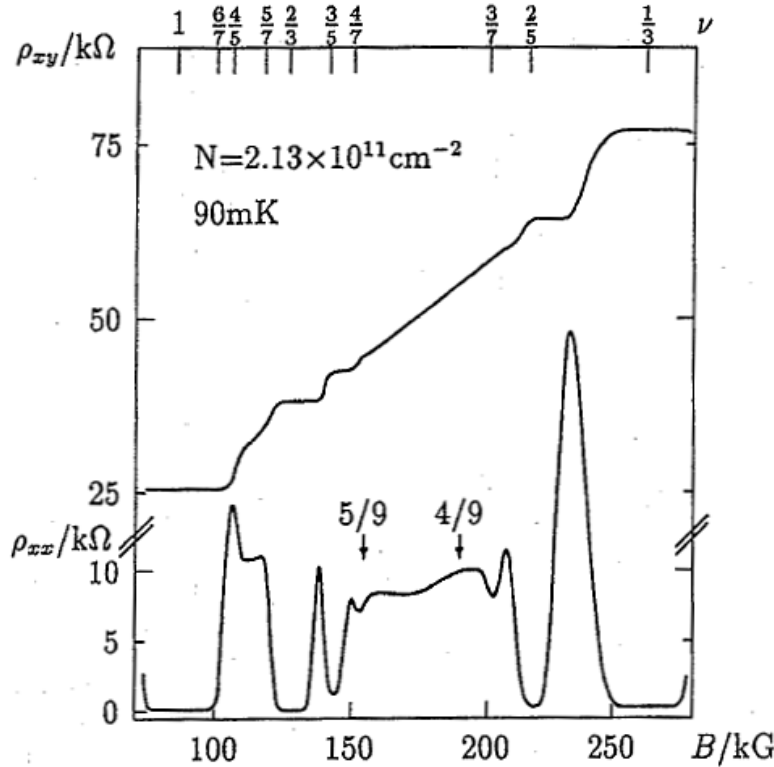
There is also a very interesting intermediate situation when

$$a_H \ll \ell \ll r_c, \quad \text{or} \quad \omega_c \tau \ll 1.$$

As was shown by Khmel'nitskii (1984), even in this region QHE plateaus can exist which are irrelevant to Landau levels.

6.4 Fractional Quantum Hall Effect

Fractional quantum Hall effect (FQHE) was discovered by the group of Tsui et Bell Laboratories [31]. Using a high-mobility GaAs/AlGaAs heterostructures they observed quantization of Hall conductance at filling factors $\nu = 1/3$ and $2/3$ at very low temperatures (below 1 K). Later more rich structure, as shown in Figs. 6.7 and 6.8 at fractional filling factors was discovered. It appears that only account of Coulomb interaction leads



The fractional quantum Hall effect. The Hall resistivity (upper curve) of the inversion layer in a high mobility AlGaAs/GaAs heterostructure shows plateaus at magnetic inductions B that correspond to the indicated filling factors ν . At the same filling factors, the magnetoresistivity (lower curve) shows minima

Figure 6.7:

to understanding of the problem. Now the studies of FQHE belong to the most active area of research. Below we shall provide a very brief sketch of the problems regarding electron-electron interaction in magnetic field and FQHE.

Few electron with Coulomb interaction

The role of electron-electron interaction is determined by the relation between the mean free distance between electrons, r_s , and the Bohr radius, $a_B = \epsilon \hbar^2 / m e^2$. At $r_s \ll a_B$ one can use the usual mean field description of interacting electrons, considering screening, plasmons, charge density waves, etc. However, at $r_s \geq a_B$ the interaction energy becomes larger than the average kinetic energy. As a result, there exists a strong electron-electron correlation, and the electrons tend to crystallize. It is known that magnetic field enhances these effects.

To get some understanding let us start with more simple problem of few electrons in a magnetic field. Historically, these studies appeared important because they led to discovery of a new state, the *incompressible electron liquid*, that is believed to transform into (Wigner) crystal at very low densities.

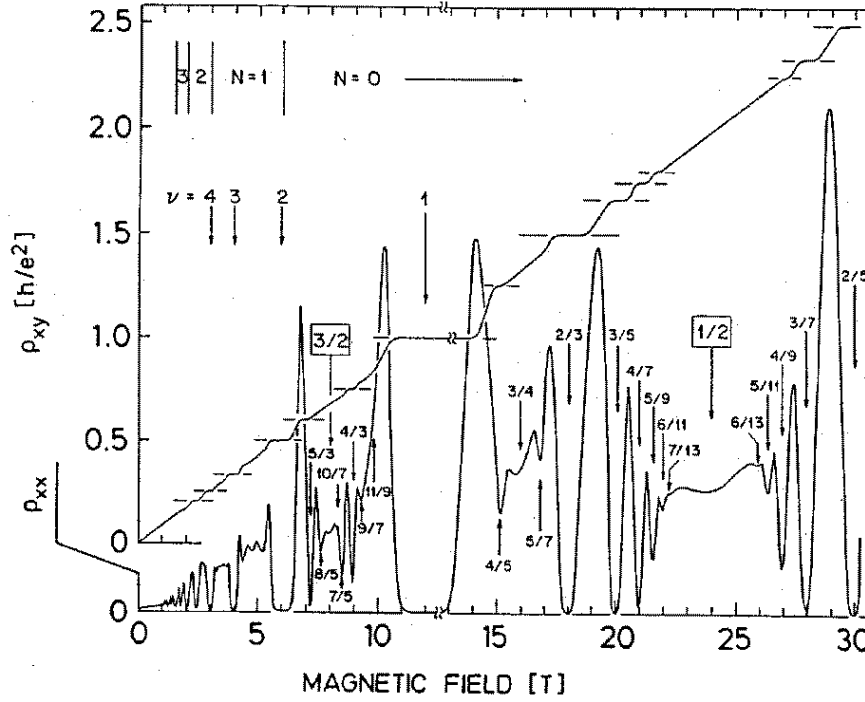


Figure 6.8: Recent results on the fractional quantum Hall effect.

Two electrons. Let us discuss the case of 2 electrons in a very strong magnetic field, $\hbar\omega_c \geq e^2/\epsilon a_H$. This inequality means that Landau levels are not mixed by the Coulomb interaction (see below).

Using symmetric gauge, $\mathbf{A} = (-Hy/2, Hx/2, 0)$ and introducing polar coordinates we easily obtain zeroth approximation Hamiltonian

$$\mathbf{H}_0 = -\frac{\hbar^2}{2m}\nabla^2 + \frac{m\omega_c^2\rho^2}{8} + \frac{\hbar\omega_c}{2i}\frac{\partial}{\partial\varphi},$$

$$\nabla^2 = \frac{\partial^2}{\partial\rho^2} + \frac{1}{\rho}\frac{\partial}{\partial\rho} + \frac{1}{\rho^2}\frac{\partial^2}{\partial\varphi^2}.$$

This Hamiltonian commutes with the angular momentum,

$$l_z = \frac{\hbar}{i}\frac{\partial}{\partial\varphi}.$$

Thus it is natural to classify the states using the eigenvalues $\hbar m$ of the angular momentum, l_z . The eigenfunctions have the form

$$\psi_{nm}(\rho, \varphi) = \frac{N_{nm}}{a_H^{|m|+1}}\rho^{|m|}e^{im\varphi}\exp\left(-\frac{\rho^2}{4a_H^2}\right)L_n^{|m|}\left(\frac{\rho^2}{2a_H^2}\right). \quad (6.5)$$

Here n is non-negative integer, m is integer, $L_n^{|m|}$ are Laguerre polynomials, while $N_{nm} = \sqrt{n!/2\pi 2^{|m|}(|m|+n)}$ are normalization factors. The energy eigenvalues are

$$E_{nm} = \hbar\omega_c[n + (|m| - m + 1)/2]. \quad (6.6)$$

The lowest Landau level corresponds to $n = 0$, $m > 0$. The Coulomb energy for the lowest state can be easily calculated as

$$E_C = \langle 0m | e^2 / \epsilon r | 0m \rangle = \frac{e^2}{\epsilon a_H} \frac{\Gamma(m + 1/2)}{m!}. \quad (6.7)$$

At large m it decays as $m^{-1/2}$.

Two electrons are described by the Hamiltonian

$$\mathcal{H}_0(1) + \mathcal{H}_0(2) + \mathcal{H}_{\text{int}}.$$

It can be rewritten through the center-of-mass coordinate, $\mathbf{R} = (\mathbf{r}_1 + \mathbf{r}_2)/\sqrt{2}$, and the relative coordinate, $\mathbf{r} = (\mathbf{r}_1 - \mathbf{r}_2)/\sqrt{2}$, as

$$\mathcal{H}_0(\mathbf{R}) + \mathcal{H}_0(\mathbf{r}) + \mathcal{H}_{\text{int}}(\mathbf{r}\sqrt{2}).$$

As a result, the center-of-mass motion is separated, and we look for a solution in the form

$$\Psi(\mathbf{R}, \mathbf{r}) = \phi(\mathbf{R})\psi(\mathbf{r}).$$

Now we are left with a *single-particle* problem for the relative motion.

Since the interaction energy is radially-symmetric one can look for a solution in the form

$$\psi(\mathbf{r}) = \mathcal{R}(r)e^{-im\varphi}$$

with odd m because of the Pauli principle [$\psi(-\mathbf{r}) = -\psi(\mathbf{r})$]. The radial Schrödinger equation is easily written in the dimensionless units as

$$-\frac{1}{2} \frac{d^2 \mathcal{R}}{dr^2} - \frac{1}{r} \frac{d\mathcal{R}}{dr} + \frac{1}{2} \left(\frac{m^2}{r^2} + m + \frac{r^2}{4} - \frac{\alpha}{r} \right) \mathcal{R} = E\mathcal{R}, \quad (6.8)$$

where r is measured in units of a_H , E is measured in the units of $\hbar\omega_c$, while dimensionless interaction constant is $\alpha = \sqrt{2}e^2/\epsilon a_H \hbar\omega_c$. At large magnetic field this equation can be solved perturbatively with respect to α . In the lowest approximation we obtain:

$$E_{0m}^{(1)} = \frac{\hbar\omega_c}{2} + \frac{e^2}{\epsilon a_H} \frac{\Gamma(m + 1/2)}{m!}. \quad (6.9)$$

The energy of the center-of-mass motion must be added.

We find that the interaction *destroys* the degeneracy of the lowest Landau level. At large m the correction decreases because the electrons are less sensitive to interaction at long distances.

Three electrons. For 3 electrons we can also strip the center-of-mass motion. It can be done by the transform $\boldsymbol{\rho} = \mathcal{O}\mathbf{r}$ where

$$\mathcal{O} = \begin{pmatrix} 1/\sqrt{2} & -1/\sqrt{2} & 0 \\ 1/\sqrt{6} & 1/\sqrt{6} & -2/\sqrt{6} \\ 1/\sqrt{3} & 1/\sqrt{3} & 1/\sqrt{3} \end{pmatrix}.$$

After the transform the interaction Hamiltonian can be written as

$$\mathcal{H}_{\text{int}} = \frac{e^2}{\epsilon\sqrt{2}} \left(\frac{1}{\rho_1} + \frac{2}{|\boldsymbol{\rho}_1 + \sqrt{3}\boldsymbol{\rho}_2|} + \frac{2}{|\sqrt{3}\boldsymbol{\rho}_2 - \boldsymbol{\rho}_1|} \right). \quad (6.10)$$

Again, we can write the eigen function as a product

$$\Psi(\boldsymbol{\rho}_1, \boldsymbol{\rho}_2, \boldsymbol{\rho}_3) = \phi(\boldsymbol{\rho}_3)\psi(\boldsymbol{\rho}_1, \boldsymbol{\rho}_2)$$

and in this way to reduce the problem to a two-particle one.

An important point is that the probability density must be invariant under rotation about multiples of $\pi/3$. The resulting Hamiltonian also commutes with the total angular momentum, \mathbf{L} . Then the states can be classified according to eigenvalues M of the orbital momentum. It was shown by R. Laughlin that a proper complete set to diagonalize a 3-electron system can be written as

$$|m, m'\rangle = \frac{F}{2} [(z_2 + iz_1)^{3m} - (z_2 - iz_1)^{3m}] (z_1^2 + z_2^2)^{m'} e^{-(|z_1|^2 + |z_2|^2)}. \quad (6.11)$$

Here $z_i = \xi_i + \eta_i$, ξ, η are the Cartesian components of the vector $\boldsymbol{\rho}_i/a_H$, F is a normalization factor. The states (6.11) are the eigenstates of the total angular momentum with $M = 3(m + m')$.

To diagonalize the system one has to solve the secular equation

$$\det |e\delta_{mm'}\delta_{m'm'} - \langle mm'|\mathcal{H}_{\text{int}}|mm'\rangle| = 0.$$

The crucial point is that the basis (6.11) is an extremely good starting approximation since off-diagonal elements of \mathcal{H}_{int} are typically at least 10 times less than the diagonal ones.

The minimum angular momentum for which a non-degenerate solution exists is $M = 3$ ($m = 0, m' = 1$). The next solution corresponds to $M = 9$, it is combined from the states (3,0) and (1,3). These states have the lowest energy at $\mathcal{H}_{\text{int}} = 0$. The ‘‘charge density’’ for the state with $M = 9$ is 1/3 comparing to the state with $M = 3$. Since the angular momentum is conserved and the angular momentum corresponds to the area of an electronic state, the 3 electrons are ‘‘incompressible’’.

Fractional quantum Hall states

It is impossible to diagonalize exactly the system of many electron states. An extremely effective approximate guess was suggested by R. Laughlin which we shall discuss for the

case of very large magnetic field when only the lowest Landau level is important. The single-electron states for that case can be written as

$$\langle \mathbf{r} | 0m \rangle = \frac{N_m}{a_H} z^m e^{-|z|^2/4},$$

where $z = x + iy$. The complete set of N -electron states with total angular momentum $M = \sum_{\nu=1}^N m_\nu$ are the Slater determinants

$$\Psi(1 \dots N) = \sum_{P(\nu_1 \dots \nu_N)} (-1)^P \prod_{\mu=1}^N N_{m_\mu} z_{\nu_\mu}^{m_\mu} \exp\left(-\frac{1}{4} \sum_{\alpha=1}^N |z_\alpha|^2\right).$$

Since the ground state in the independent band approximation is a combination of Slater determinants, its general form is

$$\Psi(1 \dots N) = \prod_{j < k} f(z_j - z_k) \exp\left(-\frac{1}{4} \sum_{\alpha=1}^N |z_\alpha|^2\right).$$

There are several requirements to the functions $f(z)$:

- The function $f(z)$ must be a polynomial of z ;
- Since Ψ should be a Fermion state, $f(-z) = -f(z)$;
- Ψ can be chosen as an eigenfunction of the total angular momentum. Therefore, the function $f(z)$ has to be *homogeneous*.

The simplest choice is

$$f(z) = z^m, \quad (n \text{ odd}).$$

Thus the approximate wave function has the form

$$\Psi(1 \dots N) = \prod_{j < k} (z_j - z_k)^m \exp\left(-\frac{1}{4} \sum_{\alpha=1}^N |z_\alpha|^2\right). \quad (6.12)$$

The *Laughlin state* (6.12) describes a liquid-like system. The two-particle correlation function

$$g_2^{(m)}(z_1, z_2) = \int \prod_{\nu=3}^N d\mathbf{r}_\nu |\Psi(1 \dots N)|^2$$

at small distances is proportional to $|z_1 - z_2|^m$ that reflects the Pauli principle for the electrons. The smallest possible value of m is 3. The total angular momentum is just $M = Nm$, while the area covered by the electrons is $A = N(2\pi m a_H^2)$. Thus the average electron density is $(2\pi m a_H^2)^{-1}$, and the filling factor is $\nu = 1/m$. To keep electrostatic stability one has to add the positive background.

The estimate for the Coulomb energy for the Laughlin state can be obtained as

$$E_C^{(m)} = \frac{N(N-1)}{2A} \frac{e^2}{\epsilon} \int \frac{d^2r}{r} [g_2^{(m)}(r) - 1].$$

Because the correlation function decays strongly at small distances the incompressible liquid state appears more stable than the Wigner crystal. An interesting fact is that the Laughlin state appears the exact ground state for $\nu = 1/m$ in the case of contact interaction, $\mathcal{H}_{\text{int}}(\mathbf{r}) \propto \delta(\mathbf{r})$.

As a consequence of the electron-hole symmetry it is easy to find the state corresponding to the filling factor $(1 - \nu)$ if the state for ν is known.

Elementary excitations

Elementary excitations are important both for transport and dynamics. Changing of energy of the electron system can be achieved by its compression, or, equivalently, by changing of angular momentum while keeping the neutralizing background.

In other words, it means that new quasielectrons or quasiholes are introduced into the state Ψ_ν if $\nu \neq 1/m$. An introduction of a quasihole can be represented as

$$\Psi_\nu^+ = A^+(z_0)\Psi_\nu(z_1 \dots z_n), \quad A^+(z_0) = \prod_{j=1}^N (z_j - z_0).$$

Let us estimate the effective charge of this excitation. The average area per particle which is covered in the state with filling factor $\nu = 1/m$ is $(N-1)(2\pi m a_H^2)$. It can be seen by direct calculation of the integral. The corresponding charge density is

$$\rho_0 = \frac{-Ne}{(N-1)(2\pi m a_H^2)} \approx -\frac{e}{2\pi m a_H^2}.$$

Thus, each electron occupies the area with m flux quanta. Its charge must be compensated by a positive background.

In the state Ψ_ν^+ the maximum angular momentum per particle is increased by $2\pi a_H^2$. This corresponds to the change in the charge density which is equivalent to the positive charge $+e/m$.

Quasielectrons can be created in a similar way,

$$\Psi_\nu^- = A^-(z_0)\Psi_\nu(z_1 \dots z_n), \quad A^-(z_0) = \prod_{j=1}^N \left(\frac{\partial}{\partial z_j} - z_0^* \right).$$

Here the partial derivative acts only on the polynomial part of the wave function Ψ_ν leaving alone the Gaussian part. It can be shown that the effective charge of the quasielectron is $-e/m$.

The gaps between the ground and excited states were observed directly from temperature dependences of conductance. It appears that the quasiparticles can be considered as

particle with so-called fractional statistics – *anyons*. Very interesting *collective excitations* were also predicted and observed experimentally by inelastic light scattering. H. Störmer, D. Tsui and R. Laughlin were awarded by the Nobel Prize 1998 for their discovery of FQHE.

However, the story is not over. Very specific features of Hall conductance were observed at $\nu = p/q$ where p, q are integers, both for odd and even denominator q . These features were not explained by original theory by Laughlin. It appears, that at odd denominators the electrons also condense in some quantum liquids. However, the properties of that liquids differ significantly from those of the incompressible Laughlin liquid.

The above discussion is definitely not an “explanation” of FQHE. It just demonstrates some basic trends in the field. More work has to be done to understand the whole physical picture and to construct a proper transport theory.

Chapter 7

Noise in mesoscopic systems

Shot noise, the time-dependent fluctuations in the electrical current due to the discreteness of the electron charge.

The shot-noise power in small conductors possesses special features which are important both for understanding correlations phenomena in mesoscopic systems and for application of mesoscopic devices. The noise is maximal if the electron transmission through the system is fully uncorrelated. This maximal value is called the Poisson limit. In mesoscopic systems it can be suppressed as a result of correlations in the electron transmission imposed by the Pauli principle. This suppression takes on simple universal values in a symmetric double-barrier junction (suppression factor $\frac{1}{2}$), a disordered metal (factor $\frac{1}{3}$), and a chaotic cavity (factor $\frac{1}{4}$). Loss of phase coherence has no effect on this shot-noise suppression, while thermalization of the electrons due to electron-electron scattering increases the shot noise slightly. Sub-Poissonian shot noise has been observed experimentally. So far unobserved phenomena involve the interplay of shot noise with the Aharonov-Bohm effect, Andreev reflection, and the fractional quantum Hall effect.

Below we discuss these processes following the review Ref. [19].

7.1 Current fluctuations

In 1918 Schottky reported that in ideal vacuum tubes, where all sources of spurious noise had been eliminated, there remained two types of noise in the electrical current, described by him as the *Wärmeeffekt* and the *Schroteffekt*. The first type of noise became known as Johnson-Nyquist noise, or simply thermal noise. We discussed this type of noise in connection with fluctuation-dissipation theorem. It is due to the thermal motion of the electrons and occurs in any conductor. The second type of noise is called shot noise, caused by the discreteness of the charge of the carriers of the electrical current. Not all conductors exhibit shot noise.

Noise is characterized by its spectral density or power spectrum $P(\omega)$, which is the

Fourier transform at frequency ω of the current-current correlation function,

$$P(\omega) = 2 \int_{-\infty}^{\infty} dt e^{i\omega t} \langle \Delta I(t + t_0) \Delta I(t_0) \rangle . \quad (7.1)$$

Here $\Delta I(t)$ denotes the time-dependent fluctuations in the current at a given voltage V and temperature T . The brackets $\langle \dots \rangle$ indicate an ensemble average or, equivalently, an average over the initial time t_0 . Both thermal and shot noise have a white power spectrum — that is, the noise power does not depend on ω over a very wide frequency range. Shot noise ($V \neq 0$, $T = 0$) is more interesting than the thermal one, because it gives information on the temporal correlation of the electrons, which is not contained in the conductance. In devices such as tunnel junctions, Schottky barrier diodes, p - n junctions, and thermionic vacuum diodes, the electrons are transmitted randomly and independently of each other. The transfer of electrons can be described by Poisson statistics, which is used to analyze events that are uncorrelated in time. For these devices the shot noise has its maximum value

$$P = 2eI \equiv P_{\text{Poisson}} , \quad (7.2)$$

proportional to the time-averaged current I .¹ Correlations suppress the low-frequency shot noise below P_{Poisson} . One source of correlations, operative even for non-interacting electrons, is the Pauli principle, which forbids multiple occupancy of the same single-particle state. A typical example is an ideal ballistic point contact, where $P = 0$ because the stream of electrons is completely correlated by the Pauli principle in the absence of impurity scattering.

Progress in nanofabrication technology has revived the interest in shot noise, because nanostructures allow measurements to be made on “mesoscopic” length scales that were previously inaccessible. The mesoscopic length scale is much greater than atomic dimensions, but small compared to the scattering lengths associated with various inelastic processes. Mesoscopic systems have been studied extensively through their conductance. Noise measurements are much more difficult, but the sensitivity of the experiments has made a remarkable progress in the last years.

To analyze the noise properties we shall apply scattering formalism. Incoming and outgoing waves are specified as shown in Fig. 7.1 Each lead contains N incoming and N outgoing modes at energy ε .² The incoming and outgoing modes are related by a $2N \times 2N$ scattering matrix S

$$\begin{pmatrix} O_1 \\ O_2 \end{pmatrix} = S \begin{pmatrix} I_1 \\ I_2 \end{pmatrix} , \quad (7.3)$$

where I_1, O_1, I_2, O_2 are the N -component vectors denoting the amplitudes of the incoming (I) and outgoing (O) modes in lead 1 and lead 2. The scattering matrix can be decomposed

¹Equation (7.2) is valid for $\omega < \tau^{-1}$, with τ the width of a one-electron current pulse. For higher frequencies the shot noise vanishes.

²We assume only elastic scattering so that energy is conserved.

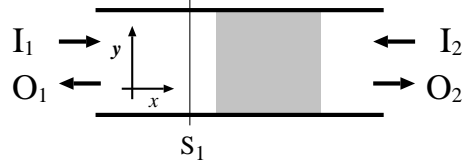


Figure 7.1: Schematic representation of the transport through the conductor. Incoming states (I) are scattered into outgoing states (O), by a scattering region (dashed). A cross section in lead 1 and its coordinates are indicated.

in $N \times N$ reflection and transmission matrices,

$$\mathbf{S} = \begin{pmatrix} s_{11} & s_{12} \\ s_{21} & s_{22} \end{pmatrix} \equiv \begin{pmatrix} r & t' \\ t & r' \end{pmatrix}, \quad (7.4)$$

where the $N \times N$ matrix s_{ba} contains the amplitudes $s_{bn,am}$ from incoming mode m in lead a to outgoing mode n in lead b . Because of flux conservation \mathbf{S} is a unitary matrix. Moreover, in the presence of time-reversal symmetry \mathbf{S} is symmetric.

The current operator in lead 1 is given by

$$\hat{I}(t) = \frac{e}{h} \sum_{\alpha,\beta} \int_0^\infty d\varepsilon \int_0^\infty d\varepsilon' I_{\alpha\beta}(\varepsilon, \varepsilon') \hat{a}_\alpha^\dagger(\varepsilon) \hat{a}_\beta(\varepsilon') e^{it(\varepsilon-\varepsilon')/\hbar}, \quad (7.5)$$

where $\hat{a}_\alpha^\dagger(\varepsilon)$ [$\hat{a}_\alpha(\varepsilon)$] is the creation [annihilation] operator of scattering state $\psi_\alpha(\mathbf{r}, \varepsilon)$. We have introduced the indices $\alpha \equiv (a, m)$, $\beta \equiv (b, n)$ and the coordinate $\mathbf{r} = (x, \mathbf{y})$. The matrix element $I_{\alpha\beta}(\varepsilon, \varepsilon')$ is determined by the value of the current at cross section S_1 in lead 1,

$$I_{\alpha\beta}(\varepsilon, \varepsilon') = \frac{1}{2} \int_{S_1} d\mathbf{y} \{ \psi_\alpha(\mathbf{r}, \varepsilon) [\hat{v}_x \psi_\beta(\mathbf{r}, \varepsilon')]^* + \psi_\beta^*(\mathbf{r}, \varepsilon') \hat{v}_x \psi_\alpha(\mathbf{r}, \varepsilon) \}. \quad (7.6)$$

Here, \hat{v}_x is the velocity operator in the x -direction. At equal energies, Eq. (7.6) simplifies to

$$I_{am,bn}(\varepsilon, \varepsilon) = \delta_{a1} \delta_{ab} \delta_{mn} - \sum_{p=1}^N s_{1p,am}(\varepsilon) s_{1p,bn}^*(\varepsilon). \quad (7.7)$$

The average current follows from

$$\langle \hat{a}_\alpha^\dagger(\varepsilon) \hat{a}_\beta(\varepsilon') \rangle = \delta_{\alpha\beta} \delta(\varepsilon - \varepsilon') f_a(\varepsilon), \quad (7.8)$$

where f_a is the Fermi-Dirac distribution function in reservoir a :

$$f_1(\varepsilon) = f(\varepsilon - E_F - eV), \quad (9a)$$

$$f_2(\varepsilon) = f(\varepsilon - E_F), \quad (9b)$$

$$f(x) = [1 + \exp(x/k_B T)]^{-1}, \quad (9c)$$

with Fermi energy E_F . The result is ³

$$\langle \hat{I}(t) \rangle = \frac{e}{h} \sum_{\alpha} \int_0^{\infty} d\varepsilon f_{\alpha}(\varepsilon) I_{\alpha\alpha}(\varepsilon, \varepsilon) = \frac{e}{h} \int_0^{\infty} d\varepsilon [f_1(\varepsilon) - f_2(\varepsilon)] \text{Tr } \mathbf{t}(\varepsilon) \mathbf{t}^{\dagger}(\varepsilon), \quad (7.10)$$

where we have substituted Eq. (7.7) and used the unitarity of \mathbf{S} . The linear-response conductance, $G \equiv \lim_{V \rightarrow 0} \langle I \rangle / V$, becomes

$$G = \frac{e^2}{h} \int_0^{\infty} d\varepsilon \left(-\frac{\partial f}{\partial \varepsilon} \right) \text{Tr } \mathbf{t}(\varepsilon) \mathbf{t}^{\dagger}(\varepsilon). \quad (7.11)$$

At zero temperature we reproduce the Landauer formula (per spin)

$$G = \frac{e^2}{h} \text{Tr } \mathbf{t} \mathbf{t}^{\dagger} = \frac{e^2}{h} \sum_{n=1}^N T_n. \quad (7.12)$$

Here \mathbf{t} is taken at E_F and $T_n \in [0, 1]$ is an eigenvalue of $\mathbf{t} \mathbf{t}^{\dagger}$. The conductance is thus fully determined by the transmission eigenvalues. Knowledge of the transmission eigenstates, each of which can be a complicated superposition of incoming modes, is not required.

In order to evaluate the shot-noise power we substitute the current operator (7.5) into Eq. (7.1) and determine the expectation value. It can be shown from direct quantum-mechanical calculation that

$$\langle \hat{a}_1^{\dagger} \hat{a}_2 \hat{a}_3^{\dagger} \hat{a}_4 \rangle - \langle \hat{a}_1^{\dagger} \hat{a}_2 \rangle \langle \hat{a}_3^{\dagger} \hat{a}_4 \rangle = \delta_{14} \delta_{23} f_1 (1 - f_2) \equiv \Delta_{1234}, \quad (7.13)$$

where *e.g.* δ_{12} stands for $\delta_{\alpha\beta} \delta(\varepsilon - \varepsilon')$. Equation (7.13) shows that there are cross correlations between different scattering states. Although this bears no effect on the time-averaged current, it is essential for the current fluctuations. For the noise power at low-frequency limit one finds,

$$P = 2 \frac{e^2}{h} \int_0^{\infty} d\varepsilon \{ [f_1(1 - f_2) + f_2(1 - f_1)] \text{Tr } \mathbf{t} \mathbf{t}^{\dagger} (1 - \mathbf{t} \mathbf{t}^{\dagger}) + [f_1(1 - f_1) + f_2(1 - f_2)] \text{Tr } \mathbf{t} \mathbf{t}^{\dagger} \mathbf{t} \mathbf{t}^{\dagger} \}, \quad (7.14)$$

where we have again used the unitarity of \mathbf{S} .

Equation (7.14) allows us to evaluate the noise for various cases. Below we will assume that eV and $k_B T$ are small enough to neglect the energy dependence of the transmission matrix, so that we can take \mathbf{t} at $\varepsilon = E_F$. Let us first determine the noise in equilibrium, *i.e.* for $V = 0$. Using the relation $f(1 - f) = -k_B T \partial f / \partial \varepsilon$ we find

$$P = 4k_B T \frac{e^2}{h} \text{Tr } \mathbf{t} \mathbf{t}^{\dagger} = 4k_B T \frac{e^2}{h} \sum_{n=1}^N T_n, \quad (7.15)$$

³Note that in the above derivations the absence of spin and valley degeneracy has been assumed for notational convenience. It can be easily included.

which is indeed the Johnson-Nyquist formula. For the shot-noise power at zero temperature we obtain

$$P = 2eV \frac{e^2}{h} \text{Tr} \mathbf{t} \mathbf{t}^\dagger (1 - \mathbf{t} \mathbf{t}^\dagger) = 2eV \frac{e^2}{h} \sum_{n=1}^N T_n (1 - T_n) . \quad (7.16)$$

One notes, that P is again only a function of the transmission eigenvalues.

It is clear from Eq. (7.16) that a transmission eigenstate for which $T_n = 1$ does not contribute to the shot noise. This is easily understood: At zero temperature there is a non-fluctuating incoming electron stream. If there is complete transmission, the transmitted electron stream will be noise free, too. If T_n decreases, the transmitted electron stream deviates in time from the average current. The resulting shot noise P is still smaller than P_{Poisson} , because the transmitted electrons are correlated due to the Pauli principle. Only if $T_n \ll 1$, the transmitted electrons are uncorrelated, yielding full Poisson noise.

The generalization of Eq. (7.16) to the non-zero voltage, non-zero temperature case is

$$P = 2 \frac{e^2}{h} \sum_{n=1}^N [2k_B T T_n^2 + T_n (1 - T_n) eV \coth(eV/2k_B T)] . \quad (7.17)$$

The crossover from the thermal noise (7.15) to the shot noise (7.16) depends on the transmission eigenvalues.

7.2 Two Simple Applications

The above results are valid for conductors with arbitrary (elastic) scattering. If the transmission eigenvalues are known, the conduction and noise properties can be readily calculated. Below, this is illustrated for two simple systems. More complicated conductors are discussed in Secs. 7.4–7.4.

Tunnel barrier

In a tunnel barrier, electrons have a very small probability of being transmitted. We model this by taking $T_n \ll 1$, for all n . Substitution into the formula for the shot noise (7.16) and the Landauer formula for the conductance (7.12) yields $P = P_{\text{Poisson}}$ at zero temperature. For arbitrary temperature we obtain from Eq. (7.17),

$$P = \coth(eV/2k_B T) P_{\text{Poisson}} . \quad (7.18)$$

This equation, describes the crossover from thermal noise to full Poisson noise. For tunnel barriers this crossover is governed entirely by the ratio $eV/k_B T$ and not by details of the conductor. This behavior has been observed in various systems.

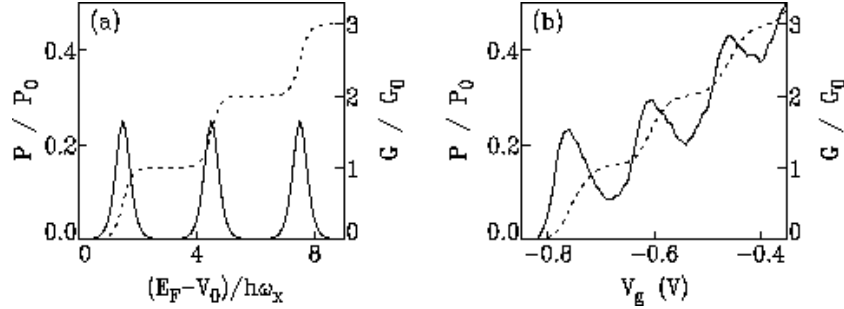


Figure 7.2: (a) Conductance G (dashed line) and shot-noise power P (full line) versus Fermi energy of a two-dimensional quantum point contact, according to the saddle-point model, with $\omega_y = 3\omega_x$. (b) Experimentally observed G and P versus gate voltage V_g (unpublished data from Reznikov *et al.* similar to the experiment of Ref. [32], but at a lower temperature $T = 0.4$ K).

Quantum Point Contact

As we know, the conductance displays a stepwise increase in units of G_0 as a function of V_g . At the conductance plateaus the shot noise is absent, as follows from Eq. (7.16). However, in between the plateaus, where the conductance increases by G_0 , there is a transmission eigenvalue which is between 0 and 1. As a consequence, the shot noise has a peak. Results for the conductance and the shot-noise power are displayed in Fig. 7.2a. The shot noise peaks in between the conductance plateaus and is absent on the plateaus. For large N , the peaks in the shot noise become negligible with respect to the Poisson noise, in agreement with the classical result.

The prediction of this quantum size-effect in the shot noise formed a challenge for experimentalists. Recent experiments at high frequencies by Reznikov *et al.* [32] have unambiguously demonstrated the occurrence of suppressed shot noise on the conductance plateaus. Experimental data of Reznikov *et al.* are shown in Fig. 7.2b.

7.3 Phase Breaking, Thermalization, and Inelastic Scattering

Noise measurements require rather high currents, which enhance the rate of scattering processes other than purely elastic scattering. The phase-coherent transmission approach is then no longer valid. Below, we discuss a model in which the conductor is divided in separate, phase-coherent parts connected by charge-conserving reservoirs. This model includes the following types of scattering:

- *Quasi-elastic scattering.* Due to weak coupling with external degrees of freedom the electron-wave function gets dephased, but its energy is conserved. In metals, this scattering is caused by fluctuations in the electromagnetic field.

- *Electron heating.* Electron-electron scattering exchanges energy between the electrons, but the total energy of the electron gas is conserved. The distribution function is therefore assumed to be a Fermi-Dirac distribution at a temperature above the lattice temperature.
- *Inelastic scattering.* Due to electron-phonon interactions the electrons exchange energy with the lattice. The electrons emerging from the reservoir are distributed according to the Fermi-Dirac distribution, at the lattice temperature T .

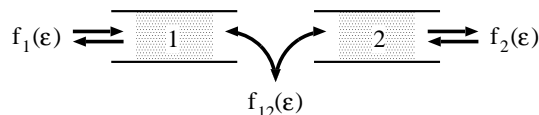


Figure 7.3: Additional scattering inside the conductor is modeled by dividing it in two parts and connecting them through another reservoir. The electron distributions in the left and the right reservoir, $f_1(\varepsilon)$ and $f_2(\varepsilon)$, are Fermi-Dirac distributions. The distribution $f_{12}(\varepsilon)$ in the intermediate reservoir depends on the type of scattering.

The model is depicted in Fig. 7.3. The conductors 1 and 2 are connected via a reservoir with distribution function $f_{12}(\varepsilon)$. The time-averaged current I_m through conductor $m = 1, 2$ is given by

$$I_1 = (G_1/e) \int d\varepsilon [f_1(\varepsilon) - f_{12}(\varepsilon)], \quad (19a)$$

$$I_2 = (G_2/e) \int d\varepsilon [f_{12}(\varepsilon) - f_2(\varepsilon)]. \quad (19b)$$

The conductance $G_m \equiv 1/R_m = G_0 \sum_{n=1}^N T_n^{(m)}$, with $T_n^{(m)}$ the n -th transmission eigenvalue of conductor m . We assume small eV and $k_B T$, so that the energy dependence of the transmission eigenvalues can be neglected.

Current conservation requires that $I_1 = I_2 \equiv I$. The total resistance of the conductor is given by Ohm's law,

$$R = R_1 + R_2, \quad (7.20)$$

for all three types of scattering that we consider.⁴

The time-averaged current (7.19) depends on the average distribution $f_{12}(\varepsilon)$ in the reservoir between conductors 1 and 2. In order to calculate the current fluctuations, we need to take into account that this distribution varies in time. We denote the time-dependent distribution by $\tilde{f}_{12}(\varepsilon, t)$. The fluctuating current through conductor 1 or 2 causes electrostatic potential fluctuations $\delta\phi_{12}(t)$ in the reservoir, which enforce charge neutrality. Assuming that the reservoir has a Fermi-Dirac distribution $\tilde{f}_{12}(\varepsilon, t) = f[\varepsilon -$

⁴The model is not suitable for transport in the ballistic regime or in the quantum Hall effect regime, where a different type of "one-way" reservoirs is required.

$E_F - eV_{12} - e\delta\phi_{12}(t)$], with $E_F + eV_{12}$ the average electrochemical potential in the reservoir. As a result, it is found that the shot-noise power P of the entire conductor is given by

$$R^2 P = R_1^2 P_1 + R_2^2 P_2. \quad (7.21)$$

In other words, the voltage fluctuations add. The noise powers of the two segments depend solely on the time-averaged distributions,

$$P_m = 2G_m \int d\varepsilon [f_m(1 - f_m) + f_{12}(1 - f_{12})] + 2S_m \int d\varepsilon (f_m - f_{12})^2, \quad (7.22)$$

where $S_m \equiv G_0 \sum_{n=1}^N T_n^{(m)}(1 - T_n^{(m)})$. The analysis first given in Ref. [33] is easily generalized to arbitrary distribution f_{12} . Then, we have $\tilde{f}_{12}(\varepsilon, t) = f_{12}[\varepsilon - e\delta\phi_{12}(t)]$. It follows that Eqs. (7.21) and (7.22) remain valid, but $f_{12}(\varepsilon)$ may be different. Let us determine the shot noise for the three types of scattering.

Quasi-elastic scattering. Here, it is not just the total current which must be conserved, but the current in each energy range. This requires

$$f_{12}(\varepsilon) = \frac{G_1 f_1(\varepsilon) + G_2 f_2(\varepsilon)}{G_1 + G_2}. \quad (7.23)$$

We note that Eq. (7.23) implies the validity of Eq. (7.20). Substitution of Eq. (7.23) into Eqs. (7.21) and (7.22) yields at zero temperature the result:

$$P = (R_1^4 S_1 + R_2^4 S_2 + R_1 R_2^2 + R_1^2 R_2) R^{-3} P_{\text{Poisson}}. \quad (7.24)$$

Electron heating. We model electron-electron scattering, where energy can be exchanged between the electrons at constant total energy. We assume that the exchange of energies establishes a Fermi-Dirac distribution $f_{12}(\varepsilon)$ at an electrochemical potential $E_F + eV_{12}$ and an elevated temperature T_{12} . From current conservation it follows that

$$V_{12} = (R_2/R) V. \quad (7.25)$$

Conservation of the energy of the electron gas requires that T_{12} is such that no energy is absorbed or emitted by the reservoir. This implies

$$T_{12}^2 = T^2 + \frac{V^2}{\mathcal{L}_0} \frac{R_1 R_2}{R^2}, \quad (7.26)$$

with the Lorentz number $\mathcal{L}_0 \equiv \frac{1}{3}(\pi k_B/e)^2$. At zero temperature in the left and right reservoir and for $R_1 = R_2$ we have $k_B T_{12} = (\sqrt{3}/2\pi)eV \simeq 0.28eV$. For the shot noise at $T = 0$, we thus obtain using Eqs. (7.21) and (7.22) the result:

$$\begin{aligned} P = & \left\{ R_1^3 S_1 + R_2^3 S_2 + \frac{1}{\pi} \sqrt{3R_1 R_2} \left[R_1(1 - R_1 S_1) + R_2(1 - R_2 S_2) \right. \right. \\ & + 2R_1^2 S_1 \ln \left(1 + e^{-\pi \sqrt{R_1/3R_2}} \right) \\ & \left. \left. + 2R_2^2 S_2 \ln \left(1 + e^{-\pi \sqrt{R_2/3R_1}} \right) \right] \right\} R^{-2} P_{\text{Poisson}}. \end{aligned} \quad (7.27)$$

Inelastic scattering. The distribution function of the intermediate reservoir is the Fermi-Dirac distribution at the lattice temperature T , with an electrochemical potential $\mu_{12} \equiv E_F + eV_{12}$, where V_{12} is given by Eq. (7.25). This reservoir absorbs energy, in contrast to the previous two cases. The zero-temperature shot-noise power is given by

$$P = (R_1^3 S_1 + R_2^3 S_2) R^{-2} P_{\text{Poisson}} . \quad (7.28)$$

This model will be applied to double-barrier junctions, and disordered conductors in the following sections. Quite generally, we will find that quasi-elastic scattering has no effect on the shot noise, while electron heating leads to a small enhancement of the shot noise. Inelastic scattering suppresses the shot noise in most cases, but not in the double-barrier junction.

7.4 Double-Barrier Junction

Resonant Tunneling

Below we will only consider the zero-frequency, low-voltage limit, in order to treat the double-barrier junction on the same footing as the other systems described in these lectures. We assume high tunnel barriers with mode-independent transmission probabilities $\Gamma_1, \Gamma_2 \ll 1$.

The transmission eigenvalues through the two barriers in series, as we have derived above, can be re-written as,

$$T_n = \frac{\Gamma_1 \Gamma_2}{2 - \Gamma_1 - \Gamma_2 - 2\sqrt{1 - \Gamma_1 - \Gamma_2} \cos \phi_n} , \quad (7.29)$$

where ϕ_n is the phase accumulated in one round trip between the barriers. The density $\rho(T) \equiv \langle \sum_n \delta(T - T_n) \rangle$ of the transmission eigenvalues follows from the uniform distribution of ϕ_n between 0 and 2π ,

$$\rho(T) = \frac{N\Gamma_1\Gamma_2}{\pi(\Gamma_1 + \Gamma_2)} \frac{1}{\sqrt{T^3(T_+ - T)}} , \quad T \in [T_-, T_+] , \quad (7.30)$$

$\rho(T) = 0$ otherwise, with $T_- = \Gamma_1\Gamma_2/\pi^2$ and $T_+ = 4\Gamma_1\Gamma_2/(\Gamma_1 + \Gamma_2)^2$. The density (7.30) is plotted in Fig. 7.4a.

The average conductance,

$$\langle G \rangle = G_0 \int_0^1 dT \rho(T) T = G_0 N \frac{\Gamma_1 \Gamma_2}{\Gamma_1 + \Gamma_2} , \quad (7.31)$$

is just the series conductance of the two tunnel conductances. The resonances are averaged out by taking a uniform distribution of the phase shifts ϕ_n . Physically, this averaging corresponds either to an average over weak disorder in the region between the barriers,

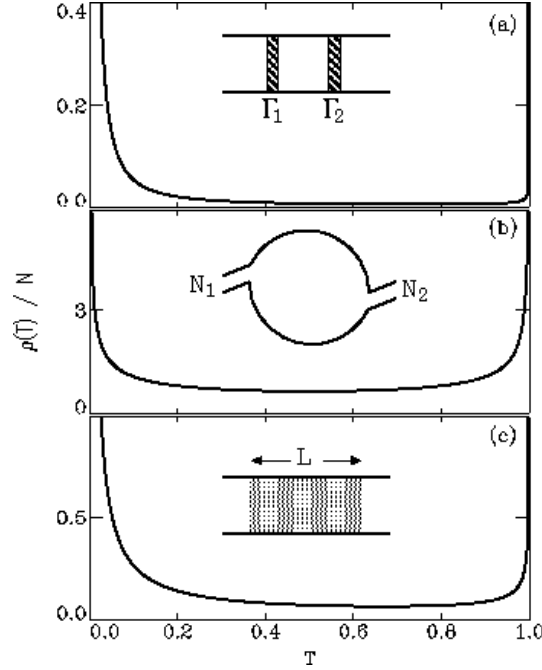


Figure 7.4: The distribution $\rho(T)$ of transmission eigenvalues T for (a) a double-barrier junction, according to Eq. (7.29) with $\Gamma_1 = \Gamma_2 = 0.01$; (b) a chaotic cavity, which we do not discuss here in detail; and (c) a disordered wire, according to Eq. (7.35) with $L = 20\ell$. Each structure has a bimodal distribution.

or to a summation over a large number of modes if the separation between the barriers is large compared to the Fermi wave length, or to an applied voltage larger than the width of the resonance. For the shot-noise power one obtains

$$\langle P \rangle = P_0 \int_0^1 dT \rho(T) T(1-T) = \frac{\Gamma_1^2 + \Gamma_2^2}{(\Gamma_1 + \Gamma_2)^2} P_{\text{Poisson}}, \quad (7.32)$$

using Eqs. (7.30) and (7.31). For asymmetric junctions, one barrier dominates the transport and the shot noise equals the Poisson noise. For symmetric junctions, the shot noise gets suppressed down to $\langle P \rangle = \frac{1}{2} P_{\text{Poisson}}$ for $\Gamma_1 = \Gamma_2$. The theoretical result (7.32) is in agreement with the several experimental observations.

The suppression of the shot noise below P_{Poisson} in symmetric junctions is a consequence of the *bimodal* distribution of transmission eigenvalues, as plotted in Fig. 7.4a. Instead of all T_n 's being close to the average transmission probability, the T_n 's are either close to 0 or to 1. This reduces the sum $T_n(1-T_n)$. A similar suppression mechanism exists for shot noise in chaotic cavities and in disordered conductors.

Phase coherence is not essential for the occurrence of suppressed shot noise. The method described above (with $G_m = S_m = G_0 N \Gamma_m$ for $m = 1, 2$) shows that both quasi-elastic scattering [see Eq. (7.24)] and inelastic scattering [see Eq. (7.28)] do not modify Eq. (7.32).

Thermalization of the electrons in the region between the barriers enhances the shot noise, as follows from Eq. (7.27). For $\Gamma_1 = \Gamma_2$ we find

$$P = \left[\frac{1}{2} + \frac{\sqrt{3}}{\pi} \ln \left(1 + e^{-\pi/\sqrt{3}} \right) \right] P_{\text{Poisson}} \simeq 0.58 P_{\text{Poisson}}, \quad (7.33)$$

which is slightly above the one-half suppression in the absence of thermalization.

Coulomb Blockade

The suppression of the shot noise described in the previous Section is due to correlations induced by the Pauli principle. Coulomb interactions are another source of correlations among the electrons. As we have discussed, a measure of the importance of Coulomb repulsion is the charging energy $E_C = e^2/2C$ of a single electron inside the conductor with a capacitance C . If $eV < E_C$, conduction through the junction is suppressed. At $eV > E_C$, one electron at a time can tunnel into the junction. The next electron can follow, only after the first electron has tunneled out of the junction. This is the single-electron tunneling regime.

Experiments on the noise suppression in Coulomb-blockade regime were reported in Ref. [34]. Here, the double-barrier junction was formed by a scanning-tunneling microscope positioned above a metal nanoparticle on an oxidized substrate. Due to the small size of the particle, $E_c \geq 1000k_B T$, at $T = 4$ K. The relative heights of the two tunnel barriers can be modified by changing the tip-particle distance. Experimental results for an asymmetric junction are plotted in Fig. 7.5. The I - V characteristics display a stepwise increase of the current with the voltage. (Rotating the plot 90° yields the usual presentation of the ‘Coulomb staircase.’) At small voltage, $I \simeq 0$ due to the Coulomb blockade. At each subsequent step in I , the number of excess electrons in the junction increases by one. The measured shot noise oscillates along with the step structure in the I - V curve. The full shot-noise level $P = P_{\text{Poisson}}$ is reached at each plateau of constant I . In between, P is suppressed down to $\frac{1}{2}P_{\text{Poisson}}$. The experimental data are in excellent agreement with the theory.

A qualitative understanding of the periodic shot-noise suppression caused by the Coulomb blockade goes as follows: On a current plateau in the I - V curve, the number of electrons in the junction is constant for most of the time. Only during a very short instance an excess electron occupies the junction, leading to the transfer of one electron. This fast transfer process is dominated by the highest tunnel barrier. Since the junction is asymmetric, Poisson noise is expected. The situation is different for voltages where there is a step in the I - V curve. Here, two charge states are degenerate in total energy. If an electron tunnels into the junction, it may stay for a longer time, during which tunneling of the next electron is forbidden. Both barriers are thus alternately blocked. This leads to a correlated current, yielding a suppression of the shot noise.

An essential requirement for the Coulomb blockade is that $G \lesssim e^2/h$. For larger G the quantum-mechanical charge fluctuations in the junction become big enough to overcome the Coulomb blockade. The next Section will discuss shot noise in a quantum dot, without

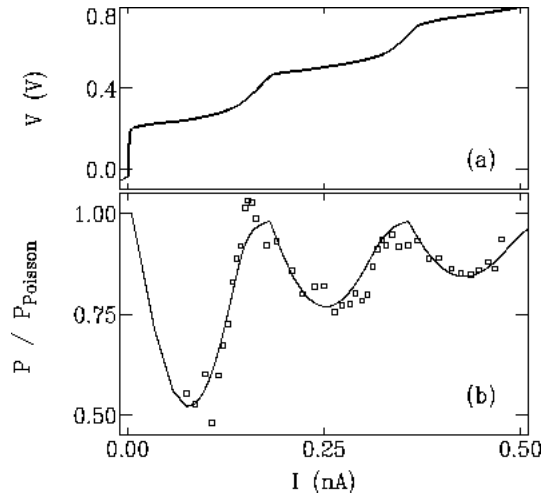


Figure 7.5: Experimental results by Birk *et al.* [34] in the single-electron tunneling regime. The double-barrier junction consists of a tip positioned above a nanoparticle on a substrate. (a) Experimental voltage V versus current I . (b) Shot-noise power P versus I . Squares: experiment; solid line: theory.

including Coulomb interactions. This is justified as long as $G \gtrsim e^2/h$. For smaller G , the quantum dot behaves essentially as the double-barrier junction considered above.

Disordered Metal

One-third suppression

We now turn to transport through a diffusive conductor of length L much greater than the mean free path ℓ , in the metallic regime ($L \ll$ localization length). The average conductance is given by the Drude formula,

$$\langle G \rangle = G_0 \frac{N\ell}{L}, \quad (7.34)$$

up to small corrections of order G_0 (due to weak localization). The mean free path $\ell = a_d \ell_{\text{tr}}$ equals the transport mean free path ℓ_{tr} times a numerical coefficient, which depends on the dimensionality d of the Fermi surface ($a_2 = \pi/2$, $a_3 = 4/3$).

From Eq. (7.34) one might surmise that for a diffusive conductor all the transmission eigenvalues are of order ℓ/L , and hence $\ll 1$. This would imply the shot-noise power $P = P_{\text{Poisson}}$ of a Poisson process. This surmise is completely incorrect. A fraction ℓ/L of the transmission eigenvalues is of order unity (open channels), the others being exponentially small (closed channels). For $\ell \ll L \ll N\ell$, the density of the T_n 's is given by

$$\rho(T) = \frac{N\ell}{2L} \frac{1}{T\sqrt{1-T}}, \quad T \in [T_-, 1], \quad (7.35)$$

$\rho(T) = 0$ otherwise, with $T_- = 4e^{-2L/\ell}$. The density $\rho(T)$, plotted in Fig. 7.4c, is again bimodal with peaks near unit and zero transmission.

One easily checks that the bimodal distribution (7.35) leads to the Drude conductance (7.34). For the average shot-noise power it implies

$$\langle P \rangle = P_0 \frac{N\ell}{3L} = \frac{1}{3} P_{\text{Poisson}} . \quad (7.36)$$

This suppression of the shot noise by a factor one-third is *universal*, in the sense that it does not depend on the specific geometry nor on any intrinsic material parameter (such as ℓ).

Dependence on wire length

The one-third suppression of the shot noise breaks down if the conductor becomes too short or too long. Upon decreasing the length of the conductor, when L becomes comparable to ℓ , the electron transport is no longer diffusive, but enters the ballistic regime. Then the shot noise is suppressed more strongly,

$$P = \frac{1}{3} [1 - (1 + L/\ell)^{-3}] P_{\text{Poisson}} . \quad (7.37)$$

For $L \ll \ell$ there is no shot noise, as in a ballistic point contact. Equation (7.37) is exact for a special model of one-dimensional scattering, but holds more generally within a few percent. The crossover of the shot noise from the ballistic to the diffusive regime is plotted in Fig. 7.6. Upon increasing L at constant cross section of the conductor, one enters the localized regime. Here, even the largest transmission eigenvalue is exponentially small, so that $P = P_{\text{Poisson}}$. Experimentally, the crossover from the metallic to the localized regime

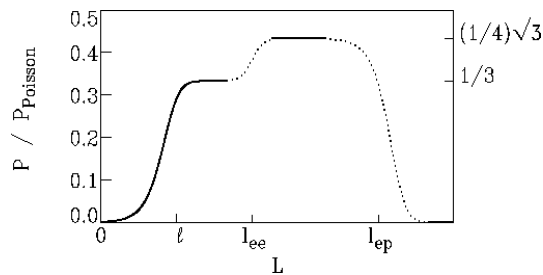


Figure 7.6: The shot-noise power P of a disordered metallic wire as a function of its length L , as predicted by theory. Indicated are the elastic mean free path ℓ , the electron-electron scattering length l_{ee} and the electron-phonon scattering length l_{ep} . Dotted lines are interpolations.

is usually not reached, because phase coherence is broken when L is still much smaller than the localization length $N\ell$. In the remainder of this Section, we apply the method of Sec. 7.3 to determine the effect of phase breaking and other inelastic scattering events on the shot noise in a disordered metal. We divide the conductor into M segments connected

by reservoirs, taking the continuum limit $M \rightarrow \infty$. The electron distribution at position x is denoted by $f(\varepsilon, x)$. At the ends of the conductor $f(\varepsilon, 0) = f_1(\varepsilon)$ and $f(\varepsilon, L) = f_2(\varepsilon)$, *i.e.* the electrons are Fermi-Dirac distributed at temperature T and with electrochemical potential $\mu(0) = E_F + eV$ and $\mu(L) = E_F$, respectively. It follows from Eqs. (7.21) and (7.22) that the noise power is given by

$$P = \frac{4}{RL} \int_0^L dx \int_0^\infty d\varepsilon f(\varepsilon, x)[1 - f(\varepsilon, x)]. \quad (7.38)$$

We evaluate Eq. (7.38) for the three types of scattering discussed in Sec. 7.3.

Quasi-elastic scattering. Current conservation and the absence of inelastic scattering requires

$$f(\varepsilon, x) = \frac{L-x}{L} f(\varepsilon, 0) + \frac{x}{L} f(\varepsilon, L). \quad (7.39)$$

The electron distribution at $x = L/2$ is plotted in the inset of Fig. 7.7. Substitution of Eq. (7.39) into Eq. (7.38) yields

$$P = \frac{2}{3} [4k_B T G + eI \coth(eV/2k_B T)]. \quad (7.40)$$

At zero temperature the shot noise is one-third of the Poisson noise. The same result follows from the phase-coherent theory [Eqs. (7.17) and (7.35)], demonstrating that quasi-elastic scattering has no effect on the shot noise. The temperature dependence of P is plotted in Fig. 7.7.

Electron heating. The electron-distribution function is a Fermi-Dirac distribution with a spatially dependent electrochemical potential $\mu(x)$ and temperature $T_e(x)$,

$$f(\varepsilon, x) = \left\{ 1 + \exp \left[\frac{\varepsilon - \mu(x)}{k_B T_e(x)} \right] \right\}^{-1}, \quad (41a)$$

$$\mu(x) = E_F + \frac{L-x}{L} eV, \quad (41b)$$

$$T_e(x) = \sqrt{T^2 + (x/L)[1 - (x/L)] V^2 / \mathcal{L}_0}, \quad (41c)$$

cf. Eqs. (7.25) and (7.26). Equations (7.38) and (7.41) yield for the noise power the result

$$P = 2k_B T G + 2eI \left[\frac{2\pi}{\sqrt{3}} \left(\frac{k_B T}{eV} \right)^2 + \frac{\sqrt{3}}{2\pi} \right] \arctan \left(\frac{\sqrt{3}}{2\pi} \frac{eV}{k_B T} \right), \quad (7.42)$$

plotted in Fig. 7.7. In the limit $eV \gg k_B T$ one finds

$$P = \frac{1}{4} \sqrt{3} P_{\text{Poisson}} \simeq 0.43 P_{\text{Poisson}}. \quad (7.43)$$

Electron-electron scattering increases the shot noise above $\frac{1}{3} P_{\text{Poisson}}$ because the exchange of energies makes the current less correlated.

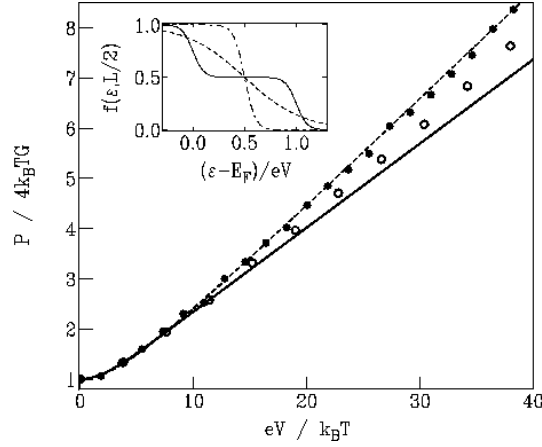


Figure 7.7: The noise power P versus voltage V for a disordered wire in the presence of quasi-elastic scattering [solid curve, from Eq. (7.40)] and of electron heating [dashed curve, from Eq. (7.42)]. The inset gives the electron distribution in the middle of the wire at $k_B T = \frac{1}{20} eV$. The distribution for inelastic scattering is included for comparison (dash-dotted). Experimental data of Steinbach, Martinis, and Devoret [35] on silver wires at $T = 50$ mK are indicated for length $L = 1 \mu\text{m}$ (circles) and $L = 30 \mu\text{m}$ (dots).

Inelastic scattering. The electron-distribution function is given by

$$f(\varepsilon, x) = \left\{ 1 + \exp \left[\frac{\varepsilon - \mu(x)}{k_B T} \right] \right\}^{-1}, \quad (7.44)$$

with $\mu(x)$ according to Eq. (41b). We obtain from Eqs. (7.38) and (7.44) that the noise power is equal to the Johnson-Nyquist noise for arbitrary V . The shot noise is thus completely suppressed by inelastic scattering.

The dependence of the shot-noise power on the length of a disordered conductor is plotted in Fig. 7.6. The phase coherence length (between ℓ and l_{ee}) does not play a role.

Results of accurate experiments by Steinbach, Martinis, and Devoret [35] on silver wires are shown in Fig. 7.7. The noise in a wire of $L = 30 \mu\text{m}$ is in excellent agreement with the hot-electron result (7.42). For the $L = 1 \mu\text{m}$ wire the noise crosses over to the elastic result (7.40), without quite reaching it.

Appendix A

Second quantization

Now we briefly discuss the way to describe many-electron states with the occupation numbers.

Bosons

In general case, the total wave function of bosons is symmetric in replacement of the particles. Thus it can be expressed as a symmetric product of individual wave functions

$$\Phi_{N_1 N_2 \dots} = \left(\frac{N_1! N_2! \dots}{N!} \right)^{1/2} \sum_P \varphi_{p_1}(\xi_1) \varphi_{p_2}(\xi_2) \dots \varphi_{p_N}(\xi_N), \quad (\text{A.1})$$

where p_i label the states, φ_{p_i} are while the sum is calculated over all the permutations of $\{p_i\}$. The coefficient is introduced to make the total function normalized: $\int |\Phi|^2 \prod_i d\xi_i = 1$.

The main idea is to consider $\Phi_{N_1 N_2 \dots}$ as a function of the *occupation numbers* N_i . Assume that we have an arbitrary one-particle symmetric operator

$$F^{(1)} = \sum_a f_a^{(1)} \quad (\text{A.2})$$

where f_a acts only upon the functions of ξ_a . It is clear that acting upon $\Phi_{N_1 N_2 \dots}$ it changes the state of only one particle. So it is reasonable to introduce the operators with matrix elements

$$(b_i)_{N_i}^{N_i-1} = \sqrt{N_i}, \quad (b_i^\dagger)_{N_i-1}^{N_i} = [(b_i)_{N_i}^{N_i-1}]^* = \sqrt{N_i} \quad (\text{A.3})$$

It is just annihilation and creation operators introduced earlier. The operator (A.2) can be expressed in terms of the creation-annihilation operators as

$$F^{(1)} = \sum_{ik} f_{ik}^{(1)} b_i^\dagger b_k \quad (\text{A.4})$$

where

$$f_{ik}^{(1)} = \int \varphi^*(\xi) f^{(1)} \varphi(\xi) d\xi. \quad (\text{A.5})$$

One can easily prove this relation comparing both diagonal and off-diagonal matrix elements of the operators. A 2-particle symmetric operator

$$F^{(2)} = \sum_{a,b} f_{ab}^{(2)} \quad (\text{A.6})$$

where $f_{ab}^{(2)}$ acts upon the functions of the variables ξ_a and ξ_b can be expressed as

$$F^{(2)} = \sum_{iklm} f_{lm}^{ik} b_i^\dagger b_k^\dagger b_l b_m \quad (\text{A.7})$$

where

$$f_{lm}^{ik} = \int \varphi_i^*(\xi_1) \varphi_k^*(\xi_2) f^{(2)} \varphi_l(\xi_1) \varphi_m(\xi_2) d\xi_1 d\xi_2. \quad (\text{A.8})$$

Electrons

Now we turn to the Fermi statistics to describe electrons. According to the Pauli principle, the total wave function should be *anti-symmetric* over all the variables. So the occupation numbers could be 0 or 1. In this case we get instead of (A.1)

$$\Phi_{N_1 N_2 \dots} = \frac{1}{\sqrt{N!}} \sum_P (-1)^P \varphi_{p_1}(\xi_1) \varphi_{p_2}(\xi_2) \dots \varphi_{p_N}(\xi_N) \quad (\text{A.9})$$

where all the numbers p_1, p_2, \dots, p_N are *different*. The symbol $(-1)^P$ shows that odd and even permutations enter the expression (A.9) with opposite signs (we take the sign ‘+’ for the term with $p_1 < p_2 < \dots < p_N$). Note that the expression (A.9) can be expressed as the determinant of the matrix with the elements $M_{ik} = (1/\sqrt{N!}) \varphi_{p_i}(\xi_k)$ which is often called the *Slater determinant*.

The diagonal matrix elements of the operator $F^{(1)}$ are

$$\bar{F}^{(1)} = \sum_i f_{ii}^{(1)} N_i \quad (\text{A.10})$$

just as for the Bose particles. But off-diagonal elements are

$$(F^{(1)})_{0_i 1_k}^{1_i 0_k} = \pm f_{ik}^{(1)} \quad (\text{A.11})$$

where the sign is determined by the parity of the total number of particles in the states between the i and k ones.¹ Consequently, for Fermi particles it is convenient to introduce the annihilation and creation operators as

$$(a_i)_1^0 = (a_i^\dagger)_0^1 = (-1)^{\sum_{l=1}^{i-1} N_l}. \quad (\text{A.12})$$

¹Note that for Bose particles similar matrix elements are $(F^{(1)})_{N_i-1, N_k}^{N_i, N_k-1} = f_{ik}^{(1)} \sqrt{N_i N_k}$.

We immediately get (Check!) the commutation rules for the Fermi operators:

$$\begin{aligned} \{a_i a_k^\dagger\} &\equiv a_i a_k^\dagger + a_i^\dagger a_k = \delta_{ik}, \\ \{a_i a_k\} &= \{a_i^\dagger a_k^\dagger\} = 0. \end{aligned} \tag{A.13}$$

The product of Fermi operators are

$$a_i^\dagger a_i = N_i, \quad a_i a_i^\dagger = 1 - N_i. \tag{A.14}$$

One can express all the operators for Fermi particles exactly in the same way as the Bose ones, Eqs. (A.4), (A.7).

Appendix B

Quantum corrections to conductivity

B.1 Diagrammatic perturbation theory

Assume the simplest model for the scattering potential a set of randomly distributed impurities with short-range potential,

$$U(\mathbf{r}) = \sum_{j=1}^{N_i} u(\mathbf{r} - \mathbf{r}_j) \approx \frac{u_0}{\mathcal{V}} \sum_{j=1}^{N_i} \delta(\mathbf{r} - \mathbf{r}_j).$$

Here N_i is the number of defects, u_0 is the potential amplitude, while \mathcal{V} is the system volume. The the correlation function of the potential is in the main approximation

$$\langle U(\mathbf{r})U(\mathbf{r}') \rangle = n_i u_0^2 \delta(\mathbf{r} - \mathbf{r}').$$

Here $n_i = N_i/\mathcal{V}$ is the impurity concentration. The following procedure is actually valid in the limiting case

$$N_i \rightarrow \infty, \quad \mathcal{V} \rightarrow \infty, \quad u_0 \rightarrow 0, \quad n_i u_0^2 = \text{const}.$$

Let us assume also zero temperature to avoid inelastic scattering.

Under these assumptions it is convenient to introduce the resolvent operator

$$\hat{G}(z) = (z - \mathcal{H})^{-1}$$

where z is a complex number, while \mathcal{H} is the Hamiltonian of the system. Since formally

$$(\varepsilon - \mathcal{H} \pm i0)^{-1} = P \frac{1}{\varepsilon - \mathcal{H}} \mp i\pi \delta(\varepsilon - \mathcal{H}),$$

where P means the principal value, we can write

$$g(\varepsilon) = \frac{1}{\mathcal{V}} \text{Tr} \delta(\varepsilon - \mathcal{H}) = \mp \frac{1}{\pi \mathcal{V}} \Im [\text{Tr} \hat{G}(\varepsilon \pm i0)].$$

The matrix elements of \hat{G} ,

$$\langle \mathbf{r} | \hat{G}(\varepsilon \pm i0) | \mathbf{r}' \rangle = \sum_{\alpha} \frac{\psi_{\alpha}(\mathbf{r}) \psi_{\alpha}^*(\mathbf{r}')}{\varepsilon - \varepsilon_{\alpha} \pm i0} = G_{\varepsilon}^{R,A}(\mathbf{r}, \mathbf{r}') \quad (\text{B.1})$$

are called retarded ($+i0$) or advanced ($-i0$) Green functions. They have a simple physical meaning of the propagation amplitudes for the states with a given energy,

$$G_{\varepsilon}^R = \frac{1}{i\hbar} A(\mathbf{r} \rightarrow \mathbf{r}') \quad \text{“along the time”}$$

while

$$G_{\varepsilon}^A = \frac{i}{\hbar} A(\mathbf{r} \rightarrow \mathbf{r}') \quad \text{“against the time”}.$$

At $k_F \ell \gg 1$ a perturbational approach is possible which allows to expand Green functions in powers of scattering potential and zeroth-order propagators

$$G^{(0)}(z, \mathbf{r} - \mathbf{r}') = \sum_{\mathbf{k}} G^{(0)}(z, \mathbf{k}) e^{i\mathbf{k}(\mathbf{r} - \mathbf{r}')}, \quad (\text{B.2})$$

where

$$G^{(0)}(z, \mathbf{k}) = \langle \mathbf{k} | \hat{G}^{(0)}(z) | \mathbf{k}' \rangle = \frac{1}{z - \varepsilon_{\mathbf{k}}} \delta_{\mathbf{k}, \mathbf{k}'}. \quad (\text{B.3})$$

It is convenient to use \mathbf{k} -representation and expand

$$G^{R,A}(\mathbf{k}, \mathbf{k}') = \sum_{\alpha} \frac{\psi_{\alpha}(\mathbf{k}) \psi_{\alpha}^*(\mathbf{k}')}{\varepsilon - \varepsilon_{\alpha} \pm i0}.$$

The result can be expressed in a diagrammatic form, as shown in Fig. B.1, panel (a). Each solid line corresponds to the non-perturbed propagator (B.3), each dashed line corresponds to the transferred momentum \mathbf{q}_j , each vertex corresponding to scattering at the defect at the point \mathbf{r}_j contributes as

$$\frac{u_0}{\mathcal{V}} e^{i\mathbf{q}_j \mathbf{r}_j} \delta(\mathbf{k}_{j+1} - \mathbf{k}_j - \mathbf{q}_j).$$

After n scattering events the incoming wave vector \mathbf{k} is changed to $\mathbf{k}' = \mathbf{k} + \sum_{j=1}^n \mathbf{q}_j$. For given \mathbf{k} and \mathbf{k}' one should sum over all \mathbf{q}_j keeping the above conservation law.

The impurity average can be performed by summing over all pairwise contractions [see Fig. B.1, panel (b)], each contraction contributes as

$$\langle U(\mathbf{q}_i) U(\mathbf{q}_j) \rangle = n_i u_0^2 \mathcal{V} \delta_{\mathbf{q}_i, -\mathbf{q}_j}.$$

The formal summation of the perturbation series can be performed by introducing the *irreducible diagrams*, Σ , which cannot be divided into parts by cutting only a single $G^{(0)}$. As it can be easily seen, in this way we arrive at the *Dyson equation* (see Fig. B.2),

$$\langle G \rangle = G^{(0)} + G^{(0)} \Sigma \langle G \rangle.$$

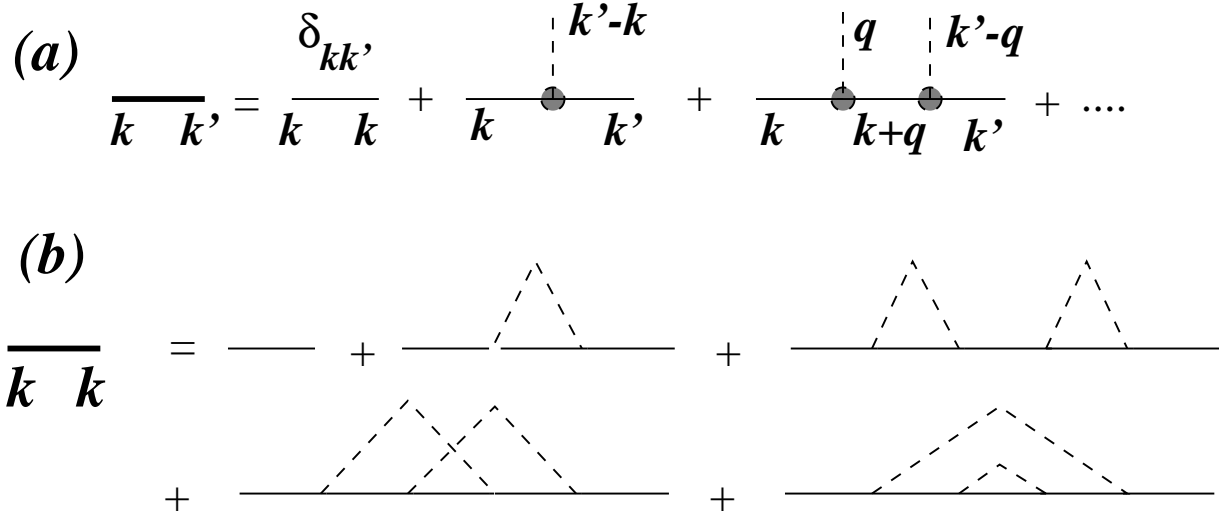


Figure B.1: a – Diagrammatic representation of the perturbations in scattering strength. b – Perturbation series for the average Green function.

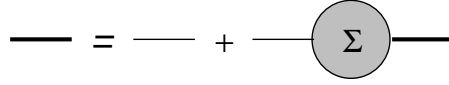


Figure B.2: Illustration of the Dyson equation.

Its formal solution is

$$\langle G \rangle = \frac{1}{(G^{(0)})^{-1} - \Sigma}.$$

Since this solution sums up an infinite series, we calculate the *self-energy* Σ in the lowest order in $n_i u_0^2$, which is just the triangle in the first diagram in Fig. B.1, panel (b). That corresponds to the Born approximation in quantum mechanical scattering. The result is

$$\Sigma_B(z, \mathbf{k}) = n_i u_0^2 \sum_{\mathbf{q}} \frac{1}{z - \varepsilon_{\mathbf{k}+\mathbf{q}}} = n_i u_0^2 \int d\epsilon \frac{g_0(\epsilon)}{z - \epsilon}. \quad (\text{B.4})$$

Taking $z = \varepsilon + i0$ the associated *retarded* self-energy has both real and imaginary part. The real part (actually divergent) can be absorbed into renormalization of bare energies $\varepsilon_{\mathbf{k}}$. The imaginary part

$$\Im \Sigma_B(\varepsilon) = -\pi n_i u_0^2 g_0(\varepsilon)$$

near the Fermi level can be replaced by a constant

$$\gamma = \hbar/2\tau = \hbar v_F/\ell$$

yielding the average Green function

$$G_\varepsilon^R(\mathbf{k}, \mathbf{k}') = \frac{\delta_{\mathbf{k},\mathbf{k}'}}{\varepsilon - \varepsilon_{\mathbf{k}} + \hbar/2\tau} \quad (\text{B.5})$$

that is equivalent in the coordinate representation to the Green function depending on $\mathbf{r} = \mathbf{r}_i - \mathbf{r}_f$ as

$$G_{\varepsilon_F}^R(\mathbf{r}) = -\frac{m}{2\pi\hbar^2} \frac{e^{ik_F r}}{r} e^{-r/2\ell}. \quad (\text{B.6})$$

This is just damped outgoing spherical wave.

B.2 Kubo-Greenwood formula

A time-dependent electric field $\mathbf{E}(\mathbf{r}, t) = -\nabla V(\mathbf{r}, t)$ leads to a change in the Hamiltonian $\mathcal{H}(t) \rightarrow \mathcal{H} - eV(\mathbf{r}, t)$. Let us for simplicity assume that

$$V(\mathbf{r}, t) = V(\mathbf{r})e^{-s|t|} \cos \omega t, \quad s \rightarrow +0.$$

Assume that the electric field is concentrated only in the region where the scattering takes place and introduce a complete orthonormal set of *exact* eigenstates $\psi_\alpha(\mathbf{r})$ indexed by continuous variable α .

To calculate current we need the nonequilibrium density matrix $\hat{\varrho}$ which is determined by von Neumann equation

$$i\hbar \frac{\partial \hat{\varrho}}{\partial t} = [\mathcal{H}(t), \hat{\varrho}].$$

The equilibrium state is described by the density matrix

$$\hat{\varrho}^{(0)} = \int d\alpha f(\varepsilon_\alpha) |\alpha\rangle \langle \alpha|,$$

where $f(\varepsilon_\alpha)$ is the Fermi function. The first-order correction is

$$i\hbar \partial_t \hat{\varrho}^{(1)} = [\mathcal{H}, \hat{\varrho}^{(1)}] + [\mathcal{H}_1, \hat{\varrho}^{(0)}].$$

Introducing $f_{\beta\alpha} = f(\varepsilon_\beta) - f(\varepsilon_\alpha)$ and $V_{\alpha\beta} = \langle \alpha | V(\mathbf{r}) | \beta \rangle$ we obtain

$$i\hbar \partial_t \varrho_{\alpha\beta}^{(1)} = -\varepsilon_{\beta\alpha} \varrho_{\alpha\beta}^{(1)} - e f_{\beta\alpha} V_{\alpha\beta} e^{-s|t|} \cos(\omega t).$$

Its solution for the initial condition $\hat{\varrho} \rightarrow 0$ at $t \rightarrow -\infty$ has the form

$$\varrho_{\alpha\beta}^{(1)}(t < 0) = -\frac{e}{2} f_{\beta\alpha} V_{\alpha\beta} e^{st} \left(\frac{e^{i\omega t}}{\varepsilon_{\beta\alpha} - \hbar\omega + i\hbar s} + (\omega \rightarrow -\omega) \right).$$

Now we can calculate the current,

$$\mathbf{j}(\mathbf{r}, t) = \text{Tr} \left(\hat{\varrho}^{(1)} \hat{\mathbf{j}}(\mathbf{r}) \right) = \int d\alpha d\beta \varrho_{\alpha\beta}^{(1)} \mathbf{j}_{\beta\alpha}(\mathbf{r}).$$

Here

$$\mathbf{j}_{\beta\alpha}(\mathbf{r}) = \frac{ie\hbar}{2m} \left[\psi_\beta^*(\mathbf{r}) \mathcal{D} \psi_\alpha(\mathbf{r}) - \psi_\alpha(\mathbf{r}) \mathcal{D}^* \psi_\beta^*(\mathbf{r}) \right],$$

where

$$\mathcal{D} = \nabla + (ie/\hbar c)\mathbf{A}(\mathbf{r})$$

is the covariant derivative. Expressing

$$eV_{\alpha\beta} = \frac{i\hbar}{\varepsilon_{\beta\alpha}} \int d^d\mathbf{r} \mathbf{j}_{\alpha\beta}(\mathbf{r}) \cdot E(\mathbf{r})$$

and collecting the contributions to the current as $\mathbf{j}(\mathbf{r}) \cos(\omega t)$, we obtain

$$\mathbf{j}(\mathbf{r}) = \int d^d\mathbf{r}' \hat{\sigma}(\mathbf{r}, \mathbf{r}') E(\mathbf{r}')$$

where non-local conductivity $\hat{\sigma}(\mathbf{r}, \mathbf{r}')$ is given by the expression

$$\hat{\sigma}(\mathbf{r}, \mathbf{r}') = \frac{\hbar}{2i} \int d\alpha d\beta \left[\frac{f_{\beta\alpha}}{\varepsilon_{\beta\alpha} - \hbar\omega + i\hbar s} + (\omega \rightarrow -\omega) \right] \mathbf{j}_{\beta\alpha}(\mathbf{r}) \otimes \mathbf{j}_{\alpha\beta}(\mathbf{r}').$$

Here \otimes means tensor product of two vectors. Having in mind the definitions of the Green functions and taking Fourier transform in the quantity $\mathbf{r} - \mathbf{r}'$ we find that non-local conductivity at $T = 0$ can be expressed as

$$\sigma_{ij}(q, \omega) = \frac{\hbar^3 e^2}{3m^2 \pi \mathcal{V}} \sum_{\mathbf{k}, \mathbf{k}'} k_i k_j' K_{\mathbf{k}\mathbf{k}'}(q, \omega), \quad (\text{B.7})$$

where

$$K_{\mathbf{k}\mathbf{k}'}(q, \omega) = G^R(\mathbf{k}_+, \mathbf{k}'_+, \varepsilon_F + \hbar\omega) G^A(\mathbf{k}_-, \mathbf{k}'_-, \varepsilon_F). \quad (\text{B.8})$$

Here $\mathbf{k}_{\pm} \mathbf{k}'_{\pm} \pm \mathbf{q}/2$. Note that the function

$$\Phi(\mathbf{q}, \omega) = \sum_{\mathbf{k}, \mathbf{k}'} K_{\mathbf{k}\mathbf{k}'}(q, \omega) \quad (\text{B.9})$$

has a physical meaning of a density relaxation function.

B.3 Weak localization corrections

The function $K_{\mathbf{k}\mathbf{k}'}(q, \omega)$ is a two-particle Green function. We are interested in its impurity average,

$$\mathcal{K}_{\mathbf{k}\mathbf{k}'}(q, \omega) \equiv \langle K_{\mathbf{k}\mathbf{k}'}(q, \omega) \rangle.$$

Again, we can extract irreducible *vertex part*, $\Gamma_{\mathbf{k}\mathbf{k}'}(\mathbf{q}, \omega)$ [see Fig. B.3, panel (a)] As a result, we rewrite K -function as

$$\mathcal{K}_{\mathbf{k}\mathbf{k}'}(q, \omega) = G_{\mathbf{k}_+}^R G_{\mathbf{k}_-}^A \delta_{\mathbf{k}, \mathbf{k}'} + G_{\mathbf{k}_+}^R G_{\mathbf{k}_-}^A \Gamma_{\mathbf{k}\mathbf{k}'}(\mathbf{q}, \omega) G_{\mathbf{k}'_+}^R G_{\mathbf{k}'_-}^A. \quad (\text{B.10})$$

Here $G^{R,A}$ denote *averaged* Green functions which take into account the impurity lines which start and finish at the same line. The vertex part Γ takes into account correlations

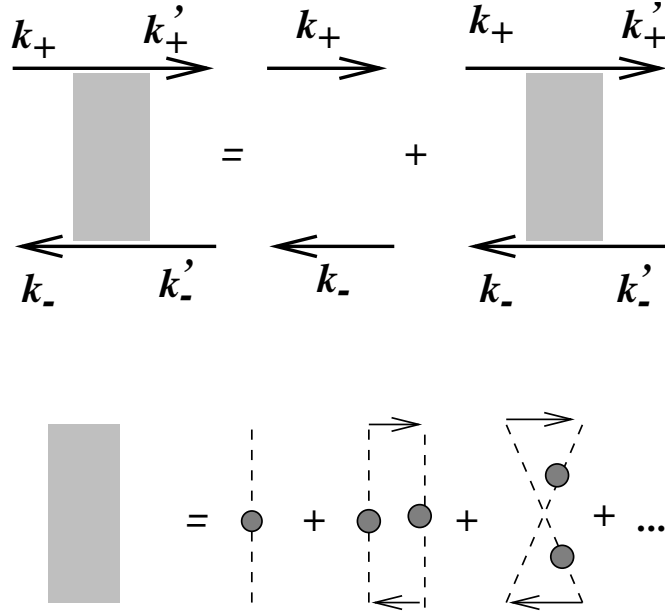


Figure B.3: Graphical representation of the disorder average of the product $G^R G^A$. The thick lines denote *averaged* Green functions.

between the quantum mechanical amplitude and the time-reversed one due to scattering against the same impurity centers.

The first term in this equation leads to the Drude formula, while the quantum corrections are incorporated in the vertex part, Γ . If the corrections are small, this part can be calculated using the main sequence of the diagrams. Two types of diagrams are usually discussed - "diffusons" and "cooperons", they leads to the main contributions provided $k_F \ell \gg 1$.

The first type is the so-called "ladder" diagrams [see Fig. B.4, panel (a)]. Summing the "ladder", diagrams we obtain

$$\Gamma_{\mathbf{k}\mathbf{k}'}^{(d)}(q, \omega) = \frac{n_i u_0^2}{\mathcal{V}} \frac{1}{1 - \zeta(q, \omega)}, \quad (\text{B.11})$$

where

$$\zeta(q, \omega) = \frac{n_i u_0^2}{\mathcal{V}} \sum_{\mathbf{k}} G_{\mathbf{k}_+}^R(\varepsilon_F + \hbar\omega) G_{\mathbf{k}_-}^A(\varepsilon_F). \quad (\text{B.12})$$

For $q, \omega \rightarrow 0$ one can expand $\varepsilon_{\mathbf{k}_{\pm}} \approx \varepsilon_{\mathbf{k}} \pm \hbar(\mathbf{q} \cdot \mathbf{v})/2$ to obtain

$$\zeta(q, \omega) = \int \frac{d\Omega_{\mathbf{k}}}{4\pi} \frac{1}{1 - i\omega\tau + i\tau(\mathbf{q} \cdot \mathbf{v})} \approx 1 + i\omega\tau - Dq^2\tau,$$

where $D = v_F \ell / 3$ is the diffusion constant. Thus, at $\omega\tau, ql \ll 1$

$$\Gamma_{\mathbf{k}\mathbf{k}'}^{(d)}(q, \omega) = \frac{n_i u_0^2}{\tau \mathcal{V}} \frac{1}{-i\omega + Dq^2}.$$

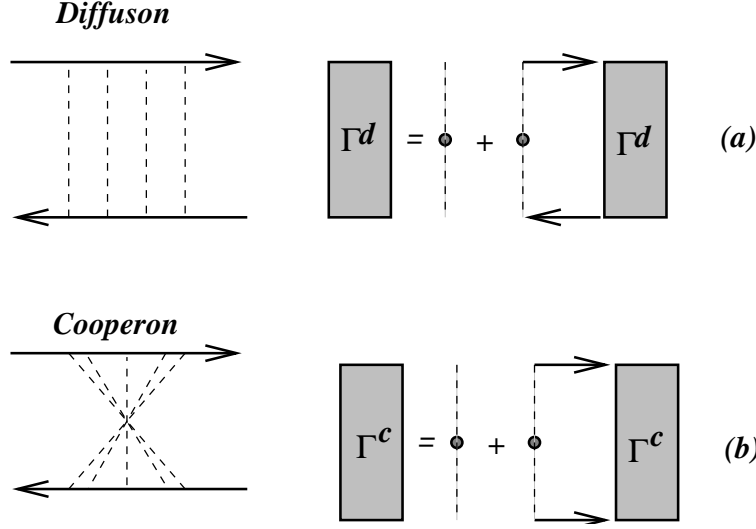


Figure B.4: On the “diffuson” and “cooperon” contributions.

One can easily check that the associated density relaxation function has a diffusion pole. At the same time, the “diffuson” part does not enter the expression (B.7) at $q \rightarrow 0$. for conductivity because of asymmetry in \mathbf{k} and \mathbf{k}' . Actually, this is a consequence of our model of point-defect scattering. For more realistic potentials “ladder” diagrams lead to renormalization of the elastic mean free time τ into the transport relaxation time τ_{tr} .

Now let us turn to the “cooperon” contribution [Fig. B.4, panel (b)]. We can obtain the result without doing a new work by exploiting time reversal symmetry and assuming ¹

$$\langle \mathbf{k}'_- | G^A | \mathbf{k}_- \rangle = \langle -\mathbf{k}_- | G^A | -\mathbf{k}'_- \rangle.$$

As a result of the invariance of the replacement $\mathbf{k} \leftrightarrow -\mathbf{k}'$

$$\Gamma_{\mathbf{k}\mathbf{k}'}(\mathbf{q}, \omega) = \Gamma_{\mathbf{k}-\mathbf{k}'+\mathbf{q}/2, \mathbf{k}'-\mathbf{k}+\mathbf{q}/2}(\mathbf{k} + \mathbf{k}', \omega).$$

As a result, at

$$\mathbf{Q} = \mathbf{k} + \mathbf{k}' \rightarrow 0, \quad \omega \rightarrow 0$$

one obtains

$$\Gamma_{\mathbf{k}\mathbf{k}'}^{(c)}(q, \omega) = \frac{n_i u_0^2}{\tau \mathcal{V}} \frac{1}{-i\omega + DQ^2}. \quad (\text{B.13})$$

The singularity at $\mathbf{k} + \mathbf{k}' \rightarrow 0$ is due to *backscattering*. The expression (B.13) is called the *cooperon* because of formal analogy with superconductivity.

Substituting (B.13) into general expression for the conductivity (B.7) and replacing $\langle k_i k_j \rangle \rightarrow k_F^2/2$ we get

$$\Delta\sigma(\omega) = -\frac{\hbar n_i e^2 u_0^2 v_F^2}{3\pi\tau} \int \frac{d^3k}{(2\pi)^3} (G^R G^A)^2 \frac{1}{\mathcal{V}} \sum_{\mathbf{Q}} \frac{1}{-i\omega + DQ^2}. \quad (\text{B.14})$$

¹This not true in the presence of magnetic field, or inelastic scattering.

Making use of the relation

$$\int \frac{d^3k}{(2\pi)^3} (G^R G^A)^2 \approx 4\pi\tau^3 g(\varepsilon_F)$$

we finally get

$$\Delta\sigma(\omega) = -\frac{2e^2 D}{\pi\hbar} \frac{1}{\mathcal{V}} \sum_{\mathbf{Q}} \frac{1}{-i\omega + DQ^2}. \quad (\text{B.15})$$

To make summation over \mathbf{Q} let us use the following trick. Namely, recall that

$$\frac{1}{-i\omega + DQ^2} = \int_0^\infty dt e^{(i\omega - DQ^2)t}.$$

On the other hand, $\exp(-DQ^2t)$ is the Fourier transform of the Green's function of the diffusion equation,

$$pdP(\mathbf{r}, t) = D\nabla^2 P(\mathbf{r}, t), \quad P(\mathbf{r}, 0) = \delta(\mathbf{r}).$$

This Green's function has the form

$$P(\mathbf{r}, t) = \frac{1}{(4\pi Dt)^{d/2}} \exp\left(-\frac{r^2}{4Dt}\right).$$

Since

$$\frac{1}{\mathcal{V}} \sum_{\mathbf{Q}} \frac{1}{-i\omega + DQ^2} = P(0, t)$$

we obtain the formal result,

$$\Delta\sigma = -\frac{2e^2 D}{\pi\hbar} \int_{t_{\min}}^{t_{\max}} \frac{dt}{(4\pi Dt)^{d/2}}. \quad (\text{B.16})$$

The results depend essentially upon cut-off times, $t_{\max, \min}$. Usually it is chosen $t_{\min} = \tau$, $t_{\max} = \tau_\varphi$. However, there are much more sophisticated ways to treat more realistic systems. The usual way is to replace the Green's function $P(\mathbf{r}, t)$ of the diffusion equation by $P(\mathbf{r}, t)e^{-t/\tau_\varphi}$. To calculate $P(\mathbf{r}, t)$ for a realistic system, a boundary problem is formulated for the eigenfunction of the diffusion operator,

$$-D\nabla^2 P_s = \lambda_s P_s, \quad \partial_n P_s|_{\text{vac}} = 0, \quad P(\mathbf{r}, t)|_{\text{lead}} = 0.$$

where subscripts ‘‘vac’’ and ‘‘lead’’ mean interfaces with vacuum and leads, respectively. Since

$$P(\mathbf{r}, t) = \sum_s P_s(\mathbf{r}) e^{-\lambda_s t},$$

we obtain

$$\Delta\sigma = -\frac{2e^2 D}{\pi\hbar} \frac{1}{\mathcal{V}} \sum_s^{(\lambda_s \geq 1/\tau)} \frac{1}{-i\omega + 1/\tau_\varphi + \lambda_s}.$$

Assuming the sample infinite in x, y -direction and $L_z \ll L_\varphi = \sqrt{D\tau_\varphi}$ we get

$$\Delta\sigma_{2d} = -\frac{e^2}{\pi\hbar} \ln\left(\frac{\tau_\varphi}{\tau}\right).$$

The above mentioned procedure allows a rather simple generalization for the case of magnetic field. It appears sufficient to change the diffusion equation to

$$-D\left(\nabla + i\frac{2e}{\hbar c}\mathbf{A}\right)^2 P_s(\mathbf{r}) = \lambda_s P_s(\mathbf{r}).$$

The boundary condition are also changed to include covariant derivatives,

$$\partial_n \rightarrow \partial_n + 2i(e/\hbar c)A_n,$$

as in the Ginzburg-Landau equations for superconductivity.

Let us apply this procedure to calculate the conductivity of an infinite slab with $L_z \ll L_\varphi$ in the perpendicular magnetic field. To find the eigenvalues we can consider a Schrödinger equation for a particle with the mass $M = \hbar/2D \approx m/k_F\ell$ and charge $-2e$ in the presence of magnetic field. As a result,

$$\lambda_s = (s + 1/2)(4DeH/\hbar).$$

As a result,

$$\Delta\sigma_{2d}(H) = -\frac{2e^2 DeH}{(\pi\hbar)^2} \sum_{s=0}^{s_{\max}} \left[\frac{1}{\tau_\varphi} + \frac{4eDH}{c\hbar} \left(s + \frac{1}{2} \right) \right]^{-1}$$

where $s_{\max} \approx c\hbar/(2eH\ell^2) \gg 1$. In the limit $\ell \ll L_\varphi, \sqrt{c\hbar/2eH}$ the result can be expressed through the standard Digamma function, Ψ :

$$\Delta\sigma_{2d}(H) = -\frac{e^2}{2\pi^2\hbar} \left[\ln\left(\frac{c\hbar}{2eH\ell^2}\right) - \Psi\left(\frac{1}{2} + \frac{1}{2} \frac{c\hbar}{2eHD\tau_\varphi}\right) \right]. \quad (\text{B.17})$$

This expression provides numerical factors. It has two clearly different regimes which cross over at

$$H_\varphi = \frac{h}{2eL_\varphi^2}.$$

Appendix C

Derivation of Landauer formula.

In this derivation I partly follow Ref. [18]. According to quantum mechanics, the expectation value of any single-particle operator \hat{A} can be expressed through the time-dependent density matrix, $\rho(t)$ as

$$\langle A \rangle = \text{Tr} \left\{ \rho(t) \hat{A} \right\},$$

where $\rho(t)$ satisfies the equation of motion

$$\dot{\rho} = -(i/\hbar)[\mathcal{H}, \rho].$$

The unperturbed system is described through the Fermi function $f(\epsilon)$ as

$$\rho_0 = \int d\alpha f(\epsilon_\alpha) |\psi_\alpha\rangle \langle \psi_\alpha|.$$

Here $|\psi_\alpha\rangle$ stand for *exact* scattering-wave states of the equilibrium system with energy ϵ_α . The integral is written to emphasize that we deal with continuous spectrum.

Let us assume that the system is perturbed by a scalar potential with frequency ω which is turned on adiabatically at $t \rightarrow -\infty$,

$$\phi \propto \exp(\nu t - i\omega t), \quad \nu \rightarrow 0.$$

We assume that the potential amplitude approaches a constant value in each lead. Then we solve the equation for ρ up to the linear terms in ϕ . In the limiting case, just as in course of derivation of the Kubo formula for extended systems, we get

$$\langle \mathbf{J}(\mathbf{r}) \rangle = \int d\mathbf{r}' \hat{\sigma}(\mathbf{r}, \mathbf{r}') \cdot \mathbf{E}(\mathbf{r}'),$$

where the local Kubo conductivity tensor is given by the expression

$$\hat{\sigma}(\mathbf{r}, \mathbf{r}') = -\hbar \int d\alpha d\beta \left[f'(\epsilon_\alpha) \pi \delta(\epsilon_{\beta\alpha}) + i \frac{f_{\beta\alpha}}{\epsilon_{\beta\alpha}} \mathcal{P} \left(\frac{1}{\epsilon_{\beta\alpha}} \right) \right] \mathbf{J}_{\beta\alpha}(\mathbf{r}) \mathbf{J}_{\alpha\beta}(\mathbf{r}'). \quad (\text{C.1})$$

Here $\epsilon_{\beta\alpha} \equiv \epsilon_\beta - \epsilon_\alpha$, $f_{\beta\alpha} \equiv f(\epsilon_\beta) - f(\epsilon_\alpha)$, $f' \equiv \partial f / \partial \epsilon$ and \mathcal{P} denotes the principal value. $\mathbf{J}_{\beta\alpha}(\mathbf{r})$ is the matrix element of the current operator between that exact eigenstates,

$$\mathbf{J}_{\beta\alpha}(\mathbf{r}) = -\frac{ie\hbar}{2m} [\psi_\beta^*(\mathbf{r})\mathcal{D}\psi_\alpha(\mathbf{r}) - \psi_\alpha(\mathbf{r})\mathcal{D}^*\psi_\beta^*(\mathbf{r})],$$

where

$$\mathcal{D} \equiv \nabla - (ie/\hbar c)\mathbf{A}(\mathbf{r})$$

denotes the gauge-invariant derivative. It follows that in the absence of magnetic field the principle value vanishes because to time-reversal invariance.

The current densities should be integrated over the surfaces of the leads. As a result, the conductance is given by the expression

$$G_{mn} = \int dS_m \int dS_n \cdot \hat{\sigma}(\mathbf{r}, \mathbf{r}') \cdot \mathbf{n}.$$

Here $\hat{\sigma}$ and \mathbf{n} are unit vectors normal to the cross-section.

In the absence of magnetic field one can immediately integrate Eq. (C.1) over energy and take the limit $T \rightarrow 0$. Then the result becomes a sum over discrete states at ϵ_F of the form

$$\frac{e^2}{2h} \sum_{\alpha,\beta} I_{\beta\alpha}(m) I_{\alpha\beta}(n), \quad (\text{C.2})$$

where

$$I_{\beta\alpha}(m) \equiv \int dS_m \cdot \mathbf{J}_{\beta\alpha}(\mathbf{r}). \quad (\text{C.3})$$

The normalization factor h^{-2} arises from the integration over the energy.

Since the energies are fixed, the states are characterized by a mode index a, b , and a lead index p, q denoting the lead and mode which contains an incoming wave from infinity.

In lead m ,

$$\begin{aligned} \psi_\alpha(\mathbf{r}) &= \phi_{ap}^-(\mathbf{r}) + \sum_{cs} t_{sc \leftarrow ap} \phi_{sc}^+(\mathbf{r}), \\ \psi_\beta^*(\mathbf{r}) &= \phi_{bq}^{-*}(\mathbf{r}) + \sum_{ds} t_{sd \leftarrow bq}^* \phi_{sd}^{+*}(\mathbf{r}). \end{aligned}$$

Here $t_{sc \leftarrow ap}$ is the transmission amplitude for an *incident* wave in lead p and mode a to scatter *to* lead s and mode c . $\phi_c^+(\mathbf{r})$ are the wavefunctions of the infinite perfect leads consisting of a longitudinal plane wave traveling *away* from the sample multiplied by the transverse wavefunction for the mode c . If we are interested in $I_{\beta\alpha}(m)$ we keep onny the items which involve the states existing in m th lead,

$$\begin{aligned} \psi_\alpha(\mathbf{r}_m) &= \phi_{mp}^-(\mathbf{r}_m) + \sum_c t_{mc \leftarrow ap} \phi_{mc}^+(\mathbf{r}_m), \\ \psi_\beta^*(\mathbf{r}_m) &= \phi_{mq}^{-*}(\mathbf{r}_m) + \sum_d t_{md \leftarrow bq}^* \phi_{md}^{+*}(\mathbf{r}_m). \end{aligned}$$

Thus,

$$\begin{aligned}
& \psi_\beta^*(\mathbf{r}_m) \partial_x \psi_\alpha(\mathbf{r}_m) - \psi_\alpha(\mathbf{r}_m) \partial_x \psi_\beta^*(\mathbf{r}_m) \\
&= \left(\phi_{mq}^{-*}(\mathbf{r}_m) + \sum_d t_{md \leftarrow bq}^* \phi_{md}^{+*}(\mathbf{r}_m) \right) \partial_x \left(\phi_{mp}^-(\mathbf{r}_m) + \sum_c t_{mc \leftarrow ap} \phi_{mc}^+(\mathbf{r}_m) \right) \\
&\quad - \left(\phi_{mp}^-(\mathbf{r}_m) + \sum_c t_{mc \leftarrow ap} \phi_{mc}^+(\mathbf{r}_m) \right) \partial_x \left(\phi_{mq}^{-*}(\mathbf{r}_m) + \sum_d t_{md \leftarrow bq}^* \phi_{md}^{+*}(\mathbf{r}_m) \right).
\end{aligned}$$

Since transverse modes are orthogonal and normalized to a unit flux we get after intergration over S_m ,

$$I_{\beta\alpha}(m) = \left[\delta_{pq} \delta_{ab} \delta_{am} - \sum_c t_{mc \leftarrow bq}^* t_{mc \leftarrow ap} \right].$$

In a similar way,

$$I_{\alpha\beta}(n) = \left[\delta_{pq} \delta_{ab} \delta_{an} - \sum_d t_{nd \leftarrow bq}^* t_{nd \leftarrow ap} \right].$$

Substituting these expressions into the Kubo formula (C.1) and using unitarity of scattering amplitudes and time reversibility, after rather long algebra we get

$$G_{mn} = \frac{e^2}{h} \text{Tr} \, t t^\dagger = \frac{e^2}{h} T_{mn}.$$

Appendix D

Coulomb blockade in a non-stationary case

Then we can use Kirchoff's second law for the 2 loops in Fig. 4.5,

$$V_e - \frac{Q_e}{C_e} + \frac{Q_g}{C_g} - V_g = 0 \quad (\text{D.1})$$

$$V_c - \frac{Q_c}{C_c} + \frac{Q_g}{C_g} - V_g = 0. \quad (\text{D.2})$$

Combining equations (4.11),(D.1) and (D.2), we find all the charges,

$$Q_e = \frac{C_e}{C} [C_c(V_e - V_c) + C_g V_e - C_g V_g - ne] ; \quad (\text{D.3})$$

$$Q_c = \frac{C_c}{C} [-(C_e + C_g)(V_e - V_c) + C_g V_e - C_g V_g - ne] ; \quad (\text{D.4})$$

$$Q_g = \frac{C_g}{C} [C_c(V_e - V_c) - (C_e + C_c)(V_e - V_g) - ne] . \quad (\text{D.5})$$

Now let us suppose that 1 electron tunnels from emitter to the grain, then the number of excess electrons is changed,

$$n \rightarrow n + 1, \quad Q_e \rightarrow Q_e - e .$$

This situation is *non equilibrium*, so a current must flow through the external circuit. The net change of charge with respect to the equilibrium value for $n + 1$ excess electrons given by Eq. (D.3) is

$$\delta Q_e = -e \frac{C_e}{C} = -e - \delta Q_c - \delta Q_g = -e + e \frac{C_c + C_g}{C} .$$

We observe that the charge transferred through the voltage source V_e is $e\alpha_{ee}$ where $\alpha_{ee} \equiv (C_c + C_g)/C$. Looking at Eq. (D.4) we find that the charge transferred through the voltage source V_c is $\alpha_{ec}e$ where $\alpha_{ec} = C_c/C$. In a similar way we can consider the jump of

the electron from the grain to collector. In this case we have the transferred charges $e\alpha_{ce}$, $\alpha_{ce} = C_e/C$ through the source V_e and $e\alpha_{cc}$, $\alpha_{cc} = (C_e + C_g)/C$ through the source V_c .

Let us define the tunneling currents through emitter and collector junctions as $I_{e/c}(t)$, respectively. Then the current in the emitter branch is

$$\begin{aligned} I_l(t) &= \alpha_{ee}I_e(t) + \alpha_{ce}I_c(t) \\ &= \frac{C_c + C_g}{C}I_e(t) + \frac{C_e}{C}I_c(t). \end{aligned}$$

In a similar way, the current in the collector lead is

$$\begin{aligned} I_r(t) &= \alpha_{ec}I_e(t) + \alpha_{cc}I_c(t) \\ &= \frac{C_c}{C}I_e(t) + \frac{C_e + C_g}{C}I_c(t). \end{aligned}$$

Usually, $C_g \ll C_e, C_c$, and $I_l \approx I_r \approx I(t)$, where

$$I(t) = \alpha_e I_e(t) + \alpha_c I_c(t), \quad \alpha_e = \frac{C_c}{C}, \quad \alpha_c = \frac{C_e}{C}. \quad (\text{D.6})$$

The partial currents can be expressed through the probability $p_n(t)$ to find n excess electrons at the grain and the tunneling rates $\Gamma_{\mu \rightarrow \nu}(n)$,

$$I_\mu(t) = e \sum_n p_n(t) [\Gamma_{\mu \rightarrow \nu} - \Gamma_{\nu \rightarrow \mu}]. \quad (\text{D.7})$$

The probability $p_n(t)$ should be calculated from the Master equation,

$$\frac{dp_n(t)}{dt} = p_{n-1}\Gamma_{n-1}^n + p_{n+1}\Gamma_{n+1}^n - (\Gamma_n^{n-1} + \Gamma_{n+1}^n) p_n(t). \quad (\text{D.8})$$

Here

$$\Gamma_{n-1}^n = \Gamma_{e \rightarrow g}(n-1) + \Gamma_{c \rightarrow g}(n-1); \quad (\text{D.9})$$

$$\Gamma_{n+1}^n = \Gamma_{g \rightarrow e}(n+1) + \Gamma_{g \rightarrow c}(n+1). \quad (\text{D.10})$$

Bibliography

Books

- [1] B. L. Altshuler, A. G. Aronov, D. E. Khmel'nitskii, and A. I. Larkin, in: *Quantum Theory of Solids*, edited by I. M. Lifshits, pp. 130-237, Advances in Science and Technology in the USSR, Mir Publishers, Moscow 1982.
- [2] H. Fukuyama and S. Hikami, *Anderson Localization*, Springer, Berlin (1982).
- [3] S. Datta, *Transport in Mesoscopic Systems*, Cambridge University Press (1996).
- [4] Y. Imry, *“Introduction to Mesoscopic Physics”*, Oxford University Press (1997).
- [5] T. Dittrich, P. Hänggi, G.-L. Ingold, B. Kramer, G. Schön, W. Zwerger, *Quantum Transport and Dissipation*, Wiley-VCH (1998).
- [6] T. Ando, Y. Arakawa, K. Furuya, S. Komiyama, H. Nakashima (Eds.), *Mesoscopic Physics and Electronics*, Springer (1998).

Review articles

- [7] T. Ando, A. B. Fowler, and F. Stern, *Rev. Mod. Phys.* **54**, 437 (1982).
- [8] B. L. Altshuler and A. G. Aronov, In: *Electron-Electron Interactions in Disordered Systems*, ed. by M. Pollak and A. L. Efros, pp. 1-151, In: *Modern Problems in Condensed Matter Physics*, North Holland (1985).
- [9] H. Fukuyama, In: *Electron-Electron Interactions in Disordered Systems*, ed. by M. Pollak and A. L. Efros, pp. 155-230, In: *Modern Problems in Condensed Matter Physics*, North Holland (1985).
- [10] C. W. J. Beenakker and H. van Houten, in “Solid State Physics” (H. Ehrenreich and D. Turnbull, eds.), v. 44, p. 1. Academic Press, Inc., 1991.
- [11] H. van Houten *et al.*, in “Physics and Technology of Submicron Structures” (H. Heinrich, G. Bauer, and F. Kuchar, eds.). Springer, Berlin, 1988.

- [12] C. W. J. Beenakker, H. van Houten and B. van Wees, *Superlattices and Microstructures*, **5**, 127 (1989)
- [13] D. A. Averin, K. K. Likharev, in: *Quantum Effects in Small Disordered Systems*, ed. by B. L. Altshuler, P. A. Lee and R. A. Webb (Elsevier, Amsterdam, 1991).
- [14] *Single Charge Tunneling*, Vol. 294 of *NATO Advanced Study Institute, Series B: Physics*, ed. by H. Grabert and M. H. Devoret (Plenum, New York, 1992).
- [15] *Single-Electron Tunneling and Mesoscopic Devices*, ed. by H. Koch and H. Lübbig (Springer-Verlag, Berlin Heidelberg, 1995).
- [16] M. P. A. Fisher, L. I. Glazman, preprint cond-mat/96010037.
- [17] C. W. J. Beenakker, *Rev. Mod. Phys.* **69**, 731 (1997).
- [18] A. D. Stone, in: *Physics of Nanostructures*, ed by J. H. Davies and A. R. Long, p. 65 (1991).
- [19] M. J. M. de Jong and C. W. J. Beenakker, *Shot Noise in mesoscopic systems*, preprint cond-mat/9611140.

Selected papers

- [20] B. L. Altshuler, A. G. Aronov and B. Z. Spivak, *JETP Lett.* **33**, 94 (1981).
- [21] D. Yu. Sharvin and Yu. V. Sharvin, *JETP Lett.* **34**, 272 (1981)
- [22] D. E. Khmelnitskii, *Physica* **126b**, 235 (1984).
- [23] V. L. Gurevich, *Phys. Rev. B* **55**, 4522 (1997).
- [24] Y. Gefen, Y. Imry, and M. Ya. Azbel, *Phys. Rev. Lett.* **52**, 129 (1984).
- [25] L. I. Glazman, G. B. Lesovik, D. E. Khmelnitskii, R. I. Shekhter, *JETP Letters*, **48**, 238 (1988).
- [26] I. O. Kulik and R. I. Shekhter, *Sov. Phys.-JETP*, **41**, 308 (1975).
- [27] P. A. Lee, *Physica* **140A**, 169 (1986).
- [28] B. L. Altshuler, *JETP Lett.* **41**, 648 (1985).
- [29] B. L. Altshuler and B. I. Shklovskii, *JETP* **64**, 127 (1986) [*Zh. Eksp. Teor. Fiz.* **91**, 220 (1986)].
- [30] Y. Imry, *Europhys. Lett.* **1**, 249 (1986).

- [31] D. C. Tsui, H. L. Störmer and A. C. Gossard, *Phys. Rev. Lett.* **48**, 1559 (1982).
- [32] M. Reznikov, M. Heiblum, H. Shtrikman, and D. Mahalu, *Phys. Rev. Lett.* **75**, 3340 (1995).
- [33] C. W. J. Beenakker and M. Büttiker, *Phys. Rev. B* **46**, 1889 (1992).
- [34] H. Birk, M. J. M. de Jong, and C. Schönenberger, *Phys. Rev. Lett.* **75**, 1610 (1995).
- [35] A. H. Steinbach, J. M. Martinis, and M. H. Devoret, *Phys. Rev. Lett.* **76**, 3806 (1996).